

DISSERTATION

Preparation and Modification of Carboxylate - Substituted Metal Oxo Clusters

ausgeführt zum Zwecke der Erlangung des akademischen Grades eines Doktors der
Naturwissenschaften

unter der Leitung von

o. Univ.-Prof. Dr. Ulrich Schubert

Institut für Materialchemie (E165)

eingereicht an der Technischen Universität Wien
Fakultät für Technische Chemie

von

Mag. rer. nat. Myhedin Jupa

9826364

Angeligasse 116/13

1100 Wien

Wien, am 23. Mai 2005



for my wife Lumturije,
and
my sons, Blendi and Bleon

Acknowledgments

I am deeply indebted to *Prof. Ulrich Schubert* for giving me the opportunity to undertake my thesis in his research group, for his support and guidance during the last three years. His guidance has allowed me to grow and mature as a scientist. My sincere thanks go to *Dr. Silvia Gross* for her help in the beginning of my work. I am also indebted to *Dr. Guido Kickelbick* and *Dr. Nicola Hüsing* for their help and support with chemistry. I want to express my gratitude to *Dr. Michael Puchberger* for his help and support with chemistry and for many discussions, which also contributes to the success of this work.

My sincere thanks go to all my colleagues from the working group Schubert: *Beatrice, Denise, Dieter H., Doris B., Doris E., Christian, Christina F., Christoph, Claudia F., Claudia V., Didi, Grace, Fatmir, Harald, Isabella, Melitta, Ralf, René, Rupert, Sorin, Susan, Thomas G., Uli, Urška, Viki,* and *Wolfgang* for the pleasant working atmosphere. I am also indebted to *Helmut* for his sense of humor and the pleasant working atmosphere.

I gratefully acknowledge the financial support by the Fonds zur Förderung der wissenschaftlichen Forschung, Austria.

I would like to thank my parents for their unwavering encouragement and support throughout my life, my sisters *Mervete* and *Florije*, and my brother *Behlul*.

Finally, this thesis is dedicated to my family, wife *Lumturije* and the sons *Blendi* and *Bleon*, who were always there for me and with me.

Kurzfassung der Arbeit

Anorganisch-organische Hybridmaterialien, in denen anorganische und organische Bestandteile kovalent miteinander verbunden sind, die zweite Klasse von Hybridmaterialien, stellen eine interessante Klasse von Materialien dar, mit sehr breiten Eigenschaften und Anwendungen. In der vorliegenden Arbeit wurden Metalloxidcluster, welche mit polymerisierbaren Gruppen substituiert waren, untersucht. Diese Cluster können als Co-Monomere in Polymerisationsreaktionen verwendet werden.

Im ersten Teil dieser Arbeit wurden organisch modifizierte Übergangsmetallcluster durch die Reaktion der entsprechenden Alkoxide mit funktionellen und nicht-funktionellen Carbonsäuren hergestellt. Die Reaktion von Gemischen aus Titanpropoxid und Yttrium-2-methoxyethoxid mit Methacrylsäure führte zur Bildung von drei gemischt-metallischen Clustern unterschiedlicher Zusammensetzung: $\text{Ti}_4\text{Y}_2\text{O}_4(\text{OMc})_{14}(\text{MeOCH}_2\text{CH}_2\text{OH})_2$, (OMc = Methacrylat), $\text{Ti}_4\text{Y}_2\text{O}_4(\text{OMc})_{14}(\text{MeOH})_2$ und $\text{Ti}_4\text{Y}_2\text{O}_4(\text{OMc})_{12}(\text{OCH}_2\text{CH}_2\text{OMe})_2(\text{MeOH})_2$. Die Reaktion von Gemischen aus Titanpropoxid und Hafniumbutoxid mit Methacrylsäure führt zur Bildung des bimetallischen Clusters $\text{Hf}_4\text{Ti}_4\text{O}_6(\text{OPr})_4(\text{OMc})_{16}$.

$\text{Zr}_{12}\text{O}_8(\text{OH})_8(\text{OProp})_{24}$, (OProp = Propionat), $\text{Zr}_{12}\text{O}_8(\text{OH})_8(\text{OAc})_{24}$ oder $\text{Hf}_{12}\text{O}_8(\text{OH})_8(\text{OAc})_{24}$ (OAc = Acetat) wurden durch Reaktion von Zirkonbutoxid oder Hafniumbutoxid mit Propion- oder Essigsäure hergestellt. $\text{Zr}_{12}\text{O}_8(\text{OH})_8(\text{OAcMe}_2)_{24}$, (OAcMe_2 = Dimethylacrylat) wurde durch Reaktion von Zirkonbutoxid mit Dimethylacrylsäure hergestellt.

Im zweiten Teil dieser Arbeit wurde versucht die Zahl der polymerisierbaren Liganden an Metall Oxo Clustern zu reduzieren. Das wurde sowohl durch Hydrosilylierungsreaktionen als auch durch Austausch von Liganden an der Oberfläche der Cluster gegen andere Carboxylate untersucht. Abhängig von molarem Verhältnis zwischen Clustern und freien Carbonsäuren wurden gemischt-substituierte Oxo Cluster mit funktionellen und nicht-funktionellen Carboxylaten erhalten, z.B. $\text{Zr}_6\text{O}_4(\text{OH})_4(\text{OMc})_6(\text{OIsob})_6$, (OIsob = Isobutyrat) und $\text{Zr}_6\text{O}_4(\text{OH})_4(\text{OMc})_7(\text{OOCEt})_5$.

Durch Radikalcopolymerisation von $\text{Hf}_4\text{Ti}_4\text{O}_6(\text{OPr})_4(\text{OMc})_{16}$ mit Methylmethacrylat wurden anorganisch-organische Hybridmaterialien hergestellt. Sowohl die thermische Stabilität als auch die mechanische Eigenschaften dieser Polymere wurden untersucht.

Abstract

Inorganic-organic hybrid materials, in which the inorganic and organic part are connected by a covalent linkage, class II of hybrid materials, are an interesting class of materials with many possibilities, interesting properties and applications. In this work, metal oxide clusters substituted by polymerizable groups were investigated. Such clusters can be used as comonomers in polymerization reactions.

In the first part organically modified transition metal oxo clusters were prepared by reaction of metal alkoxides with functional and non-functional carboxylic acids. Upon reaction of titanium propoxide and yttrium 2-methoxyethoxide with methacrylic acid, three different mixed-metal clusters were obtained, depending on the titanium to yttrium alkoxide ratio: $\text{Ti}_4\text{Y}_2\text{O}_4(\text{OMc})_{14}(\text{MeOCH}_2\text{CH}_2\text{OH})_2$, (OMc = methacrylate), $\text{Ti}_4\text{Y}_2\text{O}_4(\text{OMc})_{14}(\text{MeOH})_2$ and $\text{Ti}_4\text{Y}_2\text{O}_4(\text{OMc})_{12}(\text{OCH}_2\text{CH}_2\text{OMe})_2(\text{McOH})_2$. Reaction of mixtures of titanium propoxide and hafnium butoxide with methacrylic acid resulted in the formation of the mixed-metal cluster $\text{Hf}_4\text{Ti}_4\text{O}_6(\text{OPr})_4(\text{OMc})_{16}$.

$\text{Zr}_{12}\text{O}_8(\text{OH})_8(\text{OProp})_{24}$, (OProp = propionate), $\text{Zr}_{12}\text{O}_8(\text{OH})_8(\text{OAc})_{24}$ or $\text{Hf}_{12}\text{O}_8(\text{OH})_8(\text{OAc})_{24}$, (OAc = acetate), were prepared by the reaction of either zirconium butoxide or hafnium butoxide with propionic acid or acetic acid. $\text{Zr}_{12}\text{O}_8(\text{OH})_8(\text{OAcMe}_2)_{24}$, (OAcMe₂ = dimethylacrylate), was prepared by the reaction of zirconium butoxide with dimethylacrylic acid.

In the second part of the work, attempts were made to reduce the number of polymerizable ligands of metal oxo-clusters. This was tested by either hydrosilylation reaction of the methacrylate-substituted cluster or by exchange of surface bonded ligands for other carboxylates. Depending on the molar ratio of clusters and carboxylic acid, oxo clusters with both functional and non-functional carboxylate ligands were obtained, for example $\text{Zr}_6\text{O}_4(\text{OH})_4(\text{OMc})_6(\text{OIsob})_6$, (OIsob = isobutyrate) or $\text{Zr}_6\text{O}_4(\text{OH})_4(\text{OMc})_7(\text{OOCEt})_5$.

Free radical-initiated polymerisation of $\text{Hf}_4\text{Ti}_4\text{O}_6(\text{OPr})_4(\text{OMc})_{16}$ with methyl methacrylate, resulted in cluster-crosslinked hybrid materials. Both the thermal stability and mechanical properties of the polymers were improved by the crosslinking.

Abstrakt (in albanian)

Materialet hibride inorganik-organike, ne te cilat pjesa inorganike dhe organike jane te lidhura me lidhje kovalente, klasa II e materialeve hibride, jane klase interesante e materialeve me shume mundesi perdorimi dhe aplikimi. Per pergatitjen e ketyre materialeve hibride mund te perdoren alkoksidet e metaleve organikisht te modifikuara, te cilat ne siperfaqen e tyre permbajne ligande polimerizuese, te cilat mund te perdoren si co-monomer.

Ne pjesen e pare te ketij punimi jane pergatitur oxo *cluster*-et (komponime komplekse) te metaleve kalimtare organikisht te modifikuara nga reagimet e alkoksive me acide karboksilike funksionale dhe jo-funksionale. Pergjate reagimit te titan propoksive dhe yttrium 2-metoksiethoksive me acidin metakrilik, tre *cluster* te ndryshem jane formuar, varesisht nga raporti mes titan dhe yttrium alkoksive: $Ti_4Y_2O_4(OMc)_{14}(MeOCH_2CH_2OH)_2$, $Ti_4Y_2O_4(OMc)_{14}(MeOH)_2$ dhe $Ti_4Y_2O_4(OMc)_{12}(OCH_2CH_2OMe)_2(MeOH)_2$, (OMc = metacrylate). Reagimi i perzierjes se titan propoksive dhe hafnium butoksive me acidin metakrilik ka rezultuar ne krijimin e $Hf_4Ti_4O_6(OPr)_4(OMc)_{16}$.

$Zr_{12}O_8(OH)_8(OProp)_{24}$, (OProp = propionate), $Zr_{12}O_8(OH)_8(OAc)_{24}$ dhe $Hf_{12}O_8(OH)_8(OAc)_{24}$, (OAc = acetate), jane pergatitur nga reagimi i zirkon butoksive dhe hafnium butoksive me acidin propionik dhe acidin e uthulles, gjegjesisht. Reagimi i shtate ekuivalenteve te acidit dimetilakrilik me butokside te zirkonit shpie ne formimin e cluster-it $Zr_{12}O_8(OH)_8(OAcMe_2)_{24}$, (OAcMe₂ = dimetilacrylate).

Ne pjesen e dyte te ketij punimi jane bere perpjekje qe te reduktohet numri i ligandeve polymerizuese te oxo *cluster*-et e metaleve. Kjo eshte provuar me ane te reaksionit te hidrosililit si dhe me zevendesimin e ligandeve siperfaqesore nga acidet tjera. Varesisht nga raporti molar i *cluster*-eve dhe acideve karboksilike te lira, jane formuar oxo *cluster* me permbajtje te ligandeve karboksilike funksionale dhe jo-funksionale ne siperfaqe te tyre, si p.sh. $Zr_6O_4(OH)_4(OMc)_6(OIsob)_6$, (OIsob = isobutyrate) dhe $Zr_6O_4(OH)_4(OMc)_7(OOCeT)_5$.

Permes reaksioneve polymerizuese, te inicuar nga radikalet e lira, te $Hf_4Ti_4O_6(OPr)_4(OMc)_{16}$ me metil metakrilate, ka rezultuar ne formimin e materialeve hibride te lidhura nga cluster-i gjegjes. Jane analizuar vetite mekanike dhe stabiliteti termik i polimereve.

Part of this work has been published:

1. M. Jupa, G. Kickelbick and U. Schubert, *European Journal of Inorganic Chemistry*, 1835, 2004.
2. F. R. Kogler, M. Jupa, M. Puchberger and U. Schubert, *Journal of Materials Chemistry*, **14**, 3133, 2004.
3. Y. Gao, D. S. Dragan, M. Jupa, F. R. Kogler, M. Puchberger and U. Schubert, *Mat. Res. Soc. Symp. Proc.*, **847**, EE8.6.1, 2005.

Index of Abbreviations

Bu	Butyl group
DSC	Differential Scanning Calorimetry
Et	Ethyl group
HMBC	Heteronuclear Multiple Bond Correlation
HSQC	Heteronuclear Single Quantum Correlation
IR	Infrared
Me	Methyl group
MMA	Methyl methacrylate
NMR	Nuclear Magnetic Resonance
OAc	Acetate group
OAc _r	Acrylate group
OAc _r Me ₂	Dimethylacrylate group
OBu	Butoxide group
OEt	Ethoxide group
OIsob	Isobutyrate group
OMc	Methacrylate group
OME	Methoxyethoxide group
OPr	Propoxide group
OProp	Propionate group
ROESY	Rotating Frame Overhauser Effect Spectroscopy
Pr	Propyl group
TGA	Thermogravimetric Analysis
TOCSY	Total Correlation Spectroscopy
XRD	X-Ray Diffraction

Cluster abbreviations

- 1 $\text{Ti}_4\text{Y}_2\text{O}_4(\text{OMc})_{14}(\text{MeOCH}_2\text{CH}_2\text{OH})_2$
- 2 $\text{Ti}_4\text{Y}_2\text{O}_4(\text{OMc})_{14}(\text{MeOH})_2$
- 3 $\text{Ti}_4\text{Y}_2\text{O}_4(\text{OMc})_{12}(\text{OCH}_2\text{CH}_2\text{OMe})_2(\text{McOH})_2$
- 4 $\text{Hf}_4\text{Ti}_4\text{O}_6(\text{OPr})_4(\text{OMc})_{16}$
- 5 $\text{Zr}_{12}\text{O}_8(\text{OH})_8(\text{OProp})_{24} \cdot 6\text{PropOH}$
- 6 $\text{Zr}_{12}\text{O}_8(\text{OH})_8(\text{OAc})_{24} \cdot 6\text{AcOH} \cdot 7/2 \text{CH}_2\text{Cl}_2$
- 7 $\text{Zr}_{12}\text{O}_8(\text{OH})_8(\text{OAcMe}_2)_{24} \cdot 2\text{Me}_2\text{AcOH} \cdot \text{BuOH}$
- 8 $\text{Hf}_{12}\text{O}_8(\text{OH})_8(\text{OAc})_{24} \cdot 3\text{AcOH} \cdot 3\text{CH}_2\text{Cl}_2$
- 9 $[\text{Y}(\text{OMc})_3]_n$
- 10 $[\text{Y}(\text{OAc})_3]_n$

IR abbreviations

- | | |
|----|--------|
| s | strong |
| m | medium |
| w | weak |
| br | broad |

Contents

1. Introduction	1
1.1. Sol-gel route of inorganic-organic hybrid materials	1
1.2. Chemical reactivity of metal alkoxides	2
1.3. Control of the reactivity of metal alkoxides	4
1.4. Metal oxo clusters as co-monomer in polymerization reactions	7
2. Aim of the Work	9
3. Preparation of metal oxo clusters	10
3.1. Preparation of the mixed-metal oxo clusters	10
3.1.1. Structure of $Ti_4Y_2O_4(OMc)_{14}(MeOCH_2CH_2OH)_2$	11
3.1.2. Structure of $Ti_4Y_2O_4(OMc)_{14}(MeOH)_2$	14
3.1.3. Structure of $Ti_4Y_2O_4(OMc)_{12}(OCH_2CH_2OMe)_2(MeOH)_2$	16
3.1.4. Structure of $Hf_4Ti_4O_6(OPr)_4(OMc)_{16}$	18
3.2. Zirconium oxo clusters	22
3.2.1. Structure of $Zr_{12}O_8(OH)_8(OProp)_{24} \cdot 6PropOH$	23
3.2.2. Structure of $Zr_{12}O_8(OH)_8(OAc)_{24} \cdot 6AcOH \cdot 7/2 CH_2Cl_2$	26
3.2.3. Structure of $Zr_{12}O_8(OH)_8(OAcMe_2)_{24} \cdot 2Me_2AcOH \cdot BuOH$	30
3.3. Hafnium oxo cluster	34
3.3.1. Structure of $Hf_{12}O_8(OH)_8(OAc)_{24} \cdot 3AcOH \cdot 3CH_2Cl_2$	34
3.4. Yttrium Carboxylates	38
3.4.1. Structure of $[Y(OOCR)_3]_n$	38
4. Hydrosilylation of $Zr_4O_2(OMc)_{12}$	43
5. Ligand exchange of metal oxo clusters	47
5.1. Reaction of $Zr_6O_4(OH)_4(OMc)_{12}$ with isobutyric acid	49
5.2. Reaction of $Zr_6O_4(OH)_4(OMc)_{12}$ with propionic acid	51
5.3. Reaction of $Zr_{12}O_8(OH)_8(OProp)_{24}$ with acetic acid	54
5.4. Reaction of $Zr_{12}O_8(OH)_8(OProp)_6(OMc)_{18}$ with propionic acid	55
6. Inorganic-organic hybrid materials	61
6.1. Thermal Behavior	62
6.2. Swelling Behavior	64
7. Experimental Part	65
7.1. Sample Preparation	65
7.1.1. General techniques	65

7.1.2. Used Chemicals	65
7.2. Mixed-Metal oxo clusters	66
7.2.1. Synthesis of $Ti_4Y_2O_4(OMc)_{14}(MeOCH_2CH_2OH)_2$	66
7.2.2. Synthesis of $Ti_4Y_2O_4(OMc)_{14}(MeOH)_2$	67
7.2.3. Synthesis of $Ti_4Y_2O_4(OMc)_{12}(OCH_2CH_2OMe)_2(McOH)_2$	67
7.2.4. Synthesis of $Hf_4Ti_4O_6(OPr)_4(OMc)_{16}$	68
7.3. Zirconium oxo clusters	68
7.3.1. Synthesis of $Zr_{12}O_8(OH)_8(OProp)_{24} \cdot 6PropOH$	68
7.3.2. Synthesis of $Zr_{12}O_8(OH)_8(OAc)_{24} \cdot 6AcOH \cdot 7/2 CH_2Cl_2$	69
7.3.3. Synthesis of $Zr_{12}O_8(OH)_8(OAcMe_2)_{24} \cdot 2Me_2AcrOH \cdot BuOH$	69
7.3.4. Synthesis of $Zr_{12}O_8(OH)_8(OProp)_6(OMc)_{18}$	70
7.4. Hafnium oxo cluster	70
7.4.1. Synthesis of $Hf_{12}O_8(OH)_8(OAc)_{24} \cdot 3AcOH \cdot 3CH_2Cl_2$	70
7.5. Yttrium Carboxylates	71
7.5.1. Synthesis of $[Y(OMc)_3]_n$	71
7.5.2. Synthesis of $[Y(OAc)_3]_n$	71
7.6. Cluster Modification Reactions	72
7.6.1. Attempted hydrosilylation of $Zr_4O_2(OMc)_{12}$	72
7.6.1.1. Reaction of $Zr_4O_2(OMc)_{12}$ with $HSiPh_3$	72
7.6.1.2. Reaction of $Zr_4O_2(OMc)_{12}$ with $HSiEt_3$	72
7.7. Ligand exchange of metal oxo clusters	73
7.7.1. Reaction of $Zr_6O_4(OH)_4(OMc)_{12}$ with isobutyric acid	73
7.7.2. Reaction of $Zr_6O_4(OH)_4(OMc)_{12}$ with propionic acid	73
7.7.3. Reaction of $Zr_{12}O_8(OH)_8(OProp)_{24}$ with acetic acid	74
7.7.4. Reaction of $Zr_{12}O_8(OH)_8(OProp)_6(OMc)_{18}$ with propionic acid	74
7.8. Preparation of Inorganic-organic Hybrid Materials	75
7.8.1. Synthesis of PMMA doped with $Hf_4Ti_4O_6(OPr)_4(OMc)_{16}$	75
7.9. Analytical Techniques	76
7.9.1. Thermal Analysis (TGA, DSC)	76
7.9.2. NMR Spectroscopy	77
7.9.2.1. NMR measurements	77
7.9.3. IR Spectroscopy	77
7.9.4. Elemental Analysis	77
7.9.5. Single-Crystal X-Ray Diffraction	78

7.10. Crystallographic Data	79
7.10.1. $\text{Ti}_4\text{Y}_2\text{O}_4(\text{OMc})_{14}(\text{MeOCH}_2\text{CH}_2\text{OH})_2$	79
7.10.2. $\text{Ti}_4\text{Y}_2\text{O}_4(\text{OMc})_{14}(\text{MeOH})_2$	80
7.10.3. $\text{Ti}_4\text{Y}_2\text{O}_4(\text{OMc})_{12}(\text{OCH}_2\text{CH}_2\text{OMe})_2(\text{McOH})_2$	81
7.10.4. $\text{Hf}_4\text{Ti}_4\text{O}_6(\text{OPr})_4(\text{OMc})_{16}$	82
7.10.5. $\text{Zr}_{12}\text{O}_8(\text{OH})_8(\text{OProp})_{24} \cdot 6\text{PropOH}$	83
7.10.6. $\text{Zr}_{12}\text{O}_8(\text{OH})_8(\text{OAc})_{24} \cdot 6\text{AcOH} \cdot 7/2\text{CH}_2\text{Cl}_2$	84
7.10.7. $\text{Zr}_{12}\text{O}_8(\text{OH})_8(\text{OAcMe}_2)_{24} \cdot 2\text{Me}_2\text{AcOH} \cdot \text{BuOH}$	85
7.10.8. $\text{Hf}_{12}\text{O}_8(\text{OH})_8(\text{OAc})_{24} \cdot 3\text{AcOH} \cdot 3\text{CH}_2\text{Cl}_2$	86
7.10.9. $[\text{Y}(\text{OMc})_3]_n$	87
7.10.10. $[\text{Y}(\text{OAc})_3]_n$	88
8. Summary	89
9. Literature	94

1 Introduction

1.1. Sol-gel route of inorganic-organic hybrid materials

The sol-gel process is a versatile solution process for making ceramic, glass or glass-like materials^[1]. In general, the sol-gel process involves the transition of a system from a liquid “sol” (mostly colloidal) into a solid “gel” phase. The precursors used in the preparation of the “sol” are usually inorganic metal salts or metal-organic compounds such as metal alkoxides. In a typical sol-gel process, the precursor is subjected to a series of hydrolysis and polycondensation reactions to form a colloidal suspension, or a “sol”. The monomers which constitute the “sol” undergo hydrolysis and condensation reactions, thus they can build macroscopic molecules which extend throughout the solution. Such a system is called a “gel”. As a result, a gel can be defined as a system with a continuous skeleton enclosing a continuous liquid phase. The mild chemical conditions allowed by the sol-gel process provide a very versatile access to the inorganic-organic hybrid materials and new approaches for their preparation.

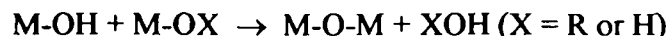
Hydrolysis and condensation of metal or semi-metal alkoxides may lead to structurally defined molecular cage compounds (clusters), instead of oligomers or polymers with broad size distributions, if the reaction with water is performed in a very controlled manner. The reaction of the sol-gel process have been extensively studied in the case of silica^[1], but less data is available for transition metal alkoxides. The reaction proceeds first through the hydrolysis of metal alkoxides, as follows:



The reaction occurs in three steps: (i) nucleophilic attack of the metal atom M by the oxygen atom of a water molecule; (ii) transfer of a proton from the water to an alkoxide group of the metal; (iii) release of the resulting ROH molecule^[2,3].

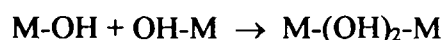
Depending on the experimental conditions, two competitive mechanisms have to be considered:

1) Oxolation (formation of Oxo bridges):



Generally, under a stoichiometric water : OR group ratio the alcohol producing condensation is favored, whereas a water forming condensation is observed for larger water : OR group ratios^[2,4].

2) Olation (formation of hydroxo bridges):



Olation is a nucleophilic addition reaction that can take place when the coordination of the metal center is not fully satisfied.

The hydrolysis, oxolation and olation can be involved in the transformation of a metal alkoxide precursor into a metal oxo macromolecular network^[5].

1.2. Chemical reactivity of metal alkoxides

Controlling the chemical reactivity of transition metal alkoxides at the molecular scale is a crucial step in sol-gel processing of high-tech materials^[2].

The chemical reactions involved in the sol-gel process can be summarized as follow^[5]:



The chemical reactivity of metal alkoxides toward nucleophilic reactions mainly depends on the strength of the nucleophile, the electrophilic character of the metal atom - the electronegativity^[2,6], and its ability to increase its coordination number. Therefore, the silicon alkoxides are not very reactive towards water, whereas transition metal akoxides are very sensitive to moisture. As result, hydrolysis-condensation reaction rates of silicon alkoxides

must be increased by using catalysts, whereas that of the metal alkoxides must be moderated by using chemical additives. Acid or base catalysis does not only increase the reaction rate of silicon alkoxides it also determines the structure of the silica materials obtained. Under acidic conditions, the alkoxy groups of silica are quickly protonated, making alcohol a better leaving group and increasing therefore the hydrolysis rate^[1]. Under basic conditions hydroxy anions and deprotonated silanol groups are better nucleophiles than water and silanol species, and thus attack the silicon atom faster. These differences in selectivity between base- or acid-catalyzed condensations result in the formation of hybrid materials of different structures.

Coordination expansion is a general tendency for transition metal alkoxides. Metal atoms tend to self-regulate their reactivity by forming aggregates, using their vacant orbitals to accept electrons from nucleophilic ligands. The molecular complexity of metal alkoxides then depends on parameters like concentration or temperature, as well as chemical factors like solvents, the oxidation state of the metal atom or the steric hindrance of alkoxy groups^[6,7,8,9]. Oligomeric species $[\text{Ti}(\text{OEt})_4]_n$ have been evidenced for titanium ethoxide, whereas titanium isopropoxide $\text{Ti}(\text{OPr}^i)_4$ remains monomeric. Therefore, the hydrolysis of $\text{Ti}(\text{OR})_4$ with bulky OPr^i groups and Ti with a lower coordination number is much faster than that of the primary alkoxides^[10].

The molecular complexity and thus the reactivity of metal alkoxides can also be influenced by an appropriate choice of a solvent which favors solvation^[11]. The stability of such solvated alkoxides increases with the positive charge of the metal atom and its tendency to acquire a higher coordination number^[8]. $[\text{Zr}(\text{OR})_4]_n$ oligomers, formed ($n \leq 4$) in nonpolar solvents such as cyclohexane, allow slow hydrolysis rates and the formation of clear gels. When alkoxides are dissolved in their parent alcohol, hydrolysis proceeds much faster and leads to precipitation^[12]. When metal alkoxides are dissolved in other alcohols, several species can be formed very fast through alcohol interchange reactions^[13].

Coordination expansion sometimes occurs through the formation of double alkoxides. Double alkoxides or oxo alkoxides are often obtained when two different alkoxides are reacted before hydrolysis^[14]. The metal atoms are linked together by alkoxo bridges or by ether elimination leading to μ -oxo bridges.

1.3. Control of the reactivity of metal alkoxides

Hydrolysis gives reactive M-OH bonds which lead to condensation and favor the formation of larger species. A large variety of oligomeric species can thus be obtained. Molecular clusters, chain polymers, or colloidal particles can be synthesized depending on the relative ratio of hydrolysis and condensation. Several possibilities have been proposed to control the reactivity of transition metal alkoxides^[15,16,17]. In most cases strongly complexing ligands, such as the anions of β -diketones, polyhydroxylated ligands such as polyols or hydroxyl acids were used^[18,19]. The chemical modification of metal alkoxides by nucleophilic ligands leads to the formation of new molecular precursors which exhibit different chemical reactivity^[2]. These organic derivatives of the metal alkoxides are more stable towards hydrolysis than the OR groups due to the chelate formation and sterical hindrance effects^[5,20,21,22].

A chelating ligand^[23] that has often been reported in the hydrolysis-condensation reactions as stabilizing agent for non-silicate metal alkoxides, is acetylacetonate for: $W(OEt)_6$ ^[24], $Zr(OR)_4$ ($OR = OPr^i, OPr^n$)^[25-28], $Ti(OR)_4$ ($OR = OPr^i, OBU^n$)^[29], $Al(OBU^s)_4$ ^[25], or $Ce(OPr^i)_4$ ^[30]. In the case of titanium alkoxide, the substitution of the two first alkoxy groups by acetylacetonate (acac) ligands occurs readily, but the replacement of a third alkoxy substituent has been not observed. The hydrolysis and condensation reactions of β -diketonate-substituted titanium alkoxides $Ti(OR)_2(acac)_2$ leads to dimers $[TiO(acac)_2]_2$ ^[31]. For a smaller amount of acac-H (~ 0.1 equivalents) larger molecular species can be obtained, i.e. $Ti_{18}O_{22}(OBU)_{26}(acac)_2$ ^[32], while $Ti_4O_2(O^iPr)_{10}(acac)_2$ ^[32] was obtained by slow hydrolysis of a 2:1 mixture of $Ti(O^iPr)_4$ and acac-H^[33]. These molecular cluster compounds are good models for the understanding of the particle growth process. For low complexation ratios, hydrolysis and condensation are very fast because the coordination of most of the metal atoms is not efficiently increased. The hydrolysis rate of alkoxy groups in complexed precursors is lower than that of alkoxy groups in unmodified alkoxides^[34].

A similar behavior is also obtained for hydrolysis of acac-modified zirconium alkoxides. The cluster $Zr_4O(OPr)_{10}(acac)_4$ ^[35] was obtained upon hydrolysis of the modified precursor $[Zr_2(OPr^n)_6(acac)_2]$. A decameric zirconium cluster $Zr_{10}O_6(OH)_4(OPr)_{18}(allylacetylacetonate)_6$ can be obtained by decreasing the complexation ratio^[36]. On the other hand, when zirconium alkoxides reacts with four equivalents of acac-H, $Zr(acac)_4$ is formed^[37].

Reaction with carboxylic acids is another common way to control the reactivity of metal alkoxides for sol-gel processing^[38]. The clusters $Ti_6O_4(O^iPr)_8(OAc)_8$ ^[39], $Ti_6O_4(O^iPr)_{12}(OAc)_4$ ^[40], $Ti_6O_4(OBu)_8(OAc)_8$ ^[41] or $Ti_6O_4(OEt)_8(OAc)_8$ ^[42] were obtained in the reaction of $Ti(OR)_4$ ($R = Et, ^iPr$ or Bu) with different molar ratio of acetic acid. When $Ti(O^iPr)_4$ was reacted with 1 or 2 equivalents of formic acid under the same conditions, the clusters $Ti_4O_2(O^iPr)_{10}(OOCH)_2$ or $Ti_6O_6(O^iPr)_6(OOCH)_6$ were obtained^[43], while $Ti_3O(OCH_2CMe_3)_8(OOCH)_2$ ^[44] is formed from the reaction of $Ti(OCH_2CMe_3)_4$ with formic acid. The formation of clusters $Ti_4O_4(OR)_4[(OOC-CCO_3(CO)_9)_4]$ ^[45,46] ($R = ^iPr, Bu, Ph$), $Ti_4O_4(OEt)_4[(OOC-CCO_2(CO)_6Mo(CO)_2Cp)_4]$ ^[47] or $Ti_4O_4(OEt)_4[(OOC-CCO_2(CO)_6W(CO)_2Cp)_4]$ ^[47] have been reported. The clusters $Ti_6O_4(OPr)_8(OMc)_8$ ^[48] or $Ti_9O_8(OPr)_4(OMc)_{16}$ ^[49] were formed in the reaction of $Ti(OPr)_4$ with 2.2 or 4 equivalents methacrylic acid, respectively. When $Ti(OEt)_4$ was reacted with 2 equivalents of methacrylic acid, the cluster $Ti_6O_4(OEt)_8(OMc)_8$ ^[50] was obtained, while $Ti_4O_2(O^iPr)_6(OMc)_6$ ^[48] is formed from $Ti(O^iPr)_4$ under the same conditions. When $Ti(OR)_4$ ($R = Et$ or O^iPr) was reacted with 2-phenoxybenzoic acid $Ti_6O_6(OEt)_6(O_2CC_4H_6-o-OPh)_6$ or $Ti_6O_6(O^iPr)_6(O_2CC_4H_6-o-OPh)_6$ were obtained^[51].

Various carboxylic acids were used in reaction with zirconium alkoxides to prepare different types of organically modified zirconium oxo clusters. When acetic acid was employed, $Zr_9O_6(OPr)_{18}(OAc)_8$ ^[52] was obtained. By varying the kind of acids, and the molecular ratio acid/alkoxide, different clusters were isolated and characterized.

The clusters $Zr_6O_4(OH)_4(OMc)_{12}$ ^[53] and $Zr_4O_2(OMc)_{12}$ ^[53] were formed in the reaction of $Zr(OR)_4$ ($R = ^nPr$ or Bu) with 4 or 7 equivalents methacrylic acid, respectively, while $Zr_6O_4(OH)_4(OMc)_{12}(PrOH)$ ^[54] is formed from the reaction of $Zr(OPr)_4$ with 9 equivalents of methacrylic acid under the same conditions. When $Zr(OPr)_4$ was reacted with 6.5 equivalents of acrylic acid, the cluster $[Zr_6O_4(OH)_4(OAc)_{12}]_2$ ^[54] was obtained, while $Zr_6O_4(OH)_4(OBz)_{12}(PrOH)$ ^[54] is formed from the reaction of $Zr(OPr)_4$ with 20 equivalents of benzoic acid ($BzOH$). The reaction of 1.6 equivalents of methacrylic acid with $Zr(OBu)_4$ lead to formation of $Zr_6O_2(OBu)_{10}(OMc)_{10}$ ^[55] in which only part of the butoxy ligands is replaced by methacrylate ligands. $Zr_6O_2(OMe)_4(OBu)_2(OMc)_{14}$ ^[55] is formed from $Zr(OBu)_4$ and a 7-fold excess of methacrylic acid in the presence of 1 equivalent of (3-methacryloxypropyl)-trimethoxysilane.

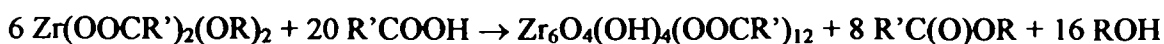
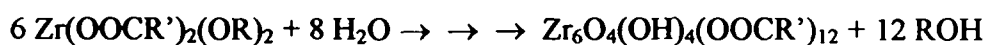
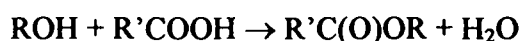
$Zr_{10}O_6(OH)_4(O_2CC_6H_4O)_8(O_2CC_6H_4OH)_8$ ^[56] and $Zr_6O_2(OPr)_{16}(O_2CC_{10}H_6O)_2(PrOH)_2$ ^[56] were obtained when zirconium propoxide was reacted with a 10-fold excess of salicylic acid or 1-hydroxy- β -naphthoic acid, respectively.

Reaction of hafnium alkoxide with methacrylic acid was also used to prepare different types of organically modified hafnium oxo clusters. When hafnium butoxide was reacted with a 4 or 7-fold excess of methacrylic acid, $Hf_4O_2(OMc)_{12}$ or $Hf_6O_4(OH)_4(OMc)_{12}(BuOH)$ ^[57] were obtained, respectively.

Simultaneous reaction of zirconium or titanium alkoxides with methacrylic acid was used to prepare different types of organically substituted mixed modified zirconium-titanium oxo clusters.

Reaction of $Ti(OBu)_4$, $Zr(OBu)_4$ and methacrylic acid in a 1:1:8.5 molar ratio resulted in the formation of $Ti_4Zr_4O_6(OBu)_4(OMc)_{16}$ ^[58], while $Ti_2Zr_4O_4(OBu)_2(OMc)_{14}$ is formed from the reaction of $Ti(OBu)_4$ and $Zr(OBu)_4$ in a 1:2 molar ratio with 4.2 equivalents of methacrylic acid per mol metal alkoxide. $Ti_4Zr_2O_4(OBu)_6(OMc)_{10}$ was obtained when $Ti(OBu)_4$ and $Zr(OPr)_4$ (instead of the butoxide) was reacted with methacrylic acid in a 1:1:8.2 molar ratio^[58], while $Ti_2Zr_6O_6(OMc)_{20}$ ^[58] was obtained when $Ti(OBu)_4$ and $Zr(OBu)_4$ in a 1:3 molar ratio were reacted with 4 equivalents of methacrylic acid per mol metal alkoxide. Mixtures of $Ti(OBu)_4$ and $Hf(OBu)_4$ in 1:1 molar ratio with 9 equivalents of methacrylic acid lead to formation of $Ti_4Hf_4O_6(OBu)_4(OMc)_{16}$ ^[57]. $Ti_2Zr_5HfO_6(OMc)_{20}$ was obtained, when a 1:1:1 mixture of $Ti(OBu)_4$, $Zr(OBu)_4$, and $Hf(OBu)_4$ was reacted with 12.5 molar equivalents of methacrylic acid^[57].

Although the reaction mechanism has not been completely elucidated so far, the following sequence of reaction steps seems to be reasonable for the formation of the carboxylate – substituted metal oxo clusters, with $Zr_6O_4(OH)_4(OOCR)_{12}$ as an example^[56]:



In the first step of this reaction, one or more alkoxide ligands are substituted by carboxylate groups. The alcohol thus liberated then undergoes an esterification reaction. The water produced along with the ester serves to hydrolyze the remaining alkoxide groups and acts as the source of the oxide or hydroxide groups in the cluster. The very slow production of water allows a very controlled growth of the carboxylate-substituted oxometallate clusters^[59]. Size and shape of the structurally well-defined clusters can be controlled by varying the alkoxide / acid ratio, and the kind of alkoxide group in the parent alkoxides.

The formation of the carboxylate-substituted clusters is in fact related to the known tendency of metal alkoxides to form clusters, when they are reacted with the water in a very controlled way. For example, by condensation reaction in the presence of water, many oxo alkoxo clusters of $Ti(OR)_4$ or $Zr(OR)_4$ ($R = Me, Et, Pr^i, Bu^t$), $Ti_7O_4(OEt)_{20}$ ^[60], $Ti_{12}O_{16}(O^iPr)_{16}$ ^[61], $Ti_{16}O_{16}(OEt)_{32}$ ^[62], $Ti_{18}O_{28}H(O^tBu)_{17}$ ^[63], $Ti_3O(O^iPr)_9(OMe)$ ^[64], $Zr_{13}O_8(OMe)_{36}$ ^[65], $Ti_{11}O_{13}(OEt)_5(OPr^j)_{13}$ ^[66], $Ti_{11}O_{13}(OPr^j)_{18}$ ^[67], $Ti_{12}O_{16}(OEt)_6(OPr^j)_{10}$ ^[67,68], $Ti_{17}O_{24}(OPr^i)_{20}$ ^[69] were obtained.

1.4. Metal oxo clusters as co-monomers in polymerization reactions

Sol-gel chemistry provides new approaches for the preparation of hybrid inorganic-organic materials. The basic idea behind the development of inorganic-organic hybrid materials is the combination of inorganic and organic moieties on a molecular scale to achieve a synergetic combination of the properties typical of each of the constituents^[48,70]. The inorganic and organic constituents can be connected with each other by strong covalent or ionic bonds^[5]. There are three approaches to prepare such hybrid materials: (i) Formation from compounds of the type $[(RO)_nM]_xY$ ($Y =$ organic group)^[5,71,72], (ii) Pre-formation of functionalized inorganic building blocks from metal alkoxides followed by polymerization of organic functions attached to the inorganic core^[70,73,74,75], (iii) Formation from bifunctional molecular precursors $(RO)_nM-X-A$ bearing a hydrolysable inorganic group $(RO)_nM$ and an organic functionality (A) capable of undergoing polymerization or crosslinking reactions^[76]. The hybrid polymers are formed by a combination of sol-gel processing and organic

polymerization reactions. For many years metal-organic precursors such as metal alkoxides have been used to produce by hydrolysis-condensation reactions metal oxo-alkoxo species that act as cross-linking reagents for many natural polymers^[77,78,79].

In this work metal oxo clusters of the general formula $M_aO_b(OH/OR)_c(OOCR)_d$ and $M_aO_b(OH/OR)_c(OOCR)_d(OOCR')_e$ were prepared by reaction of metal alkoxides $M(OR)_x$ with functional carboxylic acids, such as methacrylic acid or acrylic acid, or by reaction of metal alkoxides with mixtures of non-functional carboxylic acids ($OOCR'$), such as propionic acid or acetic acid, and functional carboxylic acids ($OOCR$). The reason for preparing this kind of clusters was to incorporate them into organic polymers by copolymerization with organic monomers, such as methyl methacrylic, (meth)acrylic acid or styrene. Small amounts of the clusters were found to efficiently crosslink the organic polymer chain. This results in a controllable swelling behaviour, a higher thermal stability, and modified dielectric properties of the resulting inorganic-organic hybrid polymers^[80,81]. Other factors that influence the material properties of the hybrid polymers are the size and shape of the cluster, the number of polymerizable groups around clusters core, or the ratio monomer : cluster^[82]. The cluster cross-linked polymers were stable at ambient atmosphere even for prolonged time, and their properties did not change^[48].

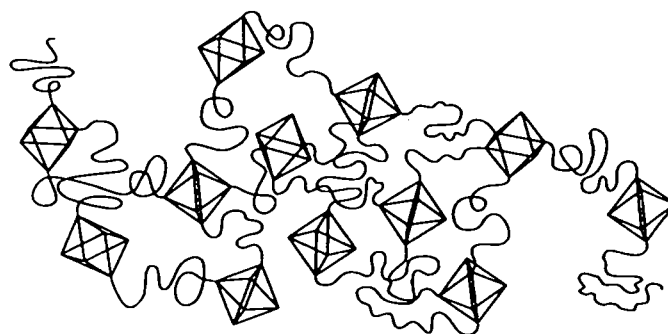


Figure 1. Idealized sketch of the cluster cross-linked polymers.

2 Aim of the Work

One of the major goals in material chemistry is to develop new materials having improved properties. To this aim, metal oxo clusters can be used for the preparation of a new type of inorganic-organic hybrid polymers in which the clusters crosslink the polymer chains and additionally introduce their specific properties. For the latter reason, clusters with different inorganic cores are needed. To control the crosslinking density and some polymer properties related to that (flexibility, swelling in organic solvents, thermal degradation, etc.), variation of the number of polymerisable ligands on the surface of a given clusters is desirable, i.e. clusters of the composition $M_aO_b(OH/OR)_c(OMc)_d(OOCR)_e$ are needed, which contain both non-reactive (OOCR) and polymerisable (OMc) ligands in an easy-to-adjust ratio.

The objective of this work is to answer the following questions:

- How important is the metal alkoxide to carboxylic acid ratio and the kind of the alkoxide group of the parent alkoxide for the size of the formed cluster?
- How does the size and shape of the cluster influence the properties or formation of the new hybrid materials?
- How can clusters be prepared with both functional and non-functional carboxylic ligand?
- Are there possibilities for a partial blocking of surface-bonded polymerisable ligands by chemical reactions at the double bond?

3. Preparation of metal oxo clusters

3.1. Preparation of the mixed-metal oxo clusters

Titanium-yttrium mixed-metal oxo clusters capped by polymerizable methacrylate ligands were prepared by reaction of mixtures of $\text{Ti}(\text{O}^n\text{Pr})_4$ and $\text{Y}(\text{OCH}_2\text{CH}_2\text{OMe})_3$ with methacrylic acid. Only the ratio between the two alkoxides was varied while the metal alkoxide/methacrylic acid ratio was kept constant.

The latter alkoxide, with a decameric ring structure^[83], was employed as a ca. 11% solution in 2-methoxyethanol. The metal alkoxide [$\text{Ti}(\text{OR})_4 + \text{Y}(\text{OME})_3$ ($\text{OME} = \text{OCH}_2\text{CH}_2\text{OMe}$)]/methacrylic acid molar ratio was kept at about 1 : 7 in each experiment, but the $\text{Ti}(\text{OR})_4/\text{Y}(\text{OME})_3$ ratio was varied from 2 : 1 to 3.5 : 1 and 18 : 1. Each precursor mixture resulted in a different metal cluster which was isolated in high yields in each case and structurally characterized by single crystal diffraction. Interestingly, all isolated clusters had the general composition $\text{Ti}_4\text{Y}_2\text{O}_4\text{X}_{14}(\text{HZ})_2$ ($\text{X}, \text{Z} = \text{OMc}$ and/or OME) despite the different Ti/Y ratio in the precursor mixture. The clusters differed by the distribution of X and Z, and by the arrangement of the titanium and yttrium polyhedra as discussed later.

A titanium-hafnium mixed-metal oxo cluster capped by polymerizable methacrylate ligands was prepared by reaction of a mixtures of $\text{Ti}(\text{O}^n\text{Pr})_4$ and $\text{Hf}(\text{O}^n\text{Bu})_4$ with methacrylic acid in a 1 : 1 : 4 ratio. The isolated cluster has the general composition $\text{Hf}_4\text{Ti}_4\text{O}_6(\text{OPr})_4(\text{OMc})_{16}$.

3.1.1. Structure of $\text{Ti}_4\text{Y}_2\text{O}_4(\text{OMc})_{14}(\text{MeOCH}_2\text{CH}_2\text{OH})_2$

The structure of $\text{Ti}_4\text{Y}_2\text{O}_4(\text{OMc})_{14}(\text{MeOCH}_2\text{CH}_2\text{OH})_2$ (1) (Figure 2, Table 1), obtained for a Ti : Y ratio of 3.5, is very similar to that of $\text{Ti}_4\text{Zr}_2\text{O}_4(\text{OBu})_6(\text{OMc})_{10}$ ^[58] (Figure 3).

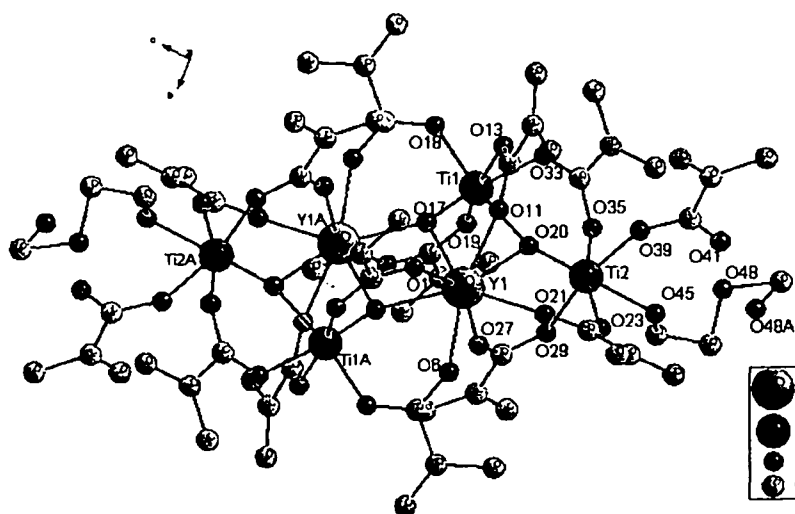
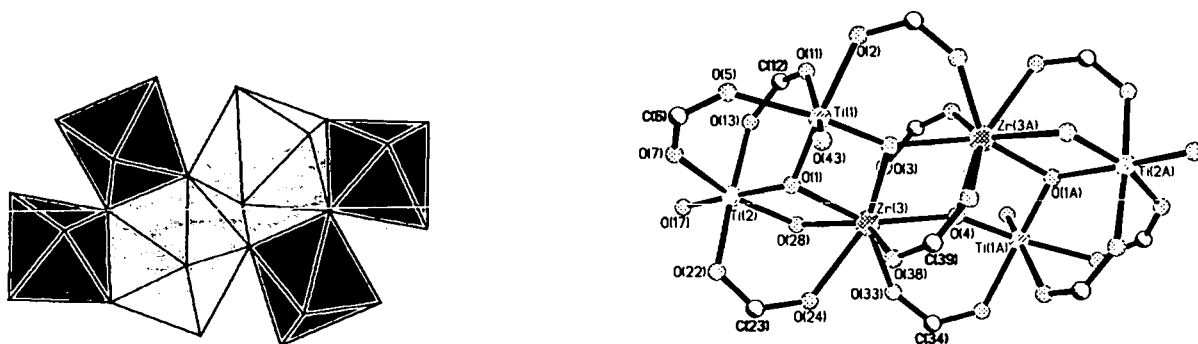


Figure 2. Molecular structure of $\text{Ti}_4\text{Y}_2\text{O}_4(\text{OMc})_{14}(\text{MeOCH}_2\text{CH}_2\text{OH})_2$.

The cluster 1 has the general composition $\text{M}_6\text{O}_4\text{X}_{14}(\text{HZ})_2$. The transition metal atoms build the cluster core and are coordinated by four μ_3 -oxygen atoms, twelve bridging and two chelating methacrylate ligands, as well as two neutral (protonated) methoxyethoxide ligands. The titanium atoms are six-coordinate, whereas the yttrium atoms are surrounded by eight oxygen atoms.

The structural motif of the hexanuclear cluster $\text{Ti}_4\text{Zr}_2\text{O}_4(\text{OBu})_6(\text{OMc})_{10}$ ^[58] is a zigzag chain of two central $[\text{ZrO}_8]$ dodecahedra and two terminal $[\text{TiO}_6]$ tetrahedra. Two additional $[\text{TiO}_6]$ octahedra are condensed to the zirconium atoms of the main chain by a shared edge.

a)



b)

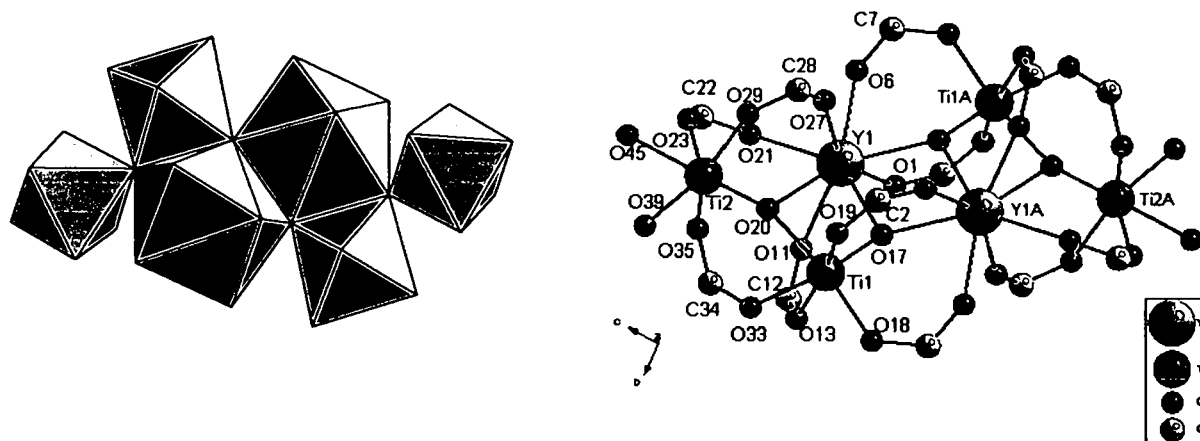


Figure 3. Clusters core and connected polyhedra of $\text{Ti}_4\text{Zr}_2\text{O}_4(\text{OBU})_6(\text{OMc})_{10}$ (a) and $\text{Ti}_4\text{Y}_2\text{O}_4(\text{OMc})_{14}(\text{MeOCH}_2\text{CH}_2\text{OH})_2 / \text{Ti}_4\text{Y}_2\text{O}_4(\text{OMc})_{14}(\text{McOH})_2$ (b). The central polyhedra are eight-coordinated Zr or Y, and the terminal polyhedra six-coordinate Ti.

The central structural motif of **1** is the same zigzag chain as in $\text{Ti}_4\text{Zr}_2\text{O}_4(\text{OBU})_6(\text{OMc})_{10}$ with $[\text{YO}_8]$ instead of $[\text{ZrO}_8]$ dodecahedra. The main structural difference is that the additional $[\text{TiO}_6]$ octahedra are condensed to the main chain via corners.

While the sum of the metal coordination numbers in $\text{Ti}_4\text{Zr}_2\text{O}_4(\text{OBU})_6(\text{OMc})_{10}$ and **1** is the same, the total metal charge in **1** is smaller by two units (Y(III) instead of Zr(IV)). That means that two of the 16 ligands in **1** must be neutral, i.e. must be coordinated in their protonated form. The protonated ligands are clearly identified by comparing the Ti-O and Y-O distances. The Ti-O distance associated with the OME group in **1** [Ti(2)-O(45) 218.0(2) pm] is much longer than comparable Ti-OR distances trans to a μ_3 -oxo ligand (for example, Ti-OPr 180.3(2) in $\text{Ti}_3\text{O}(\text{OPr})_9(\text{OOCPh})_2$ ^[97], 179.3(3) in $\text{Ti}_6\text{O}_4(\text{OEt})_8(\text{OAc})_8$ ^[42], or 178.7(2) in $\text{Ti}_4\text{O}_2(\text{OPr})_6(\text{OMc})_6$ ^[48]). Thus, O(45) trans to the μ_3 -oxo group at Ti(2) is the oxygen atom of

a coordinated alcohol rather than an alkoxide ligand. The alcoholic hydrogen atom at O(45) undergoes an intramolecular hydrogen bridge with the non-coordinated oxygen atom O(41) of the neighboring μ_1 -OMc ligand [O(41)-O(45) 259.4 pm]. The presence of a weakly coordinating ROH ligand also manifests itself in the very short Ti(2)- μ -O(20) distance (173.4(2) pm) (for comparison, Ti- μ_3 -O distances trans to Ti-OR are 185.6(2) in $\text{Ti}_3\text{O}(\text{OPr})_9(\text{OOCPh})_2$, 209.9(1) in $\text{Ti}_6\text{O}_4(\text{OEt})_8(\text{OMc})_8$ and 208.9(2) in $\text{Ti}_4\text{O}_2(\text{OPr})_6(\text{OMc})_6$). Metal-oxygen bond lengths and selected angles are listed in Table 1.

Table 1. Bond lengths [pm] and angles [deg] for $\text{Ti}_4\text{Y}_2\text{O}_4(\text{OMc})_{14}(\text{MeOCH}_2\text{CH}_2\text{OH})_2$
(* = -x+1, -y+1, -z+1).

Y(1)-Ti(1)	333.59(6)	Ti(2)-O(35)	199.3(2)
Y(1)-Ti(1)*	372.62(6)	Ti(2)-O(39)	195.6(2)
Y(1)-Y(1)*	388.16(5)	Ti(2)-O(45)	218.0(2)
Ti(1)-O(13)	198.7(2)	Y(1)-O(1)	229.2(2)
Ti(1)-O(17)	171.9(2)	Y(1)-O(6)	235.4(2)
Ti(1)-O(18)	195.8(2)	Y(1)-O(11)	233.6(2)
Ti(1)-O(19)	201.1(2)	Y(1)-O(17)	233.0(2)
Ti(1)-O(20)	202.3(2)	Y(1)-O(17)*	235.8(2)
Ti(1)-O(33)	212.2(2)	Y(1)-O(20)	250.6(2)
Ti(2)-O(20)	173.4(2)	Y(1)-O(21)	231.6(2)
Ti(2)-O(23)	197.0(2)	Y(1)-O(27)	231.4(2)
Ti(2)-O(29)	198.8(2)		
O(1)-Y(1)-O(27)	148.73(7)	O(13)-Ti(1)-O(19)	165.95(9)
O(21)-Y(1)-O(17)	141.26(7)	O(18)-Ti(1)-O(20)	172.49(8)
O(27)-Y(1)-O(11)	139.52(7)	O(17)-Ti(1)-O(33)	172.38(9)
O(17)-Y(1)-O(6)	144.57(7)	O(23)-Ti(2)-O(35)	165.09(9)
O(11)-Y(1)-O(6)	130.69(7)	O(20)-Ti(2)-O(45)	174.45(9)
O(21)-Y(1)-O(17)*	149.25(7)	Ti(1)-O(17)-Y(1)	110.01(8)
O(11)-Y(1)-O(17)*	130.56(7)	Ti(1)-O(17)-Y(1)*	131.45(9)
O(1)-Y(1)-O(20)	140.29(6)	Y(1)-O(17)-Y(1)*	111.76(7)
O(6)-Y(1)-O(20)	137.31(7)	Ti(2)-O(20)-Ti(1)	136.96(11)
O(17)*-Y(1)-O(20)	121.42(6)	Ti(2)-O(20)-Y(1)	125.48(9)
		Ti(1)-O(20)-Y(1)	94.29(7)

3.1.2. Structure of $\text{Ti}_4\text{Y}_2\text{O}_4(\text{OMc})_{14}(\text{McOH})_2$

$\text{Ti}_4\text{Y}_2\text{O}_4(\text{OMc})_{14}(\text{McOH})_2$ (**2**) was obtained when $\text{Ti}(\text{OPr})_4$ and $\text{Y}(\text{OCH}_2\text{CH}_2\text{OMe})_3$ were reacted in a 18 : 1 ratio.

The structure of **2** (Figure 4, Table 2) is basically the same as that of **1** with coordinated methacrylic acid molecules instead of the coordinated alcohol molecules. This can be rationalized by the smaller concentration of methoxyethanol in the starting mixture due to the low portion of $\text{Y}(\text{OME})_3$.

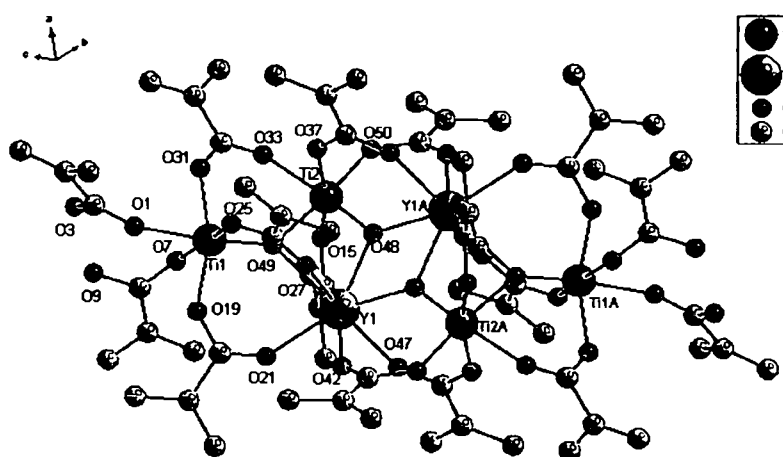


Fig. 4. Molecular structure of $\text{Ti}_4\text{Y}_2\text{O}_4(\text{OMc})_{14}(\text{McOH})_2$.

In the Y/Ti cluster **2**, an (anionic) OMc and a (neutral) HOMc ligand are bonded to the same metal atom. The coordinated methacrylic acid molecules are coordinated via the oxygen atom of their C=O double bond, while the OH hydrogen atom forms a hydrogen bridge to the non-coordinated oxygen atom of the neighboring μ_1 -OMc ligand [O(3)-O(9) 222.1 (11) pm]. The Ti(1)-O(1) distance of the (neutral) methacrylic acid ligand (212.6(2) pm) is clearly longer than that of the (anionic) μ_1 -methacrylate ligand [Ti(1)-O(7) 198.0(3) pm].

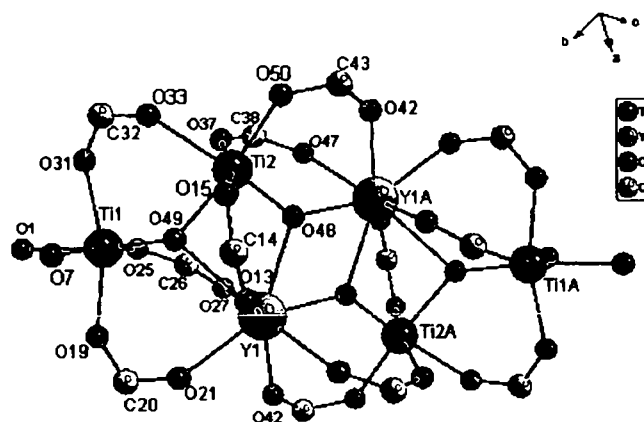


Figure 5. Cluster core of connected titanium, yttrium, oxygen and carbon atoms in $\text{Ti}_4\text{Y}_2\text{O}_4(\text{OMc})_{14}(\text{McOH})_2$.

Table 2. Bond lengths [pm] and angles [deg] for $\text{Ti}_4\text{Y}_2\text{O}_4(\text{OMc})_{14}(\text{McOH})_2$ (2) (* = $-x+1, -y, -z+1$).

Ti(2)-Y(1)	333.85(6)	Ti(2)-O(37)	201.1(2)
Y(1)-Y(1)*	386.35(6)	Ti(2)-O(49)	202.0(2)
Ti(1)-O(1)	212.6(2)	Ti(2)-O(50)	194.6(2)
Ti(1)-O(7)	198.0(3)	Y(1)-O(13)	234.6(2)
Ti(1)-O(19)	198.8(3)	Y(1)-O(21)	228.5(2)
Ti(1)-O(25)	197.4(3)	Y(1)-O(27)	231.3(2)
Ti(1)-O(31)	199.2(3)	Y(1)-O(42)	234.9(2)
Ti(1)-O(49)	173.3(2)	Y(1)-O(47)	228.3(2)
Ti(2)-O(48)	172.0(2)	Y(1)-O(48)	232.0(2)
Ti(2)-O(15)	199.0(3)	Y(1)-O(48)*	235.8(2)
Ti(2)-O(33)	212.7(2)	Y(1)-O(49)	255.1(2)
O(25)-Ti(1)-O(7)	169.58(11)	O(13)-Y(1)-O(48)*	127.15(8)
O(19)-Ti(1)-O(31)	163.52(11)	O(47)-Y(1)-O(49)	143.68(8)
O(49)-Ti(1)-O(1)	174.10(12)	O(42)-Y(1)-O(49)	132.29(8)
O(15)-Ti(2)-O(37)	166.86(10)	O(48)*-Y(1)-O(49)	123.39(7)
O(50)-Ti(2)-O(49)	172.21(10)	Ti(2)-O(48)-Y(1)	110.59(10)
O(48)-Ti(2)-O(33)	173.03(10)	Ti(2)-O(48)-Y(1)*	132.48(11)
O(47)-Y(1)-O(27)	147.33(9)	Y(1)-O(48)-Y(1)*	111.37(8)
O(21)-Y(1)-O(48)	140.14(8)	Ti(1)-O(49)-Ti(2)	137.10(13)
O(27)-Y(1)-O(13)	139.65(8)	Ti(1)-O(49)-Y(1)	125.80(11)

O(48)-Y(1)-O(42)	142.57(9)	Ti(2)-O(49)-Y(1)	93.10(8)
O(13)-Y(1)-O(42)	136.40(9)	C(43)*-O(50)-Ti(2)	130.5(2)
O(21)-Y(1)-O(48)*	149.29(8)		

3.1.3. Structure of $\text{Ti}_4\text{Y}_2\text{O}_4(\text{OMc})_{12}(\text{OCH}_2\text{CH}_2\text{OMe})_2(\text{McOH})_2$

The blueprint of $\text{Ti}_4\text{Y}_2\text{O}_4(\text{OMc})_{12}(\text{OCH}_2\text{CH}_2\text{OMe})_2(\text{McOH})_2$ (**3**) is completely different to that of **1** and **2**, although cluster **3** has the same overall composition as **1**, i.e. clusters **1** and **3** are geometric isomers. The neutral (protonated) ligand in **3** is McOH rather than $\text{HOCH}_2\text{CH}_2\text{OMe}$ in **1**. This shift in protons results in dramatic structural changes. The structure (Figure 6, Table 3) consists of a ring of four corner-sharing $[\text{TiO}_6]$ octahedra to which two $[\text{YO}_8]$ dodecahedra are condensed (Figure 7). This arrangement of the polyhedra implies that only two of the oxo ligands are μ_3 [O(26)], while the other two oxo ligands are μ_2 [O(39)].

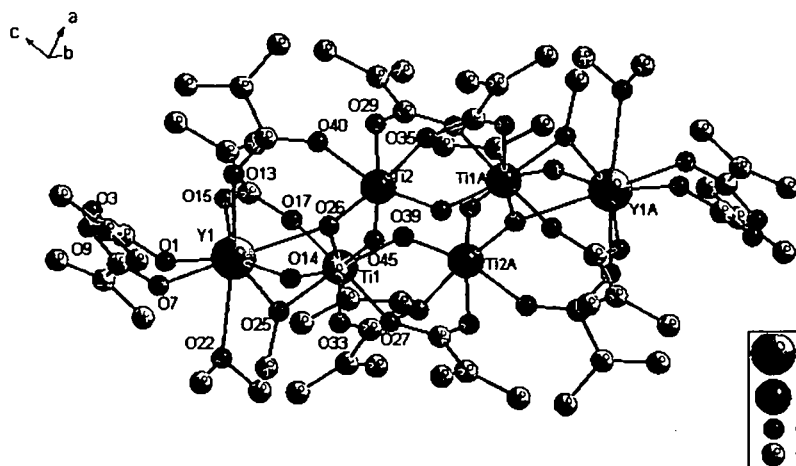


Figure 6. Molecular structure of $\text{Ti}_4\text{Y}_2\text{O}_4(\text{OMc})_{12}(\text{OCH}_2\text{CH}_2\text{OMe})_2(\text{McOH})_2$ (**3**).

However, in **3** both the monodentate OMc and HOMc ligands are bonded to the same yttrium atoms. The methacrylic acid ligands are again coordinated via the oxygen atom of their C=O double bonds, and there is again a hydrogen bridge between the OH hydrogen atom of the methacrylic acid and the non-coordinated oxygen atom of the neighboring μ_1 -OMc ligand [O(3)-O(9) 240.8 pm].

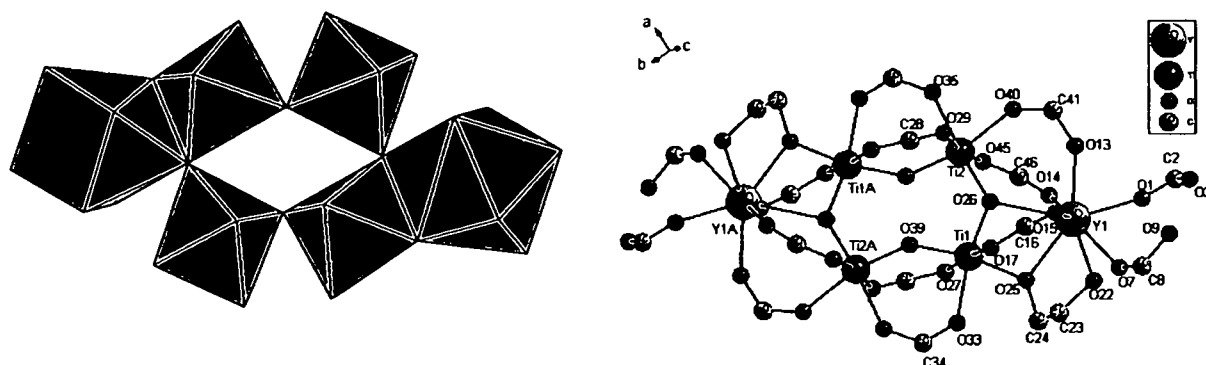


Figure 7. Cluster core and connected polyhedra of $\text{Ti}_4\text{Y}_2\text{O}_4(\text{OMc})_{12}(\text{OCH}_2\text{CH}_2\text{OMe})_2(\text{McOH})_2$ (**3**). The central polyhedra are six-coordinate Ti and the terminal eight-coordinated Y.

Table 3. Bond lengths [pm] and angles [deg] for $\text{Ti}_4\text{Y}_2\text{O}_4(\text{OMc})_{12}(\text{OCH}_2\text{CH}_2\text{OMe})_2(\text{McOH})_2$ (**3**) (* = $-x, -y, -z+1$).

Ti(1)-Ti(2)	338.62(9)	Ti(2)-O(39)	178.1(2)
Y(1)-Ti(1)	338.20(7)	Ti(2)-O(40)	204.6(2)
Y(1)-O(26)	251.9(2)	Ti(2)-O(45)	196.9(3)
Ti(1)-O(17)	197.5(2)	Y(1)-O(1)	228.3(3)
Ti(1)-O(25)	194.2(2)	Y(1)-O(7)	233.4(3)
Ti(1)-O(26)	184.4(2)	Y(1)-O(13)	223.9(3)
Ti(1)-O(27)	204.4(2)	Y(1)-O(14)	232.6(3)
Ti(1)-O(33)	208.2(2)	Y(1)-O(15)	235.4(3)
Ti(1)-O(39)	185.3(2)	Y(1)-O(22)	250.4(3)
Ti(2)-O(26)*	187.3(2)	Y(1)-O(25)	230.1(2)
Ti(2)-O(29)	203.3(3)	Y(1)-O(26)	251.9(2)
Ti(2)-O(35)	207.4(3)		

O(39)-Ti(1)-O(25)	169.27(10)	O(14)-Y(1)-O(15)	142.70(9)
O(17)-Ti(1)-O(27)	174.44(11)	O(13)-Y(1)-O(22)	146.33(10)
O(26)-Ti(1)-O(33)	168.72(10)	O(15)-Y(1)-O(22)	136.14(9)
O(45)-Ti(2)-O(29)	170.67(11)	O(1)-Y(1)-O(26)	148.76(11)
O(39)-Ti(2)-O(40)	165.55(11)	O(7)-Y(1)-O(26)	130.95(10)
O(26)*-Ti(2)-O(35)	173.84(10)	Ti(1)-O(26)-Ti(2)*	131.14(12)
O(13)-Y(1)-O(25)	142.15(9)	Ti(1)-O(26)-Y(1)	100.48(10)
O(1)-Y(1)-O(25)	141.37(10)	Ti(2)*-O(26)-Y(1)	126.29(11)
O(14)-Y(1)-O(7)	145.82(11)	Ti(2)-O(39)-Ti(1)	137.43(13)

Due to two oxo ligands now being μ_2 (rather than μ_3 as in 1 and 2), each $\text{OCH}_2\text{CH}_2\text{OMe}$ ligand in 3 must now occupy three coordination sites. In fact, the alkoxy oxygen atom [O(25)] bridges Ti(1) and Y(1), and the ether oxygen [O(22)] additionally coordinates to Y(1), thus 3 is $\text{Ti}_4\text{Y}_2(\mu_3\text{-O})_2(\mu_2\text{-O})_2(\mu_2\text{-OMc})_{10}(\mu_1\text{-OMc})_2(\mu\text{-OCH}_2\text{CH}_2\text{OMe})_2(\text{McOH})_2$.

3.1.4. Structure of $\text{Hf}_4\text{Ti}_4\text{O}_6(\text{OPr})_4(\text{OMc})_{16}$

The structure of $\text{Hf}_4\text{Ti}_4\text{O}_6(\text{OPr})_4(\text{OMc})_{16}$ (4), prepared by reaction of $\text{Hf}(\text{OBu})_4$ and $\text{Ti}(\text{OPr})_4$ with methacrylic acid in a molar ratio to 1 : 1 : 4, shows a lower degree of condensation of the mixed titan/yttrium clusters and has the general composition $\text{M}_2\text{O}_6\text{X}_{20}$. The cluster 4 (Fig. 8) is isostructural and isomorphous to the cluster $\text{Zr}_4\text{Ti}_4\text{O}_6(\text{OBu})_4(\text{OMc})_{16}$ [58]. The cluster core is formed of metal atoms and six $\mu_3\text{-O}$ atoms [$\text{Hf}_4\text{Ti}_4\text{O}_6$]. Fourteen of sixteen methacrylate ligands are bridging and two chelating. Four terminal propoxide groups coordinate to Ti atoms and complete the structure.

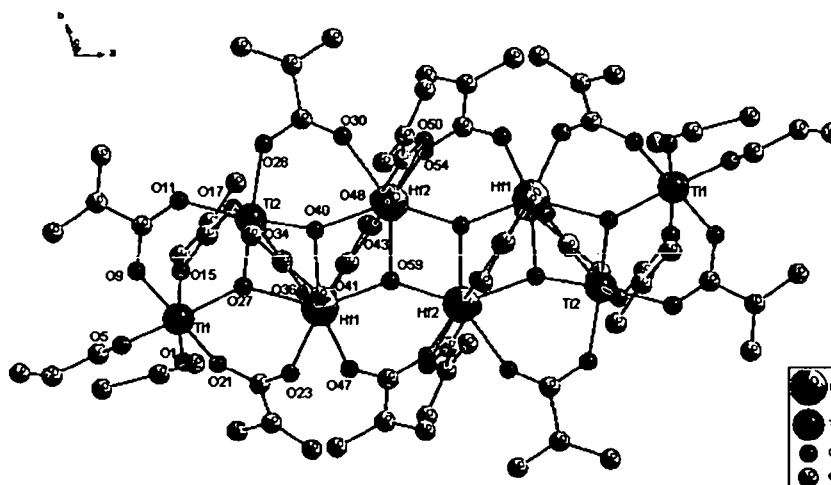


Figure 8. Molecular structure of $\text{Hf}_4\text{Ti}_4\text{O}_4(\text{OPr})_4(\text{OMc})_{16}$.

The structural motif is a zigzag chain formed by four oxo hafnium polyhedra. Edge-sharing $[\text{TiO}_6]$ octahedra terminate the main chain, and there are also additional $[\text{TiO}_6]$ octahedra at the flank of this main chain. The four polyhedra of the zigzag chain are two distorted $[\text{HfO}_7]$ pentagonal bipyramids, adjacent to the terminal $[\text{TiO}_6]$ octahedra and two central $[\text{HfO}_8]$ dodecahedra.



Figure 9. The linkage of the coordination polyhedra in $\text{Hf}_4\text{Ti}_4\text{O}_4(\text{OPr})_4(\text{OMc})_{16}$.

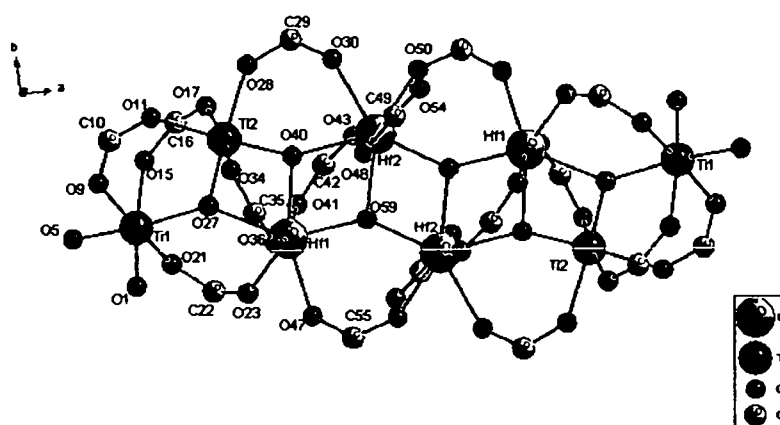


Figure 10. Cluster core of connected titanium, hafnium, oxygen and carbon atoms in $\text{Hf}_2\text{Ti}_4\text{O}_4(\text{OPr})_4(\text{OMc})_{16}$.

Ti(1) is condensed by one μ_3 -oxygen atom [O(27)], three bridging [O(9), O(15) and O(21)] methacrylate ligands and two terminal propoxy ligands [O(1) and O(5)] to the main chain.

Ti(2) is linked by two μ_3 -oxygen atoms [O(27) and O(40)], and four bridging methacrylate ligands [O(11), O(17), O(28) and O(34)].

Three sorts of oxygen donors are bound to Hf(2): three μ_3 -oxygen bridges [O(40), O(59) and O(59A)], three bridging [O(30), O(43) and O(54)] and two chelating [O(48) and O(50)] methacrylate ligands. Two sorts of oxygen donors are bonded to Hf(1): three μ_3 -oxo bridges [O(27), O(40) and O(59A)], and four bridging [O(23), O(36), O(41) and O(47)] methacrylate ligands.

Table 4. Bond lengths [pm] and angles [deg] for $\text{Hf}_2\text{Ti}_4\text{O}_4(\text{OPr})_4(\text{OMc})_{16}$ (4).

Hf(1)-Ti(2)	307.5(2)	Hf(1)-O(47)	212.4(8)
Hf(1)-Hf(2)	346.05(9)	Hf(1)-O(41)	216.3(7)
Ti(1)-O(1)	176.6(11)	Hf(1)-O(40)	212.6(8)
Ti(1)-O(5)	191.5(11)	Hf(1)-O(36)	217.4(8)
Ti(1)-O(9)	196.1(11)	Hf(1)-O(27)	217.4(8)
Ti(1)-O(21)	212.2(9)	Hf(1)-O(23)	200.7(9)
Ti(1)-O(27)	215.6(8)	Hf(2)-O(59)	204.0(7)

3. Preparation of metal oxo clusters

Ti(1)-O(15)	212.4(10)	Hf(2)-O(54)	220.4(10)
Ti(2)-O(40)	179.3(7)	Hf(2)-O(50)	234.4(8)
Ti(2)-O(27)	185.5(8)	Hf(2)-O(48)	221.5(8)
Ti(2)-O(17)	199.4(8)	Hf(2)-O(43)	217.6(7)
Ti(2)-O(28)	204.6(9)	Hf(2)-O(40)	218.1(8)
Ti(2)-O(34)	205.1(8)	Hf(2)-O(30)	212.2(9)
Ti(2)-O(11)	206.1(10)	Hf(1)-O(59)	205.7(7)
O(5)-Ti(1)-O(27)	164.7(5)	O(40)-Hf(2)-O(54)	131.2(3)
O(9)-Ti(1)-O(21)	168.3(4)	O(59)-Hf(2)-O(30)	144.2(3)
O(1)-Ti(1)-O(15)	172.7(5)	O(43)-Hf(2)-O(48)	153.9(3)
O(28)-Ti(2)-O(28)	174.1(4)	O(43)-Hf(2)-O(50)	147.0(3)
O(17)-Ti(2)-O(34)	170.2(4)	Ti(2)-O(27)-Ti(1)	124.1(4)
O(40)-Ti(2)-O(11)	172.4(4)	Ti(2)-O(40)-Hf(1)	103.0(4)
O(47)-Hf(1)-O(40)	146.0(3)	Ti(2)-O(40)-Hf(2)	149.5(4)
O(47)-Hf(1)-O(27)	126.3(3)	Hf(1)*-O(59)-Hf(2)	140.8(4)
O(41)-Hf(1)-O(36)	160.0(3)	Hf(1)-O(40)-Hf(2)	106.9(3)

3.2. Zirconium oxo clusters

New zirconium oxoclusters of the composition $Zr_{12}O_8(OH)_8(OOCR)_{24}$ were prepared by reaction of zirconium alkoxide with propionic acid, acetic acid or dimethylacrylic acid. The same type of the cluster was previously obtained when $Zr(OBu)_4$ was reacted with acrylic acid^[54]. This kind of zirconium oxo clusters has dimeric structures with the same stoichiometry as the cluster $Zr_6O_4(OH)_4(OOCR)_{12}$ ^[53]. $Zr_6O_4(OH)_4(OMc)_{12}$ consists of a $Zr_6O_4(OH)_4$ core in which the faces of the Zr_6 octahedron are capped by μ_3-O and μ_3-OH groups. Three of twelve methacrylate ligands chelate the zirconium atom at one triangular face, while the remaining nine ligands bridge the other edges. The basic structural of $Zr_6O_4(OH)_4(OMc)_{12}$ (Fig. 11) is retained in the sub-units of $Zr_{12}O_8(OH)_8(OOCR)_{24}$. However, two carboxylate ligands that bridge a $Zr - Zr$ edge in $Zr_6O_4(OH)_4(OOCR)_{12}$ change their coordinate made in a way that they bridge two cluster sub-units in the $Zr_{12}O_8(OH)_8(OOCR)_{24}$ cluster.

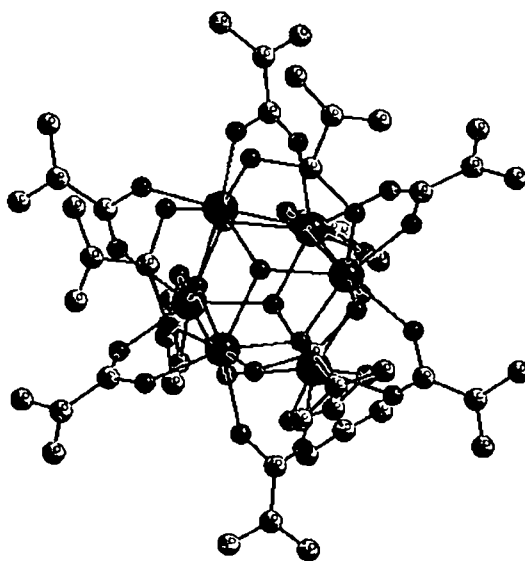


Figure 11. Structure of $Zr_6O_4(OH)_4(OMc)_{12}$

3.2.1. Structure of $Zr_{12}O_8(OH)_8(OProp)_{24} \cdot 6PropOH$

$Zr_{12}O_8(OH)_8(OProp)_{24} \cdot 6PropOH$ (5), (OProp = propionate) was quantitatively formed when a 80 % solution of $Zr(OBu)_4$ in *n*-butanol was reacted with a 10-fold excess of propionic acid (PropOH). When the reaction was repeated with a 2, 4 and 7-fold excess of propionic acid under the same conditions, the same cluster was obtained. The cluster had the same stoichiometry as the methacrylate cluster $Zr_6O_4(OH)_4(OMc)_{12}$ (Fig. 11). The most obvious difference is that in 5 (Fig.12, Table 5), two of the carboxylate ligands opposite the chelated face are no longer edge-bridging as in $Zr_6O_4(OH)_4(OMc)_{12}$ ^[53] but instead linking two cluster units.

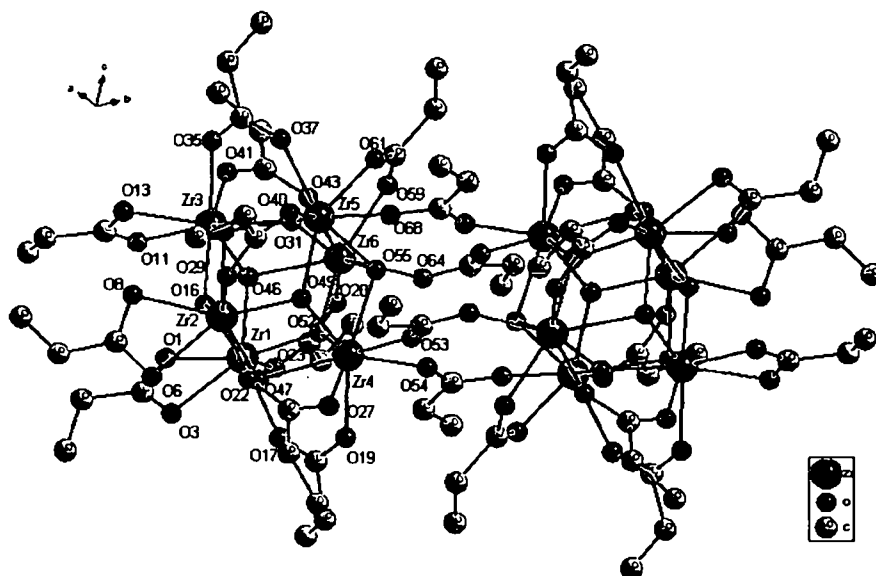


Figure 12. The structure of $[Zr_6O_4(OH)_4(OProp)_{12}]_2 \cdot 6PropOH$ (5). The hydrogen-bonded propionate molecules are omitted for clarity.

The cluster has a crystallographic C_{2h} symmetry. This symmetry leads to following chemically non-equivalent carboxylates: four cluster-bridging-, six chelating- and fourteen edge-bridging carboxylates, i.e. The crystal structure of 5 contains six propionic acid molecules interacting with the cluster via two hydrogen bridges each (Fig. 13). The carbonyl

oxygen is hydrogen bonded to a μ_3 -OH group [O(152)---O(114) 279.4 pm, O(155)---O(90) 278.9 pm, O(162)---O(22) 276.9 pm, O(165)---O(102) 276.7 pm, O(170)---O(8) 275.7 pm, O(176)---O(46) 277.2 pm] and the OH group with an oxygen atom of chelating propionate ligand [O(150)---O(81) 265.8 pm, O(157)---O(71) 271.6 pm, O(160)---O(6) 266.5 pm, O(167)---O(76) 264.6 pm, O(172)---O(34) 275.0 pm, O(175)---O(1) 263.7 pm].

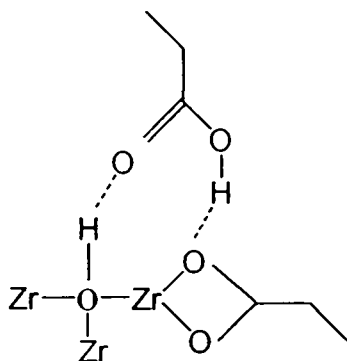
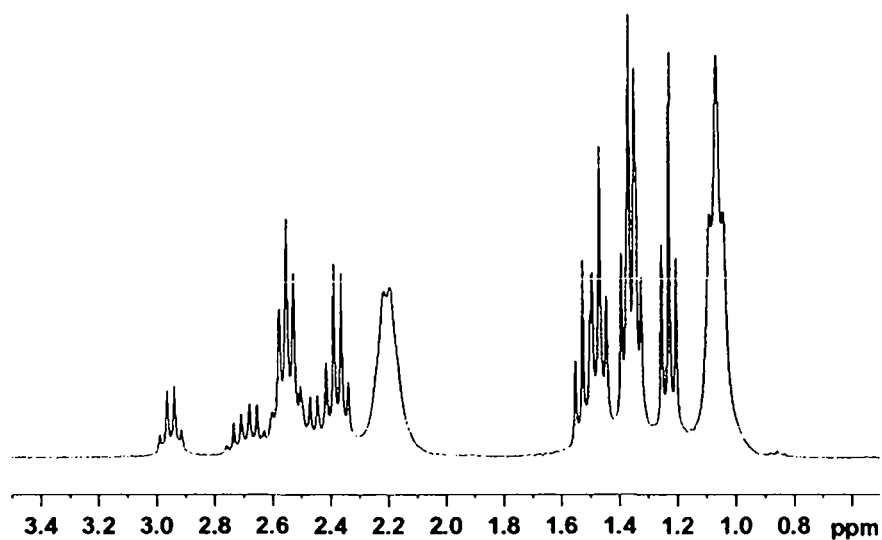


Figure 13. Schematic structure of propionic acid hydrogen bonded to the cluster 5

NMR spectroscopy was carried out to analyse the cluster 5 in solution (Figure 14). The $^1\text{H}/^{13}\text{C}$ -HSQC and COSY spectrum at room temperature shows that only six ligand signals were observed. The $^1\text{H}/^{13}\text{C}$ -HMBC spectrum didn't show long range correlation from protons to the carbonyl carbons. Different to other zirconium oxo clusters (discussed later), the ^1H -NMR spectrum of 5 in room temperature showed sharp signals, which broadened upon cooling the solution to -40°C and below.

Figure 14. ^1H -NMR spectrum of $\text{Zr}_{12}\text{O}_8(\text{OH})_8(\text{OProp})_{24}$ in d_6 -benzene.Table 5. $^1\text{H}/^{13}\text{C}$ chemical shifts [ppm] of the propionate ligands (OProp) of $\text{Zr}_{12}\text{O}_8(\text{OH})_8(\text{OProp})_{24}$ in C_6D_6 at room temperature

	OProp1	OProp2	OProp3	OProp4	OProp5	OProp6
CH_3	1.06/8.5	1.23/9.8	1.35/9.5	1.37/9.5	1.47/9.9	1.49/10.2
CH_2	2.20/28.4	2.36/30.5	2.39/30.5	2.55/30.6	2.69/30.0	2.95/30.2
$\text{C}=\text{O}$	n.o.*	180.2	180.8	179.9	184.3	178.6
$-\text{OH}$	11.96					

* not observed due to mutual exchange

Table 6. Bond lengths [pm] and angles [deg] for $\text{Zr}_{12}\text{O}_8(\text{OH})_8(\text{OProp})_{24} \cdot 6\text{PropOH}$

Zr(1)-O(1)	227,8(8)	Zr(3)-O(40)	203,4(7)
Zr(1)-O(3)	230,1(8)	Zr(3)-O(16)	210,8(8)
Zr(1)-O(17)	219,7(7)	Zr(3)-O(41)	221,9(8)
Zr(1)-O(47)	222,4(8)	Zr(3)-O(34)	222,9(7)
Zr(1)-O(46)	221,6(8)	Zr(3)-O(46)	222,9(7)
Zr(1)-O(52)	205,4(7)	Zr(3)-O(11)	229,0(8)
Zr(1)-Zr(6)	351,4(2)	Zr(4)-O(28)	207,6(7)

Zr(1)-Zr(3)	352,9(2)	Zr(4)-O(52)	207,6(7)
Zr(1)-Zr(4)	347,2(2)	Zr(4)-O(53)	220,2(7)
Zr(2)-O(6)	231,8(7)	Zr(4)-O(27)	223,2(8)
Zr(2)-O(16)	211,2(7)	Zr(4)-Zr(6)	360,9(2)
Zr(2)-O(8)	232,3(7)	Zr(4)-Zr(5)	361,1(2)
Zr(2)-O(28)	203,0(7)	Zr(5)-O(40)	207,6(7)
Zr(2)-O(23)	222,7(7)	Zr(5)-O(28)	211,8(7)
Zr(2)-O(34)	218,8(7)	Zr(5)-O(55)	217,5(7)
Zr(2)-O(22)	221,4(7)	Zr(5)-O(37)	219,0(7)
Zr(2)-Zr(4)	346,6(2)	Zr(5)-O(31)	220,5(8)
Zr(2)-Zr(5)	350,5(2)	Zr(5)-O(59)	222,4(8)
Zr(2)-Zr(3)	352,2(2)	Zr(5)-O(68)	230,0(7)
Zr(5)-O(34)	240,1(7)	Zr(5)-Zr(6)	352,4(2)
Zr(6)-O(40)	205,3(7)	Zr(6)-O(52)	209,5(8)
Zr(6)-O(61)	220,1(8)	Zr(6)-O(46)	238,0(7)
Zr(1)-O(3)-Zr(6)	171,2(2)	Zr(4)-O(53)-Zr(1)	169,3(2)
O(17)-Zr(1)-O(1)	109,2(3)	Zr(6)-Zr(3)-Zr(2)	90,1(4)
Zr(2)-O(8)-Zr(5)	120,9(2)	Zr(3)-O(41)-Zr(5)	109,3(2)
Zr(2)-O(16)-Zr(4)	85,8(2)	Zr(4)-O(28)-Zr(1)	83,5(2)
O(23)-Zr(2)-O(8)	109,4(3)	Zr(4)-O(68)-Zr(2)	94,9(2)
Zr(4)-O(27)-Zr(1)	109,5(2)	Zr(4)-O(27)-Zr(5)	111,2(2)
Zr(4)-O(54)-Zr(1)	112,4(2)	Zr(6)-O(43)-Zr(4)	161,7(2)

3.2.2. Structure of $Zr_{12}O_8(OH)_8(OAc)_{24} \cdot 6AcOH \cdot 7/2 CH_2Cl_2$

Reaction of $Zr(OBu)_4$ (80 % solution in *n*-butanol) in CH_2Cl_2 with a 10 molar ratio of acetic acid (AcOH) led to the formation of $Zr_{12}O_8(OH)_8(OAc)_{24} \cdot 6AcOH \cdot 7/2 CH_2Cl_2$ (**6**). The

cluster (Fig. 15) has the general composition $M_{12}O_8(OH)_8X_{24}$. The zirconium atoms form the cluster core and are surrounded by eight oxygen atoms.

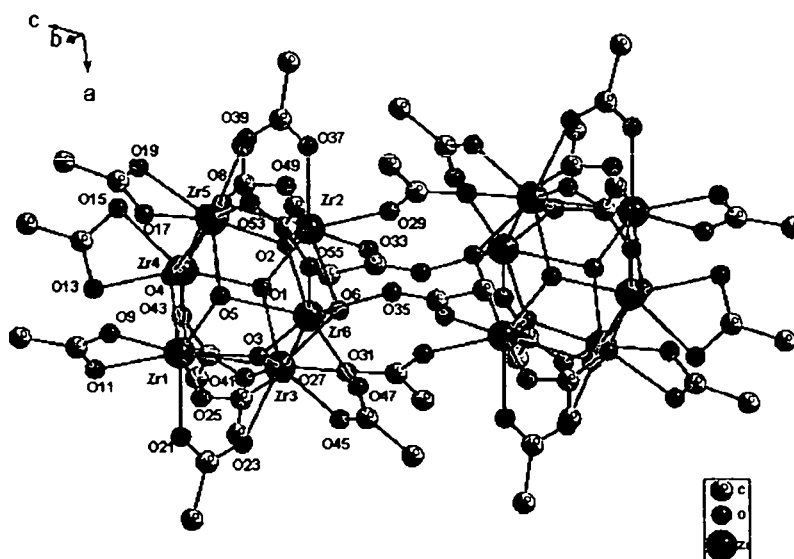


Figure 15. The structure of $Zr_{12}O_8(OH)_8(OAc)_{24}$ (6). The hydrogen-bonded acetate molecules are omitted for clarity.

The Zr-O bond lengths of the cluster-bridging acetate ligands 6 are shorter [Zr-O 217.6(3)-221.5(3) pm] than the bond lengths to the cluster-bridging propionate ligands of 5 [Zr-O 222.2(7)-230.0(7) pm].

The crystal structure of 6 contained strongly disordered dichloromethane molecules and three acid molecules per asymmetric unit which interact with the cluster via two hydrogen bridges. As in the cluster 5, the carbonyl oxygen of the acid in the cluster 6 is hydrogen bonded to a μ_3 -OH group [O(57)—O(5) 273.0 pm, O(61)—O(7) 275.3 pm, O(65)—O(8) 270.8 pm] and the OH group of the acetic acid molecules with an oxygen atom of a chelating acetate ligand [O(59)—O(17) 266.2 pm, O(64)—O(11) 265.7 pm, O(67)—O(15) 265.1 pm]. The bond lengths of hydrogen bonded acetic acid in the cluster 6 [265.1 – 275.3 pm] are shorter than that of hydrogen bonded propionic acid in cluster 5 [263.7 – 279.4 pm].

The dynamic behaviour of compound 6 in toluene was studied by NMR spectroscopy. The 1H and ^{13}C chemical shifts of the acetate ligands at room temperature or at $-40^\circ C$ are given in Table 7 or 8. The proton spectrum at room temperature (Fig. 16) showed five methyl signals of acetate ligands.

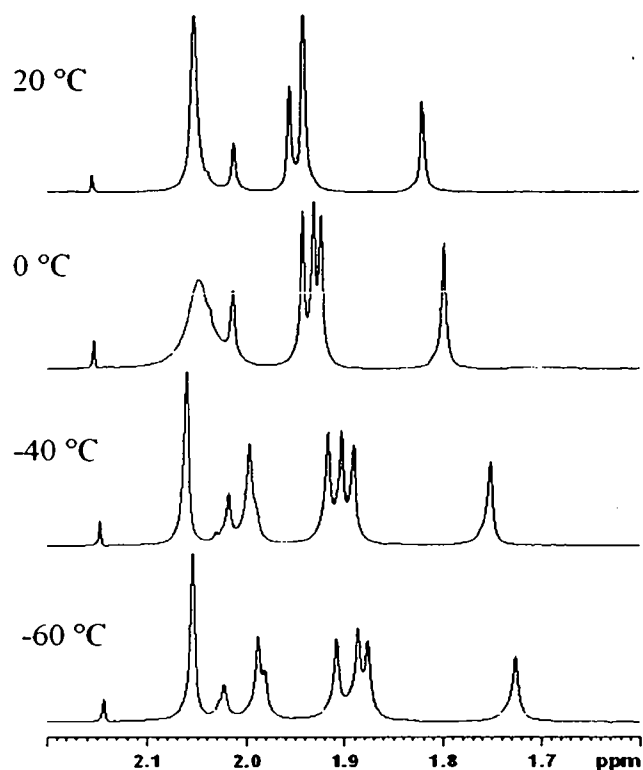


Figure 16. ^1H -NMR spectra of $\text{Zr}_{12}\text{O}_8(\text{OH})_8(\text{OAc})_{24}$ in d_8 -toluene at different temperature.

More signals were obtained at temperature below 0°C . By cooling the solution to -40°C , seven signals of ligands were observed, and a further splitting of the signals are seen. When the solution was further cooled to -60°C nine broad signals were seen and the inversion symmetry of the cluster was broken.

Table 7. $^1\text{H}/^{13}\text{C}$ chemical shifts [ppm] of the acetate ligands (OAc) of **6** in d_8 -toluene at room temperature

	OAc1	OAc2	OAc3	OAc4	OAc5
CH_3	1.82/23.5	1.94/23.8	1.96/23.7	2.01/22.9	2.05/20.9
$\text{C}=\text{O}$	181.0	177.5	176.6	n.o.*	n.o.*
$-\text{OH}$	10.01				

* not observed due to mutual exchange

Table 8. $^1\text{H}/^{13}\text{C}$ chemical shifts [ppm] of the acetate ligands (OAc) of **6** in d_8 -toluene at -40°C

	OAc1	OAc2	OAc3	OAc4	OAc5	OAc6	OAc7
CH ₃	1.75/23.6	1.89/24.1	1.90/23.9	1.92/23.9	1.99/22.8	2.02/23.5	2.06/21.0
C=O	181.1	177.4	177.3	177.5	176.5	175.9	175.9
-OH	11.51						

Table 9. Bond lengths [pm] and angles [deg] for **6**

Zr(1)-O(3)	203,3(3)	Zr(4)-O(43)	220,0(4)
Zr(1)-O(4)	209,5(4)	Zr(5)-O(2)	204,6(3)
Zr(1)-O(7)	221,1(4)	Zr(5)-O(4)	209,2(4)
Zr(1)-O(9)	228,8(4)	Zr(5)-O(5)	219,8(4)
Zr(1)-O(11)	225,3(4)	Zr(5)-O(17)	225,8(4)
Zr(1)-O(25)	219,8(4)	Zr(5)-O(19)	229,6(4)
Zr(2)-O(1)	206,6(4)	Zr(5)-O(39)	221,7(4)
Zr(2)-O(6)	229,3(3)	Zr(6)-O(3)	204,5(4)
Zr(2)-O(8)	230,8(3)	Zr(6)-O(5)	238,2(3)
Zr(2)-O(37)	220,2(4)	Zr(6)-O(27)	221,9(4)
Zr(2)-O(29)	221,5(3)	Zr(6)-O(47)	219,6(4)
Zr(3)-O(1)	208,1(3)	Zr(6)-O(55)	222,9(4)
Zr(3)-O(3)	204,6(3)	Zr(1)-Zr(3)	349,3(7)
Zr(3)-O(6)	230,2(4)	Zr(1)-Zr(5)	350,7(8)
Zr(3)-O(7)	239,6(3)	Zr(1)-Zr(6)	348,8(7)
Zr(3)-O(23)	219,3(4)	Zr(2)-Zr(3)	358,3(7)
Zr(3)-O(31)	217,6(3)	Zr(2)-Zr(4)	346,2(7)
Zr(4)-O(1)	205,6(3)	Zr(2)-Zr(5)	344,8(7)
Zr(4)-O(4)	210,2(4)	Zr(2)-Zr(6)	358,8(7)
Zr(4)-O(7)	219,7(4)	Zr(3)-Zr(4)	349,7(7)
Zr(4)-O(8)	221,0(4)	Zr(3)-Zr(6)	350,8(7)
Zr(4)-O(13)	229,9(4)	Zr(4)-Zr(1)	350,9(7)
Zr(4)-O(15)	225,9(4)	Zr(5)-Zr(6)	349,5(7)

O(3)-Zr(1)-O(9)	152,9(16)	Zr(2)-O(49)-Zr(5)	110,6(9)
O(21)-Zr(1)-O(4)	143,2(15)	Zr(2)-O(33)-Zr(4)	113,1(10)
O(1)-Zr(2)-O(29)	143,9(13)	Zr(3)-O(31)-Zr(4)	120,0(10)
O(6)-Zr(2)-O(37)	140,7(13)	Zr(3)-O(45)-Zr(2)	114,5(10)
O(1)-Zr(3)-O(3)	90,2(14)	Zr(3)-O(23)-Zr(1)	73,5(10)
O(23)-Zr(3)-O(31)	109,3(14)	Zr(3)-O(31)-Zr(6)	116,4(10)
O(1)-Zr(4)-O(15)	148,5(16)	Zr(4)-O(43)-Zr(1)	111,5(10)
O(8)-Zr(4)-O(43)	143,0(14)	Zr(5)-O(39)-Zr(1)	165,8(10)
O(2)-Zr(5)-O(17)	149,5(15)	Zr(5)-O(5)-Zr(2)	100,7(10)
O(8)-Zr(5)-O(53)	141,6(15)	Zr(6)-O(35)-Zr(1)	177,0(9)
O(3)-Zr(6)-O(35)	146,5(13)	Zr(6)-O(47)-Zr(5)	162,7(10)
O(5)-Zr(6)-O(47)	136,8(14)	Zr(1)-O(25)-Zr(3)	109,5(10)
Zr(1)-O(3)-Zr(5)	80,6(11)	Zr(6)-O(55)-Zr(3)	163,2(10)

3.2.3. Structure of $Zr_{12}O_8(OH)_8(OAcMe_2)_{24} \cdot 2Me_2AcOH \cdot BuOH$

$Zr_{12}O_8(OH)_8(OAcMe_2)_{24} \cdot 2Me_2AcOH \cdot BuOH$ (7), was quantitatively formed, when a 80 % solution of $Zr(OBu)_4$ in *n*-butanol was reacted with a 7-fold excess of dimethylacrylic acid (Me_2AcOH), dissolved in *n*-butanol. The X-ray structure analysis showed that the dimethylacrylate derivative is dimeric, i.e., its composition is $Zr_{12}O_8(OH)_8(OAcMe_2)_{24} \cdot 2Me_2AcOH \cdot BuOH$ (Fig. 17).

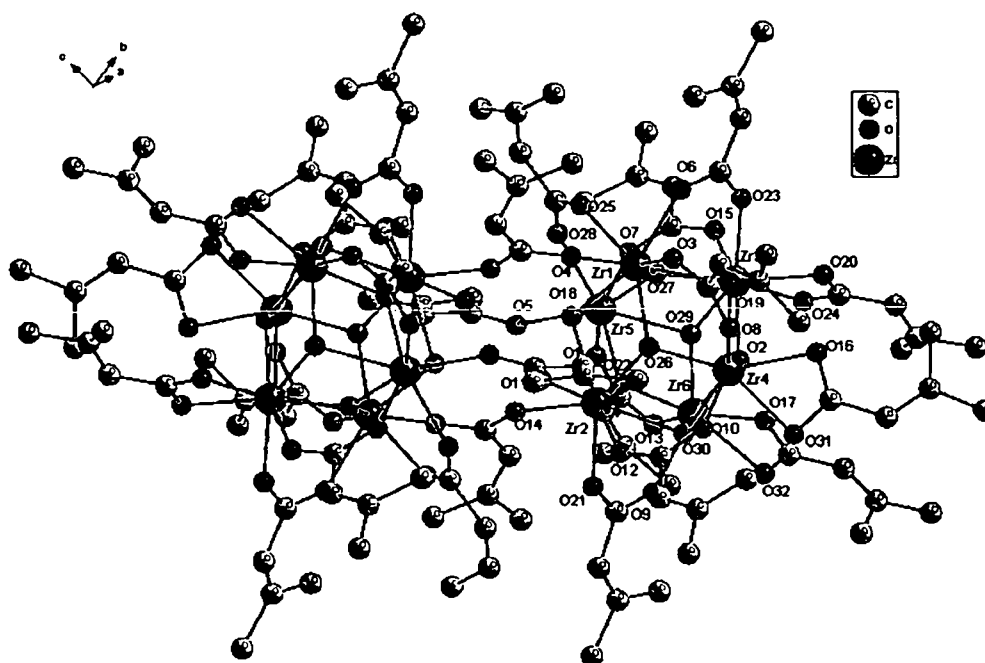


Figure 17. The structure of $Zr_{12}O_8(OH)_8(OAcMe_2)_{24} \cdot 2Me_2AcrOH \cdot BuOH$ (7).

The cluster 7 contains to one butanol molecule bonded through hydrogen-bonds to the cluster core, and two dimethylacrylic acid molecules which are hydrogen-bonded to the cluster units as the acetic acid molecules of 6 or the propionic acid molecules of 5. In the cluster 7 the carbonyl oxygen of dimethylacrylic acid is hydrogen bonded to a μ_3 -OH group [O(33)---O(29) 275.2 pm, O(36)---O(19) 269.3 pm] and the OH group with an oxygen atom of a chelating dimethylacrylate ligand [O(34)---O(17) 262.4 pm, O(37)---O(20) 256.1 pm], while the oxygen of butanol is hydrogen-bonded to a μ_3 -OH group [O(35)---O(30) 273.0 pm] and to an oxygen atom of a chelating dimethylacrylate ligand [O(35)---O(31) 283.3 pm].

The zirconium atoms form the cluster core and are coordinated by eight oxygen atoms. The zirconium atoms triangles are bridged by μ_3 -OH groups with short bonds [Zr-O 219.7(7)-230.1(7) pm] and long bonds [231.5(6)-241.9(7)], and by μ_3 -oxygens [Zr-O 202.8(6)-211.2(7) pm]. The Zr-Zr distances in 7 [346.3(1)-358.3(1) pm] are the same as in $Zr_6O_4(OH)_4(OMe)_{12}(PrOH)$ [346.27(7)-358.02(7) pm]^[54]. The longest Zr-Zr distances in 7 are the non-bridged edges opposite the chelated face. In the clusters $Zr_{12}O_8(OH)_8(OOCR)_{24}$ the shortest Zr-Zr distances are in 6 [344.8(7)-358.8(7) pm], and the longest ones are in 5 [346.6(2)-361.1(2) pm].

The 1H NMR spectrum of cluster 7 in CD_2Cl_2 at room temperature (Fig. 18) shows seven different signal of protons and seven different signals of methyl groups. This is an good

agreement with the symmetry of the cluster. The $^1\text{H}/^{13}\text{C}$ chemical shifts of the carboxylate ligands at room temperature are given in Table 10.

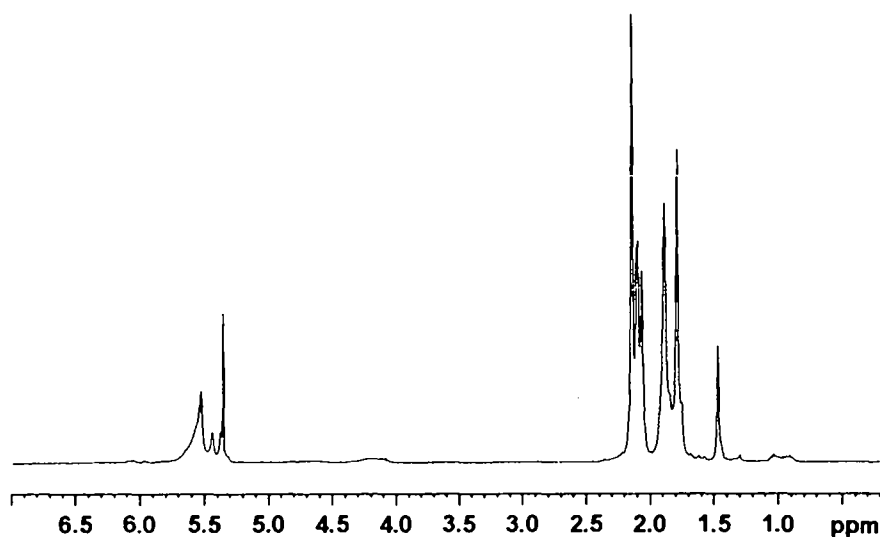


Figure 18. ^1H -NMR spectrum of $\text{Zr}_{12}\text{O}_8(\text{OH})_8(\text{OAcMe}_2)_{24}$ in CD_2Cl_2 at room temperature.

Table 10. $^1\text{H}/^{13}\text{C}$ chemical shifts [ppm] of the dimethylacrylate ligands (OAcMe_2) of 7 in CD_2Cl_2 at room temperature

	OAcMe_21	OAcMe_22	OAcMe_23	OAcMe_24	OAcMe_25	OAcMe_26	OAcMe_27
C^1	171.5	174.3	171.7	n.o.*	n.o.*	n.o.*	n.o.*
C^2	150.7	152.5	157.0	n.o.*	n.o.*	n.o.*	n.o.*
C^3	5.57/	5.56/	5.52/	5.57/	5.53/	5.44/	5.37/
	118.3	120.2	120.5	121.7	121.4	121.9	121.1
C^4	2.1/20.0	2.08/19.9	2.07/20.7	1.92/19.7	1.88/27.0	1.79/27.0	1.47/27.0
-OH	10.63						

^a the labelling of the atoms is as follows: $\text{OOC}^1\text{C}^3\text{HC}^2(\text{C}^4\text{H}_3)_2$
 * not ordered signal protons

Table 11. Bond lengths [pm] and angles [deg] for 7

$\text{Zr}(1)\text{-O}(27)$	205.9(7)	$\text{Zr}(1)\text{-O}(6)$	220.5(7)
$\text{Zr}(1)\text{-O}(26)$	208.6(6)	$\text{Zr}(1)\text{-O}(3)$	220.5(7)
$\text{Zr}(1)\text{-O}(4)$	216.0(7)	$\text{Zr}(1)\text{-O}(25)$	221.3(6)

Zr(1)-O(18) 230.1(7)	Zr(4)-O(26) 207.0(6)
Zr(1)-O(19) 239.5(6)	Zr(4)-O(2) 211.2(7)
Zr(1)-Zr(4) 349.5(1)	Zr(4)-O(19) 219.1(7)
Zr(1)-Zr(3) 349.7(1)	Zr(4)-O(10) 220.7(7)
Zr(1)-Zr(5) 349.7(1)	Zr(4)-O(8) 220.9(7)
Zr(1)-Zr(2) 359.9(1)	Zr(4)-O(30) 223.2(7)
Zr(2)-O(26) 205.3(6)	Zr(4)-O(16) 226.2(7)
Zr(2)-O(22) 208.3(6)	Zr(4)-O(31) 229.0(7)
Zr(2)-O(14) 218.8(7)	Zr(5)-O(27) 204.6(7)
Zr(2)-O(12) 219.8(7)	Zr(5)-O(22) 207.5(6)
Zr(2)-O(21) 223.3(7)	Zr(5)-O(5) 216.2(7)
Zr(2)-O(18) 231.5(6)	Zr(5)-O(28) 219.6(7)
Zr(2)-O(30) 231.6(6)	Zr(5)-O(1) 221.5(8)
Zr(2)-Zr(4) 346.3(1)	Zr(5)-O(18) 228.0(6)
Zr(2)-Zr(6) 347.0(1)	Zr(5)-O(29) 241.9(7)
Zr(2)-Zr(5) 358.3(1)	Zr(5)-Zr(6) 349.9(1)
Zr(3)-O(2) 208.3(7)	Zr(6)-O(22) 204.9(6)
Zr(3)-O(23) 219.1(8)	Zr(6)-O(2) 210.5(7)
Zr(3)-O(15) 221.6(7)	Zr(6)-O(29) 218.3(7)
Zr(3)-O(29) 223.6(7)	Zr(6)-O(9) 219.6(8)
Zr(3)-O(19) 224.7(7)	Zr(6)-O(13) 221.8(7)
Zr(3)-O(20) 227.0(8)	Zr(6)-O(30) 221.9(7)
Zr(3)-O(24) 228.5(8)	Zr(6)-O(32) 231.1(7)
Zr(3)-Zr(5) 350.5(1)	Zr(6)-O(17) 229.0(8)
Zr(3)-Zr(6) 350.7(1)	
O(27)-Zr(1)-O(4) 145.5(2)	Zr(1)-O(25)-Zr(4) 162.57(19)
O(4)-Zr(1)-O(6) 109.2(3)	Zr(1)-O(4)-Zr(3) 176.35(18)
O(26)-Zr(1)-O(25) 144.7(3)	Zr(1)-O(3)-Zr(5) 163.44(18)
Zr(1)-O(6)-Zr(2) 161.9(2)	O(22)-Zr(2)-O(11) 142.8(2)
O(18)-Zr(2)-O(30) 121.9(2)	Zr(2)-O(14)-Zr(4) 169.23(17)
Zr(2)-O(11)-Zr(6) 168.73(17)	O(27)-Zr(3)-O(20) 151.7(3)
Zr(2)-O(21)-Zr(1) 162.32(19)	O(29)-Zr(3)-O(20) 132.2(3)
O(2)-Zr(3)-O(15) 143.2(3)	O(27)-Zr(3)-O(24) 152.1(3)

O(20)-Zr(3)-Zr(1) 120.9(2)	O(5)-Zr(5)-Zr(3) 176.59(19)
Zr(3)-O(20)-Zr(5) 172.4(2)	Zr(5)-O(7)-Zr(2) 162.16(19)
Zr(3)-O(23)-Zr(6) 164.1(2)	O(2)-Zr(6)-O(13) 143.9(3)
O(2)-Zr(4)-O(8) 144.1(3)	O(22)-Zr(6)-O(17) 151.9(3)
O(26)-Zr(4)-O(16) 151.3(3)	O(30)-Zr(6)-O(17) 133.0(3)
Zr(4)-O(16)-Zr(2) 174.8(2)	O(22)-Zr(6)-O(32) 151.7(3)
Zr(4)-O(31)-Zr(1) 171.3(2)	O(29)-Zr(6)-O(32) 131.3(3)
Zr(4)-O(10)-Zr(3) 164.86(18)	Zr(6)-O(17)-Zr(2) 173.3(2)
O(27)-Zr(5)-O(5) 146.2(3)	Zr(6)-O(32)-Zr(5) 171.6(2)
O(5)-Zr(5)-O(29) 143.8(3)	Zr(6)-O(9)-Zr(3) 166.1(2)
Zr(5)-O(28)-Zr(6) 162.63(18)	

3.3. Hafnium oxo cluster

3.3.1. Structure of $\text{Hf}_{12}\text{O}_8(\text{OH})_8(\text{OAc})_{24} \cdot 3\text{AcOH} \cdot 3\text{CH}_2\text{Cl}_2$

Reaction of hafnium butoxide (95% in n-butanol) in CH_2Cl_2 with a 10-fold molar excess of acetic acid (AcOH) led to the formation of $\text{Hf}_{12}\text{O}_8(\text{OH})_8(\text{OAc})_{24} \cdot 3\text{AcOH} \cdot 3\text{CH}_2\text{Cl}_2$ (**8**). The molecular structure of the cluster is the same as that of zirconium oxo clusters of the type $\text{Zr}_{12}\text{O}_8(\text{OH})_8(\text{OOCR})_{24}$, C_{2h} symmetry. The crystal structure of **8** (Fig. 19) contained strongly disordered dichloromethane molecules and three acetic acid per cluster asymmetric unit. Each acetic acid interacts with the cluster via two hydrogen bridges. In the cluster **8**, the carbonyl oxygen is hydrogen bonded to a μ_3 -OH group [O(34)---O(23) 271.2 pm, O(35)---O(15) 272.5 pm, O(38)---O(22) 274.3 pm] and the OH group with an oxygen atom of a chelating acetate ligand [O(33)---O(28) 269.0 pm, O(36)---O(30) 269.8 pm, O(37)---O(25) 267.2 pm].

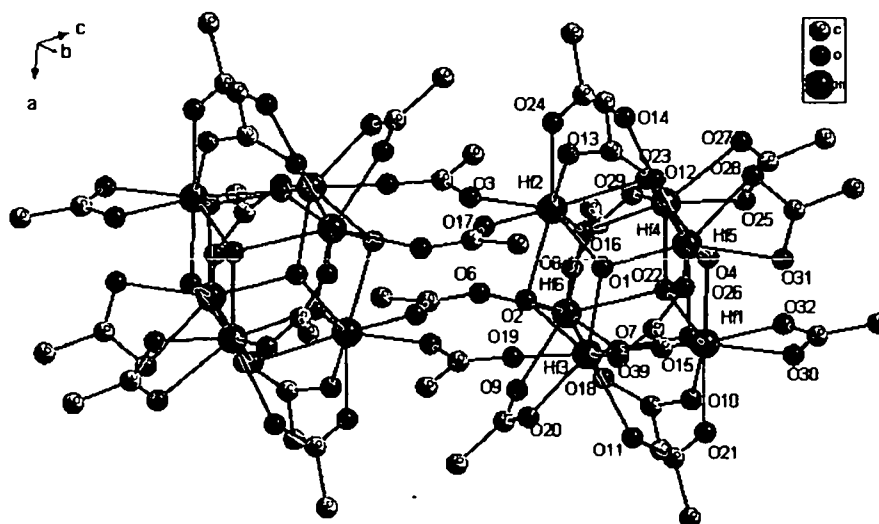


Figure 19. The structure of $\text{Hf}_{12}\text{O}_8(\text{OH})_8(\text{OAc})_{24} \cdot 3\text{AcOH} \cdot 3\text{CH}_2\text{Cl}_2$ (**8**).

The hafnium atoms form the cluster core and are coordinated by eight oxygen atoms. From the bond distances, the Hf(2)/Hf(3)/Hf(6), Hf(2)/Hf(4)/Hf(5), Hf(1)/Hf(3)/Hf(6) and Hf(1)/Hf(4)/Hf(6) triangles are bridged by μ_3 -OH groups [Hf-O 219.4(11)-240.5(11) pm], and the other triangles by μ_3 -oxygens [Hf-O 203.3(10)-209.1(11) pm]. The μ_3 -OH group bridging the face Hf(2)/Hf(3)/Hf(6), i.e., the face opposite the second cluster unit in the dimer is not hydrogen-bonded to an acetate molecule. The Hf-Hf distances in **8** [343.5(10)-357.4(10) pm] are the same as in **6** [344.8(7)-358.8(7) pm]. This finding can be ascribed to the well known resemblances between the two metals. The zirconium and hafnium atoms have a very similar covalent radius, i.e. 1.44 and 1.45 Å respectively.

The similarity of hafnium and zirconium acetate clusters in their structure was also proven by NMR analysis. The ^1H NMR spectrum (Fig.20) of the cluster **8** at room temperature gives five methyl signals as cluster **6**, but two signals are shifted relative to **8**, with the same peak pattern of the both clusters. The $^1\text{H}/^{13}\text{C}$ chemical shifts of the acetate ligands of **8** are given in Table 12.

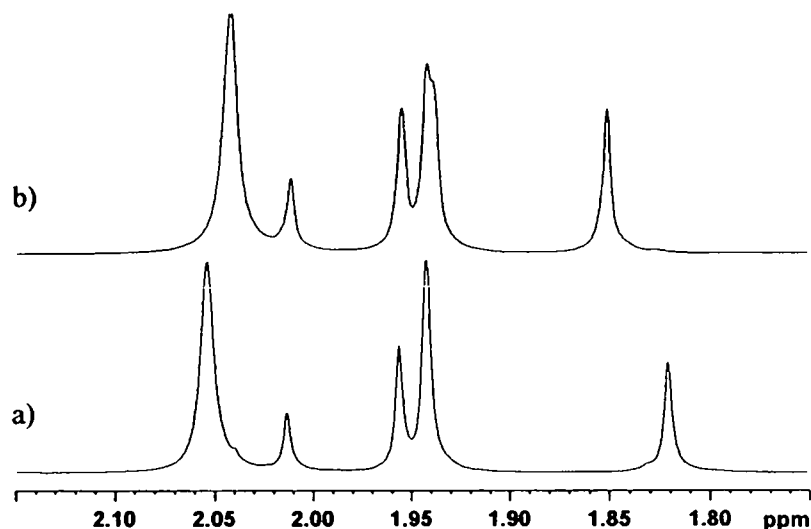


Figure 20. ^1H -NMR spectra of: a) $\text{Zr}_{12}\text{O}_8(\text{OH})_8(\text{OAc})_{24}$ in d_8 -toluene at room temperature and b) $\text{Hf}_{12}\text{O}_8(\text{OH})_8(\text{OAc})_{24}$ in CD_2Cl_2 at room temperature.

Table 12. $^1\text{H}/^{13}\text{C}$ chemical shifts [ppm] of the acetate ligands (OAc) of $\text{Hf}_{12}\text{O}_8(\text{OH})_8(\text{OAc})_{24}$ in CD_2Cl_2 at room temperature

	OAc1	OAc2	OAc3	OAc4	OAc5
CH_3	1.84/23.5	1.94/23.8	2.01/23.0	2.04/21.8	2.04/21.1
$\text{C}=\text{O}$	181.9	177.8	176.7	n.o.*	n.o.*
$-\text{OH}$	10.32				

* not observed due to mutual exchange

Table 13. Bond lengths [pm] and angles [deg] for $\text{Hf}_{12}\text{O}_8(\text{OH})_8(\text{OAc})_{24} \cdot 3\text{AcOH} \cdot 3\text{CH}_2\text{Cl}_2$.

$\text{Hf}(1)-\text{O}(7)$	203.3(10)	$\text{Hf}(2)-\text{O}(24)$	217.5(11)
$\text{Hf}(1)-\text{O}(4)$	209.1(11)	$\text{Hf}(2)-\text{O}(3)$	217.9(11)
$\text{Hf}(1)-\text{O}(10)$	218.5(12)	$\text{Hf}(2)-\text{O}(17)$	218.2(11)
$\text{Hf}(1)-\text{O}(22)$	220.3(11)	$\text{Hf}(2)-\text{O}(13)$	222.8(11)
$\text{Hf}(1)-\text{O}(21)$	220.9(11)	$\text{Hf}(2)-\text{O}(2)$	228.4(10)
$\text{Hf}(1)-\text{O}(15)$	221.6(11)	$\text{Hf}(2)-\text{O}(23)$	230.3(10)
$\text{Hf}(1)-\text{O}(30)$	223.1(12)	$\text{Hf}(2)-\text{Hf}(4)$	343.5(10)
$\text{Hf}(1)-\text{O}(32)$	224.3(12)	$\text{Hf}(2)-\text{Hf}(5)$	344.6(10)

Hf(1)-Hf(6)	347.5(10)	Hf(2)-Hf(3)	356.7(10)
Hf(1)-Hf(3)	348.5(10)	Hf(2)-Hf(6)	357.4(10)
Hf(1)-Hf(5)	348.8(10)	Hf(3)-O(7)	204.8(10)
Hf(2)-O(1)	205.3(10)	Hf(3)-O(1)	208.3(10)
Hf(3)-O(11)	220.4(11)	Hf(5)-O(4)	208.1(11)
Hf(3)-O(39)	221.2(11)	Hf(5)-O(15)	218.8(11)
Hf(3)-O(2)	229.0(10)	Hf(5)-O(23)	219.4(11)
Hf(3)-O(15)	240.5(11)	Hf(5)-O(12)	221.1(12)
Hf(3)-Hf(5)	348.2(9)	Hf(5)-O(28)	222.7(11)
Hf(3)-Hf(6)	349.2(9)	Hf(5)-O(31)	226.8(12)
Hf(4)-O(16)	204.8(10)	Hf(6)-O(7)	203.4(11)
Hf(4)-O(4)	208.9(11)	Hf(6)-O(16)	207.9(10)
Hf(4)-O(29)	219.4(11)	Hf(6)-O(9)	217.7(11)
Hf(4)-O(23)	220.7(11)	Hf(6)-O(18)	218.2(11)
Hf(4)-O(14)	222.0(12)	Hf(6)-O(8)	221.2(11)
Hf(4)-O(25)	223.7(12)	Hf(6)-O(2)	227.5(10)
Hf(4)-O(27)	229.1(11)	Hf(6)-O(22)	238.5(10)
Hf(4)-Hf(6)	347.9(9)	Hf(5)-O(1)	204.9(10)
O(4)-Hf(1)-O(10)	143.1(5)	O(7)-Hf(1)-O(30)	150.0(4)
O(7)-Hf(1)-O(32)	153.0(4)	O(22)-Hf(1)-O(21)	141.8(4)
O(30)-Hf(1)-Hf(6)	175.1(3)	O(22)-Hf(4)-O(27)	130.1(4)
O(32)-Hf(1)-Hf(3)	171.1(3)	O(25)-Hf(4)-Hf(2)	176.1(3)
O(10)-Hf(1)-Hf(5)	164.6(3)	O(3)-Hf(2)-Hf(5)	169.6(3)
O(17)-Hf(2)-Hf(4)	170.8(3)	O(14)-Hf(4)-Hf(1)	165.7(3)
O(1)-Hf(5)-O(28)	148.1(4)	O(15)-Hf(5)-O(12)	143.2(4)
O(3)-Hf(2)-Hf(3)	114.6(3)	O(1)-Hf(5)-O(31)	155.7(4)
O(13)-Hf(2)-Hf(6)	163.1(3)	O(31)-Hf(5)-Hf(2)	168.1(4)
O(7)-Hf(3)-O(19)	145.9(4)	O(28)-Hf(5)-Hf(3)	172.7(3)
O(20)-Hf(3)-Hf(5)	162.7(3)	O(12)-Hf(5)-Hf(1)	165.6(3)
O(19)-Hf(3)-Hf(1)	176.4(3)	O(7)-Hf(6)-O(6)	146.1(4)
O(11)-Hf(3)-Hf(2)	162.6(3)	O(16)-Hf(6)-O(9)	144.3(4)
O(16)-Hf(4)-O(25)	149.3(4)	O(6)-Hf(6)-Hf(1)	176.5(3)

3.4. Yttrium Carboxylates

The chemistry of yttrium carboxylates has not been investigated in detail. Crystals of the anhydrous yttrium and lanthanide (La-Tm) formates have a rhombohedral symmetry, while the hydrates either have a orthorhombic (Y, Ho, Er) or triclinic (Yb, Ln) symmetry^[84,85]. With neutral donor ligands, yttrium (III) formate forms compounds of the type $Y(\text{OOCH})_3 \cdot 2\text{H}_2\text{O}$ or $Y(\text{OOCH})_3 \cdot 1.5\text{NH}_3$ ^[86,87,88], but their structures are little characterized^[89]. $Y(\text{OOCCH}_3)_3 \cdot 4\text{H}_2\text{O}$ has a dimeric structure where the yttrium atoms have a ninefold coordination^[90]. Yttrium atoms are linked by two chelating bridging acetates, by two other chelating acetate groups and two water molecules. The lower carboxylates of yttrium are insoluble in common organic solvents.

3.4.1. Synthesis of $[\text{Y}(\text{OOCR})_3]_n$

$[\text{Y}(\text{OMc})_3]_n$ (**9**) or $[\text{Y}(\text{OAc})_3]_n$ (**10**) were prepared by reaction of a CH_2Cl_2 solution of $\text{Y}(\text{OCH}_2\text{CH}_2\text{OMe})_3$ (15-18 % solution in 2-methoxyethoxide) with a 3-fold excess of methacrylic acid or acetic acid, respectively. In an attempt to obtain a yttrium oxo cluster with carboxylate ligands, such as methacrylate or acetate, the reactions were repeated with an 1- or 10-fold excess of methacrylic acid or acetic acid under the same conditions. However, crystals with the same molecular chain of **9** or **10** were obtained.

The overall structures can thus be viewed as a polymers of MX_3 , and display chain structures (Fig. 21 and 22).

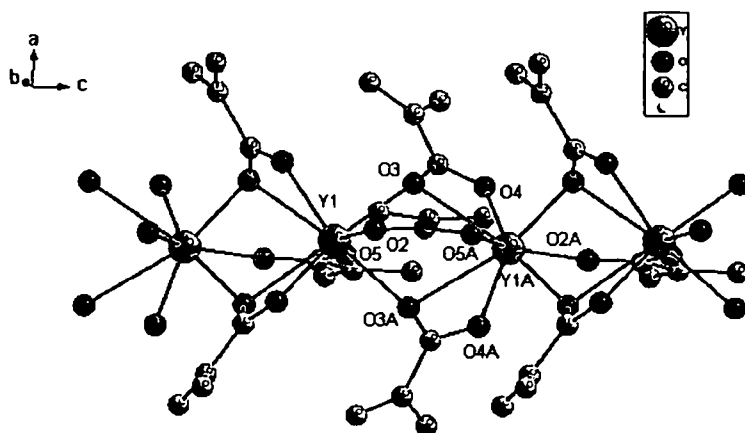


Figure 21. Structure of $[\text{Y}(\text{OMc})_3]_n$ chain.

The **9** and **10** polymers are insoluble in solvents such as benzene, toluene, dichloromethane or chloroform. Characterisation with spectroscopic methods in solution at was not possible.

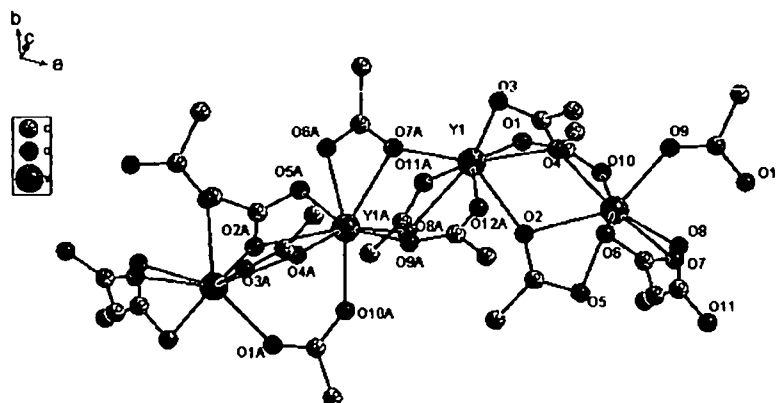


Figure 22. Structure of $[Y(OAc)_3]_n$ chain.

The yttrium atom in the chains of **9** or **10** are surrounded by eight oxygen atoms of two chemically non-equivalent methacrylate or acetate ligands: four bridging-chelating ligands and two bridging ligands (Fig. 23). Metal-metal distances along the chain in **9** are longer [Y(1) – Y(1A) 401.41 pm] than in **10** [Y(1)–Y(1A) 394.98(15) pm]. The angle metal-metal-metal in **9** [Y(1)-Y(1A)-Y(1) 146.1°] is bigger than that in **10** [Y(1A)-Y(1)-Y(1A) 129.05(2)°].

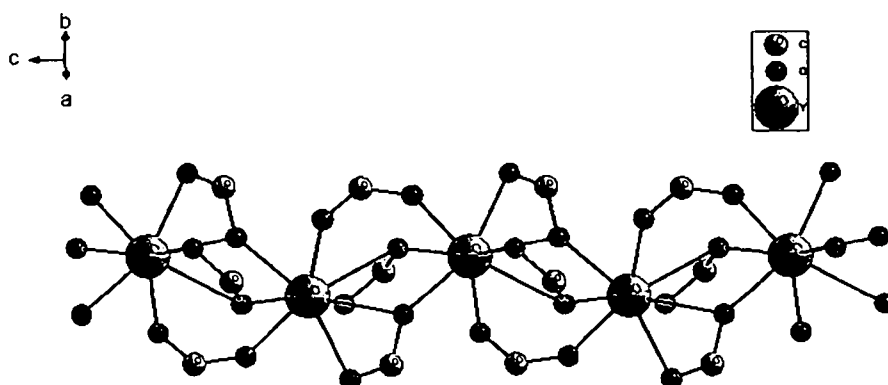


Figure 23. Zig-zag chain of $[Y(OMc)_3]_n$ or $[Y(OAc)_3]_n$. For clarity, the organic groups were omitted.

The geometry of the bridge within the chain is non-planar. The common structural motif of $Y(OOCR)_3$ is a zigzag chain of $[YO_8]$ dodecahedra connected by a shared edge (Fig 24).

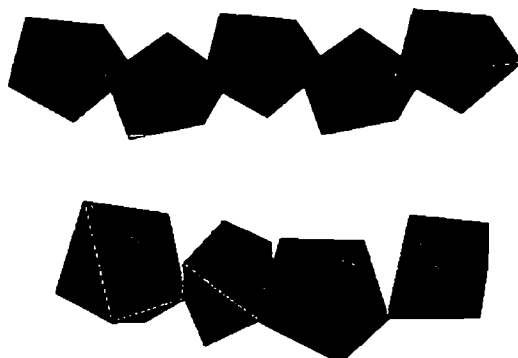


Figure 24. Polyhedra of $[Y(OMc)_3]_n$ (top) and $[Y(OAc)_3]_n$ (bottom) chains.

Metal-oxygen bond lengths and selected angles are listed for **9** in Table 14 and for **10** in Table 15.

Table 14. Bond lengths [pm] and angles [deg] for $[Y(OMc)_3]_n$ (**9**).

Y(1)-O(5)#1	225.80	Y(1)-O(3)#1	267.01
Y(1)-O(2)	225.99	Y(1)-O(3)#3	267.01
Y(1)-O(3)	231.41	Y(1)-Y(1A)#1	401.41
Y(1)-O(3)#2	231.41	Y(1)-Y(1A)#4	401.41
Y(1)-O(4)	231.59	O(3)-Y(1)#4	267.01
Y(1)-O(4)#2	231.59	O(5)-Y(1)#4	225.80
O(5)#1-Y(1)-O(2)	148.9	O(2)-Y(1)-O(3)#1	129.9
O(5)#1-Y(1)-O(3)	77.3	O(3)-Y(1)-O(3)#1	151.0
O(2)-Y(1)-O(3)	78.7	O(3)#2-Y(1)-O(3)#1	101.0
O(2)-Y(1)-O(3)#2	78.7	O(4)-Y(1)-O(3)#1	97.6
O(3)-Y(1)-O(3)#2	77.9	O(4)#2-Y(1)-O(3)#1	50.4
O(5)#1-Y(1)-O(4)	120.6	O(5)#1-Y(1)-O(3)#3	74.3
O(2)-Y(1)-O(4)	79.5	O(2)-Y(1)-O(3)#3	129.9
O(3)-Y(1)-O(4)	92.0	O(3)-Y(1)-O(3)#3	101.0

O(3)#2-Y(1)-O(4)	157.4	O(3)#2-Y(1)-O(3)#3	151.0
O(5)#1-Y(1)-O(4)#2	120.6	O(4)-Y(1)-O(3)#3	50.4
O(2)-Y(1)-O(4)#2	79.5	O(4)#2-Y(1)-O(3)#3	97.6
O(3)-Y(1)-O(4)#2	157.4	O(3)#1-Y(1)-O(3)#3	66.0
O(3)#2-Y(1)-O(4)#2	92.0	O(5)#1-Y(1)-Y(1)#1	65.4
O(4)-Y(1)-O(4)#2	90.0	O(2)-Y(1)-Y(1)#1	145.6
O(5)#1-Y(1)-O(3)#1	74.3	O(3)#2-Y(1)-Y(1)#1	125.9
O(4)-Y(1)-Y(1)#1	76.4	O(3)-Y(1)-Y(1)#4	39.5
O(3)#1-Y(1)-Y(1)#1	33.4	O(4)-Y(1)-Y(1)#4	124.6
O(5)#1-Y(1)-Y(1)#4	80.7	Y(1)-O(3)-Y(1)#4	107.1
O(2)-Y(1)-Y(1)#4	68.2	Y(1)#1-Y(1)-Y(1)#4	146.1
O(3)#1-Y(1)-Y(1)#4	137.7		

Symmetry transformations used to generate equivalent atoms:

#1 -x,-y,z-1/2 #2 -x,y,z #3 x,-y,z-1/2 #4 -x,-y,z+1/2 #5 x,-y,z+1/2

Table 15. Bond lengths [pm] and angles [deg] for $[Y(OAc)_3]_n$ (10).

Y(1)-O(12)#1	233.4(9)	Y(2)-O(9)	226.4(9)
Y(2)-O(4)	230.7(9)	Y(1)-O(7)#1	237.1(8)
Y(2)-O(8)#2	235.1(9)	Y(2)-O(10)	224.6(10)
Y(1)-O(2)	238.0(9)	Y(2)-O(6)	238.4(10)
Y(1)-O(4)	242.5(9)	Y(1)-O(1)	233.9(8)
Y(1)-O(11)	242.6(9)	Y(2)-O(7)	246.9(8)
Y(1)-O(3)	246.5(8)	Y(2)-O(2)	255.0(9)
Y(1)-O(8)	254.6(10)	Y(1)-Y(1A)#1	399.32(15)
Y(1)-Y(1A)	394.98(15)		
O(12)#1-Y(1)-O(1)	139.1(3)	Y(1A)#1-O(8)-Y(1)	109.2(4)
O(1)-Y(1)-O(7)#1	145.3(3)	Y(1)#2-O(7)-Y(1A)	111.2(3)
O(7)#1-Y(1)-O(2)	135.2(3)	Y(1A)-O(4)-Y(1)	113.1(4)
O(7)#1-Y(1)-O(4)	127.4(3)	Y(1)-O(2)-Y(1A)	106.4(3)
O(12)#1-Y(1)-O(11)	128.5(3)	Y(1)-Y(1A)-Y(1)#2	175.4(4)
O(4)-Y(1)-O(11)	145.0(3)	O(2)-Y(1A)-Y(1)#2	140.3(2)

3. Preparation of metal oxo clusters

O(2)-Y(1)-O(3)	119.2(3)	O(4)-Y(1A)-Y(1)#2	149.4(2)
O(11)-Y(1)-O(3)	150.9(3)	O(10)-Y(1A)-Y(1)#2	110.8(2)
O(1)-Y(1)-O(8)	116.4(3)	O(7)-Y(1A)-Y(1)	144.5(2)
O(4)-Y(1)-O(8)	140.1(3)	O(8)#2-Y(1A)-Y(1)	141.8(2)
O(3)-Y(1)-O(8)	139.0(3)	O(7)-Y(1A)-O(2)	127.8(3)
O(7)#1-Y(1)-Y(1A)	148.3(2)	O(9)-Y(1A)-O(2)	147.9(3)
O(11)-Y(1)-Y(1A)	118.2(2)	O(4)-Y(1A)-O(7)	129.3(3)
O(1)-Y(1)-Y(1A)#1	147.4(2)	O(4)-Y(1A)-O(5)	115.6(3)
O(2)-Y(1)-Y(1A)#1	101.1(2)	O(9)-Y(1A)-O(5)	159.4(3)
O(4)-Y(1)-Y(1A)#1	134.3(2)	O(8)#2-Y(1A)-O(6)	119.5(3)
O(3)-Y(1)-Y(1A)#1	105.9(2)	O(10)-Y(1A)-O(6)	162.1(3)
Y(1)-Y(1A)-Y(1)#1	129.05(2)	O(4)-Y(1A)-O(8)#2	157.4(3)

Symmetry transformations used to generate equivalent atoms: #1 $x-1/2, -y+3/2, z-1/2$

#2 $x+1/2, -y+3/2, z+1/2$

4. Hydrosilylation of $Zr_4O_2(OMc)_{12}$

An attempt was made to reduce the number of polymerizable ligands in $Zr_4O_2(OMc)_{12}$ ^[64,80] (Fig.25) by reducing part of the methacrylate groups through hydrosilylation reactions.

Hydrosilylation allows the formation of a Si-C bond by addition of a Si-H to a double or triple bond. The process of hydrosilylation was used by Agaskar^[91] for preparation of another type of hybrid materials. $[Si_{10}O_{25}][Si(CH_3)_2(CHCH_2)]_{10}$ was allowed to react with a stoichiometric amount of the bifunctional compound $[HSi(CH_3)_2C_6H_4O_{0.5}]_2$ in the presence of a catalyst, $PtCl_2(C_6H_5CN)_2$. In the mixture the two terminal $\equiv SiH$ groups react with the $\equiv SiCH=CH_2$ groups on separate spherosilicate cores.

The kinetics of hydrosilylation reactions and the final products are strongly influenced by the catalyst. The reaction is generally catalyzed by platinum derivatives, among which hexachloroplatinic acid (H_2PtCl_6) and Pt-divinyltetramethyl-disiloxane, also known as Karstedt catalyst^[92], are the most widely used^[93,94,95,96]. Hydrosilylation may be to Markovnikov or anti-Markovnikov (terminal) addition:

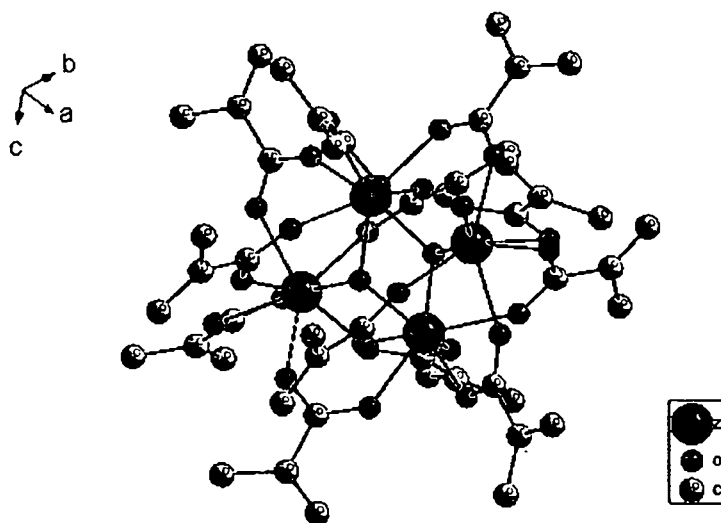


Figure 25. Structure of $Zr_4O_2(OMc)_{12}$

When silanes (HSiEt_3 or HSiPh_3) were reacted with the methacrylate ligands of $\text{Zr}_4\text{O}_2(\text{OMc})_{12}$ in the presence of catalytic amounts of either $\text{Pt}[\text{Si}(\text{CH}_3)_2\text{CH}=\text{CH}_2]_2\text{O}$ or H_2PtCl_6 under various conditions, such as different temperatures and molar ratios, the $\nu_{\text{C}=\text{C}}$ band at 1644 cm^{-1} in the IR spectra (Fig.26) and the Si-H band ($\nu_{\text{Si-H}}$, 2080 cm^{-1}) were consumed.

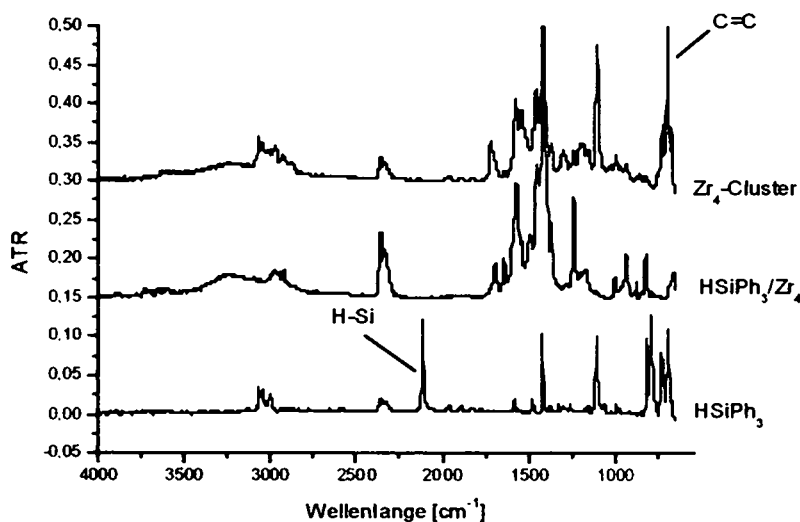


Figure 26. IR-ATR spectra of hydrosilylation reaction of $\text{Zr}_4\text{O}_2(\text{OMc})_{12}$.

Several reactions with an stoichiometric or over-stoichiometric ratio of cluster : HSiPh_3 were carried out. Neither NMR or IR showed that the hydrosilylation reaction took place in one of the reactions mixtures.

A higher reactivity of HSiEt_3 towards $\text{C}=\text{C}$ double bonds was expected, compared to HSiPh_3 , due to steric reasons. Several reactions between $\text{Zr}_4\text{O}_2(\text{OMc})_{12}$ and HSiEt_3 were performed, using different molar ratios of cluster : HSiEt_3 . NMR and IR analysis after reactions indicated only that the cluster decomposed during the reaction.

To investigate the hydrosilylation of $\text{C}=\text{C}$ double bonds of methacrylate ligands of the cluster, some reference reactions were carried out. Methyl methacrylate was allowed to react directly with HSiEt_3 in a stoichiometric molar ratio. Karstedt catalyst was used. A polymeric precipitate was formed from the liquid product after some days. The product were not analysed in detail.

The conditions of some reference reactions for the platinum-catalyzed hydrosilylation of $Zr_4O_2(OMc)_{12}$ are presented in Table 16.

Table 16. Experimental conditions for the hydrosilylation of $Zr_4O_2(OMc)_{12}$.

Conditions time/temp.	Educts	Ratio between Educts	Catalyst
20 h / 65°C	MMA / HSiEt ₃	1 : 1	Pt[Si(CH ₃) ₂ CH=CH ₂] ₂ O
RT	Zr ₄ / Karstedt	4 : 1	Pt[Si(CH ₃) ₂ CH=CH ₂] ₂ O
16 h / 65°C	Zr ₄ / HSiEt ₃	1 : 8	H ₂ PtCl ₆
1 h / RT	Zr ₄ / HSiEt ₃	1 : 1	-
24 h / 65°C	Zr ₄ / HSiEt ₃	1 : 1	Pt[Si(CH ₃) ₂ CH=CH ₂] ₂ O
20 h / 65°C	Zr ₄ / HSiPh ₃	1:10 / 1:12 / 1:20	H ₂ PtCl ₆

The $Zr_4O_2(OMc)_{12}$ cluster was allowed to react directly with Karstedt catalyst in a 4 : 1 molar ratio at room temperature, in order to see whether the cluster was destroyed by the Pt compound. The NMR spectrum (Fig.27) of the product was difficult to interpret. The conclusion is that the Karstedt catalyst does not promote hydrosilylation reactions but reacts with the $Zr_4O_2(OMc)_{12}$ cluster.

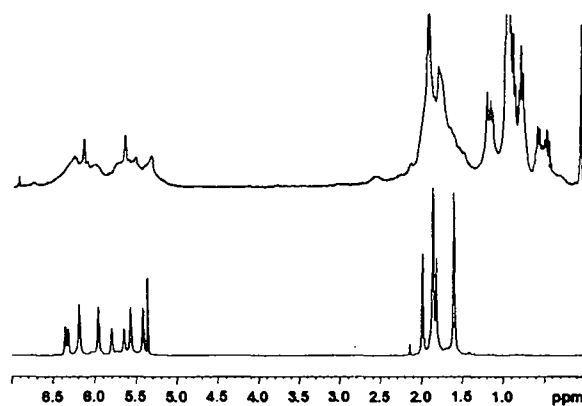


Figure 27. ¹H-NMR spectrum, methylene protons of product $Zr_4O_2(OMc)_{12}$ + Karstedt catalyst at -80°C in C_7D_8 (top), and pure $Zr_4O_2(OMc)_{12}$ at -80°C in CD_2Cl_2 (bottom).

After analysis of the reaction mixture of cluster and silane, given in Table 16, it was not possible to verify how much silane had reacted with the cluster, whether Zr (IV) of the cluster was (partially) reduced to Zr (III), or how many methacrylate were modified by the silane and in which position exactly. For these reasons, an exact interpretation was difficult. Different reactions can apparently take place at the same time, leading to the formation of product mixtures.

5. Ligand exchange of metal oxo clusters

Transition metal oxo clusters with capping organic ligands can be prepared by two strategies. The organic groups can either be grafted to a pre-formed cluster ("surface modification" method) or introduced during the cluster synthesis ("in situ" method). One problem associated with the "surface modification" method is that substitution of reactive groups bonded to the surface metal atoms requires the simultaneous balancing of charges and co-ordination numbers^[3,49]. Substitution of mono-anionic, monodentate groups (OR, OH, etc) by mono-anionic, bidentate ligands (carboxylates, β -diketonates, etc.) therefore requires either rearrangement of the cluster and/or changing the co-ordination mode of bridging groups (e.g. bridging OR or OH to terminal, or μ_3 oxygens to μ_2 oxygens) to make additional co-ordination sites available. The modification of clusters at the surface was carried out by few researchers to exchange alkoxid groups^[60,67,97], for example in $\text{Ti}_{12}\text{O}_{16}(\text{OPr}^i)_{16}$ ^[61], $\text{Ti}_{11}\text{O}_{13}(\text{OPr}^i)_{18}$ ^[67] and $\text{Ti}_{16}\text{O}_{16}(\text{OEt})_{32}$ ^[62]. While some of the alkoxo ligands in large clusters such a $\text{Ti}_{11}\text{O}_{13}(\text{OPr}^i)_{18}$ ^[67] can be replaced by other alkoxo groups, the opposite is true for the exchange of alkoxo groups against carboxylate ligands. When $\text{Ti}_{11}\text{O}_{13}(\text{OPr}^i)_{18}$ was reacted with benzoic acid, complete degradation was observed. The same was observed for $\text{Ti}_{12}\text{O}_{16}(\text{OPr}^i)_{16}$ ^[61].

When $\text{Ti}_{16}\text{O}_{16}(\text{OEt})_{32}$ was reacted with small proportions of carboxylic acids, a fraction of the bridging OEt groups was replaced by bridging carboxylate groups, but the resulting cluster has not been structurally characterized. When a toluene solution of $\text{Ti}_3\text{O}(\text{OPr}^i)_9(\mu_3\text{-OR})$ ^[64] (R = Me or ⁱPr) was reacted with benzoic acid, the new cluster $\text{Ti}_3\text{O}(\text{OPr}^i)_8(\text{OOCPh})_2$ ^[98] was obtained in high yield. One benzoate ligand substitutes a bridging OPr ligand (this substitution preserves both the charge and the coordination numbers), while the second benzoate ligand substitutes the $\mu_3\text{-OR}$ group. Preservation of the overall cluster structure is only possible because one titanium atom changes its coordination number from six to five thus balancing the decreased coordination capability of the ligands.

The formation of $\text{Ti}_6\text{O}_4(\text{OEt})_{14}(\text{OOCPh})_2$ ^[99] upon reaction of $\text{Ti}_7\text{O}_4(\text{OEt})_{20}$ ^[60] with benzoic acid, where the cluster structure is completely re-organized, illustrates the structural problems associated with the exchange of the alkoxide groups for carboxylate.

The exchange of carboxylate ligands for other carboxylates is known from cluster chemistry. For example, exchange of carboxylate ligands, was used for the preparation of $\text{Mn}_{12}\text{O}_{12}(\text{acrylate})_{16}$ from $\text{Mn}_{12}\text{O}_{12}(\text{acetate})_{16}$ ^[100].

The new idea is to control the ratio of functional and non-functional ligands in the clusters by partial exchange.

In this work, the exchange of carboxylate ligands at the surface of metal oxo clusters such as $Zr_4O_2(OMc)_{12}$, $Zr_6O_4(OH)_4(OMc)_{12}$, $Zr_{12}O_8(OH)_8(OProp)_{24}$, and $Zr_{12}O_8(OH)_8(OProp)_6(OMc)_{18}$ was carried out. On the surface of zirconium oxo clusters there is fast ligands intramolecular exchange of non-equivalent ligands, as previously shown by NMR spectroscopic investigations.

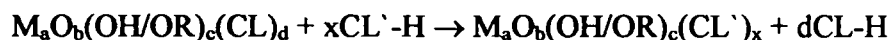
To see whether exchange of methacrylate for other carboxylate ligands is possible, $Zr_4O_2(OMc)_{12}$ was treated with an excess of propionic, isobutyric or acetic acid. The NMR spectra of the reaction products were very difficult to interpret. The treatment of the cluster with an excess of propionic acid lead to one product with a uninterpreted NMR spectrum. Similar results were obtained by reacting the cluster with 400 equivalents of isobutyric acid or acetic acid, respectively.

However, promising results were obtained, when $Zr_6O_4(OH)_4(OMc)_{12}$, $Zr_{12}O_8(OH)_8(OProp)_{24}$, and $Zr_{12}O_8(OH)_8(OProp)_6(OMc)_{18}$ were treated with carboxylic acids such as propionic, isobutyric, methacrylic or acetic acid. Depending on the molar cluster/acid ratio, partial or complete exchange of carboxylate ligands was observed and clusters were obtained with mixed functional and non-functional ligands.

The partial exchange of non-functional carboxylate ligands (CL = acetate, propionate, etc.) for functional carboxylate ligands (CL' = methacrylate, etc.) can be summarized as follows:



The complete exchange of the ligands can be summarized as follows:



5.1. Reaction of $Zr_6O_4(OH)_4(OMc)_{12}$ with isobutyric acid

Crystals of the cluster $Zr_6O_4(OH)_4(OMc)_{12}$ ^[53] (Fig. 11) are obtained by reaction of $Zr(OPr)_4$ or $Zr(OBu)_4$ with four molar equivalents of methacrylic acid. Its structure consists of a Zr_6 octahedron, the triangular faces of which are alternatively capped by μ_3 -O and μ_3 -OH groups. Three of the twelve methacrylate ligands chelate the zirconium atoms of one triangular face, while the other nine ligands bridge the remaining Zr-Zr edges. In the crystal structure of $Zr_6O_4(OH)_4(OMc)_{12}$, the clusters are packed in a way that broad channels parallel to the hexagonal c-axis are formed that contain highly disordered solvate molecules. Owing to the disorder, the nature of the intra-channel molecules could not be identified crystallographically; related studies indicated that hydrogen bridges to the OH groups of the cluster probably play an important role^[54].

The molecular symmetry of $Zr_6O_4(OH)_4(OMc)_{12}$ is C_{3v} , therefore NMR signals for three non-equivalent methacrylate ligands are expected if the symmetry is preserved in solution and ligand conformation is neglected. The ¹H-NMR spectrum of solvate-free $Zr_6O_4(OH)_4(OMc)_{12}$ is shown in Fig. 28a. Five separated signals were observed in the CH₂ region of the spectrum. They were relatively broad due to mutual exchange, which was verified by 2D-EXSY spectra. Successive addition of three molar equivalents of methacrylic acid to a solution of solvate-free $Zr_6O_4(OH)_4(OMc)_{12}$ resulted in a broadening and finally collapsing of the methacrylate ligand signals. The obtained ¹H-NMR spectrum was very similar to the spectrum of the crystalline cluster^[101]. The degenerate exchange between methacrylic acid and $Zr_6O_4(OH)_4(OMc)_{12}$ led to the conclusion that (partial) exchange of the methacrylate ligands against other carboxylates should be possible. This exchange was probed with iso-butyric acid. As a reference for the exchange experiments, $Zr_6O_4(OH)_4(OIsob)_{12}$ (OIsob = iso-butyrate) was prepared by reaction of $Zr(OBu)_4$ with about seven equivalents of iso-butyric acid. To remove the solvate molecules, the compounds were washed with n-heptane, and then dissolved in CH₂Cl₂ and all volatiles were removed in *vacuo*. This process was repeated with toluene and once more with CH₂Cl₂ as the solvent. The obtained solid was dried at room temperature ($\sim 10^{-5}$ mbar).

The cluster $Zr_6O_4(OH)_4(OMc)_{12}$ was first reacted with six molar equivalents of iso-butyric acid in toluene. The NMR spectra of the resulting solid clearly showed that the cluster contains both methacrylate and iso-butyrate ligands. Their ratio was in this case approximately 1:1, that means the cluster with the formula $Zr_6O_4(OH)_4(OMc)_6(OIsob)_6$ was

obtained. Due to the cluster symmetry, two non-equivalent methacrylate ligands and three non-equivalent iso-butyrate ligands were observed at -40°C (Table 17). ROESY spectra at that temperature showed again cross-peaks between the two ligands and therefore their close proximity on the cluster surface.

Table 17. $^1\text{H} / ^{13}\text{C}$ chemical shifts [ppm] of the reaction product of $\text{Zr}_6\text{O}_4(\text{OH})_4(\text{OMc})_{12}$ with six equivalents of iso-butyric acid in CD_2Cl_2 at -40°C .

	OMc1	OMc2	OIsob1	OIsob2	OIsob3
C^1	- / 172.3	n.o.*	- / 182.6	n.o.*	183.0
C^2	- / 139.6	- / 137.8	2.53 / 34.3	2.33 / 35.8	2.34 / 36.7
C^3	6.05, 5.40 / 123.5	6.17, 5.60 / 126.3	1.13 / 18.4	1.10 / 18.7	0.99 / 19.0
C^4	1.86 / 18.0	1.91 / 17.5	-	-	-
-OH	10.86				

The labelling of the atoms is as follows: $\text{OOC}^1\text{C}^2(\text{C}^4\text{H}_3)=\text{C}^3\text{H}_2$ or $\text{OOC}^1\text{C}^2(\text{C}^3\text{H}_3)_2$
 * not observed due to mutual exchange

Treatment of $\text{Zr}_6\text{O}_4(\text{OH})_4(\text{OMc})_{12}$ with a large excess of iso-butyric acid led to nearly complete exchange of the methacrylate ligands. The ^1H -NMR spectrum of the reaction product in CD_2Cl_2 at room temperature (Fig. 28b) shows the same number of inequivalent ligands as $\text{Zr}_6\text{O}_4(\text{OH})_4(\text{OMc})_{12}$. At room temperature, only two resolved signal sets of the iso-butyrate ligand were observed. The cluster core remains unchanged, and the symmetry of the reaction product is the same as $\text{Zr}_6\text{O}_4(\text{OH})_4(\text{OMc})_{12}$.

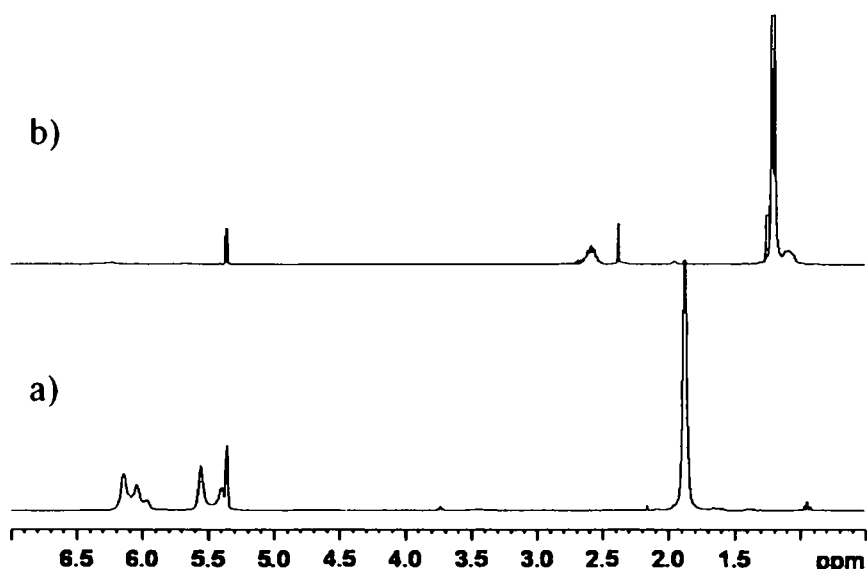


Figure 28. a) ^1H -NMR spectrum of re-crystallised $\text{Zr}_6\text{O}_4(\text{OH})_4(\text{OMc})_{12}$, b) ^1H -NMR spectrum of the reaction product of $\text{Zr}_6\text{O}_4(\text{OH})_4(\text{OMc})_{12}$ with an excess of iso-butyric acid in CD_2Cl_2 at room temperature.

5.2. Reaction of $Zr_6O_4(OH)_4(OMc)_{12}$ with propionic acid

The addition of six equivalents of propionic acid to the cluster $Zr_6O_4(OH)_4(OMc)_{12}$ (Fig. 11) led to a compound with the methacrylate : propionate ratio of approximately 7 : 5, i.e., the approximate composition was $Zr_6O_4(OH)_4(OMc)_7(OOCEt)_5$ (determined by integration of the 1H NMR signals). The 1H and ^{13}C chemical shifts of the carboxylate ligands at $-40^\circ C$ are given in Table 18. Two non-equivalent methacrylate and propionate ligands each were observed at $-40^\circ C$ and again assigned to bridging and chelating positions. The observation of cross-peaks between the $-CH_3$ groups of the propionate ligands (at 0.95 and 1.00 ppm) and the $-CH_3$ (at 1.87 ppm) and $=CH_2$ (at 5.40–6.14 ppm) groups of the methacrylate ligands in the ROESY spectrum (Fig. 29) clearly shows that both types of ligands are neighbouring and therefore bonded to the same cluster.

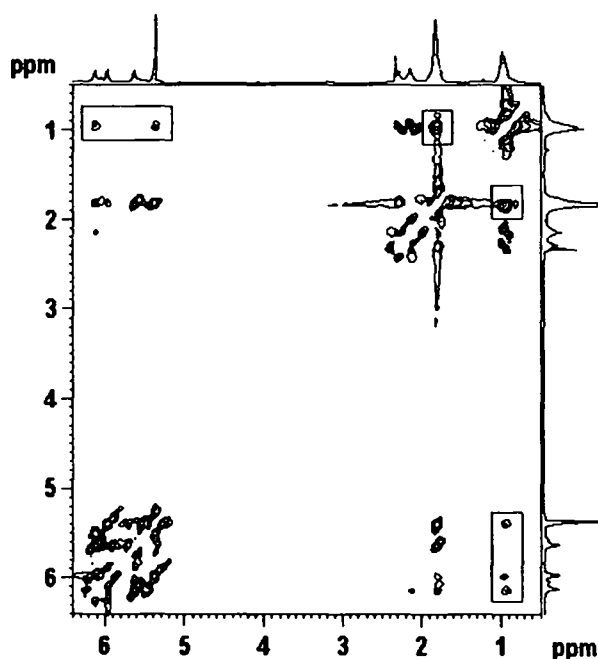


Figure 29. ROESY spectrum of the reaction product of $Zr_6O_4(OH)_4(OMc)_{12}$ with six equivalents of propionic acid in CH_2Cl_2 at -40° . Crosspeaks between the different kinds of ligands are marked. The other crosspeaks are from the same ligand type.

Table 18. $^1\text{H} / ^{13}\text{C}$ chemical shifts [ppm] of the reaction product of $\text{Zr}_6\text{O}_4(\text{OH})_4(\text{OMc})_{12}$ with six equivalents of propionic acid in CD_2Cl_2 at -40°C

	OMc1	OMc2	OProp1	OProp2
C^1	-172.1	-184.7	-179.1	-193.6
C^2	-139.8	-137.0	2.30/27.2	2.15/29.3
C^3	5.97, 5.36/ 124.2	6.11, 5.50/ 127.4	1.00/8.36	0.95/8.20
C^4	1.83/18.6	1.83/17.2	-	-
-OH	11.70			

The labelling of the atoms is as follows:
 $\text{OOC}^1\text{C}^2(\text{C}^4\text{H}_3)=\text{C}^3\text{H}_2$ or $\text{OOC}^1\text{C}^2\text{H}_2\text{C}^3\text{H}_3$

Treatment of $\text{Zr}_6\text{O}_4(\text{OH})_4(\text{OMc})_{12}$ with a large excess of either propionic acid led to nearly complete exchange of the methacrylate ligands. Figure 30 shows the carbonyl region of the $^1\text{H}/^{13}\text{C}$ HMBC spectra of $\text{Zr}_6\text{O}_4(\text{OH})_4(\text{OMc})_{12}$ and of the reaction product of a treating the cluster with a large excess of propionic acid. Each of the two spectra showed two carbonyl signals at higher field and one carbonyl signal at lower field, which, according to our previous tentative assignment, correspond to bridging and chelating carboxylates. From the signal patterns of the two HMBC spectra it appears that the cluster core and the overall symmetry of both compounds is the same. The ^1H and ^{13}C chemical shifts of the propionate-substituted compound are given in Table 19. The appearance of three sets of signals, corresponding to three non-equivalent propionate ligands, corresponds to the NMR data of $\text{Zr}_6\text{O}_4(\text{OH})_4(\text{OMc})_{12}$.

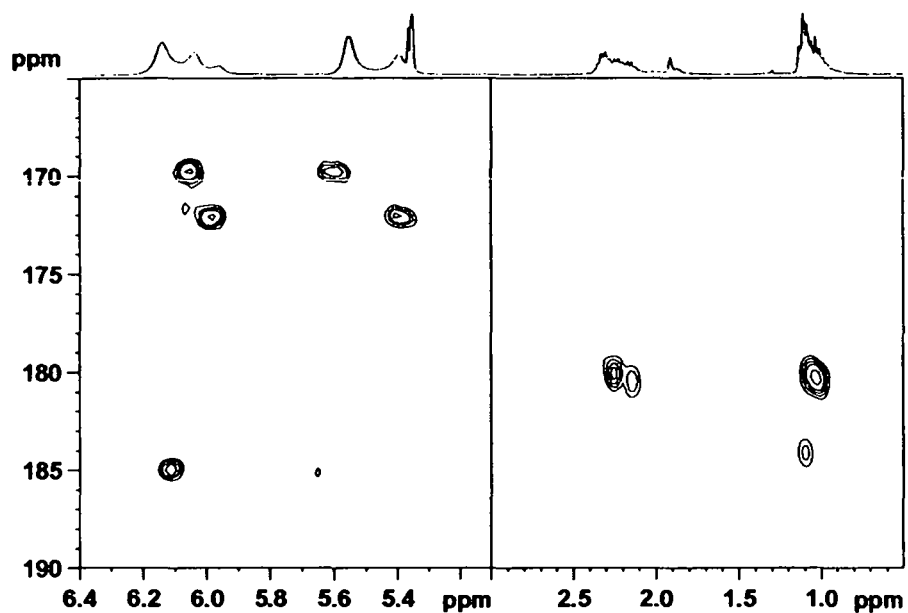


Figure 30. $^1\text{H}/^{13}\text{C}$ HMBC spectra of the carbonyl region of $\text{Zr}_6(\text{OH})_4\text{O}_4(\text{OMc})_{12}$ (left side, room temperature, = CH_2/CO_2 - correlation) and the reaction product of the propionic acid treatment (right side, room temperature, $-\text{CH}_2$ and $-\text{CH}_3/\text{CO}_2$ - correlations).

Table 19. $^1\text{H}/^{13}\text{C}$ chemical shifts [ppm] of the reaction product of $\text{Zr}_6\text{O}_4(\text{OH})_4(\text{OMc})_{12}$ with an excess of propionic acid in CD_2Cl_2 at room temperature

	OProp1	OProp2	OProp3
C^1	- / 179.8	- / 180.3	- / 183.9
C^2	2.24 / 27.9	2.13 / 30.2	2.17 / 30.2
C^3	1.04 / 9.27	1.01 / 9.16	1.09 / 8.43
$-\text{OH}$	11.40		

The labelling of the atoms is as follows: $\text{OOC}^1\text{C}^2\text{H}_2\text{C}^3\text{H}_3$

5.6. Reaction of $Zr_{12}O_8(OH)_8(OProp)_{24}$ with acetic acid

The exchange of the propionate ligands in $Zr_{12}O_8(OH)_8(OProp)_{24}$ (Fig.19) was done by dissolving in CH_2Cl_2 and adding a 400-fold molar amount of acetic acid related to the cluster, i.e. 17-fold related to propionate. This procedure was twice repeated.

The 1H -NMR spectra (Fig. 31) show that there is an exchange between the cluster-bonded propionate ligands and acetic acid in solution, resulting in a propionate : acetate ratio of 1:2, i.e. the composition of the cluster is approximately $Zr_{12}O_8(OH)_8(OProp)_8(OAc)_{16}$ (determined by integration of the 1H NMR signals).

The $^1H/^{13}C$ chemical shifts of the reaction product of $Zr_{12}O_8(OH)_8(OProp)_{24}$ treated with acetic acid at room temperature are given in Table 20.

In the HSQC and HMBC spectra, eight resolved methyl signals were observed. Four were assigned to non-equivalent propionate and four to non-equivalent acetate ligands.

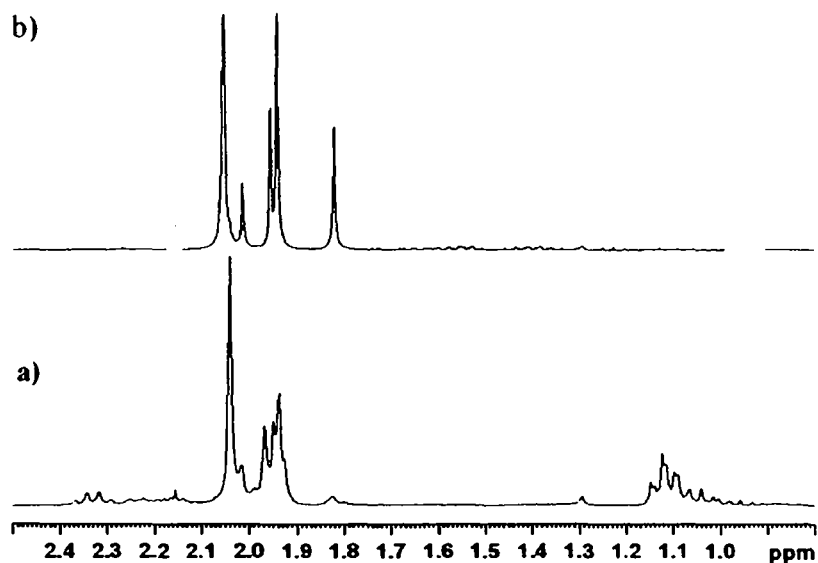


Figure 31. a) 1H -NMR spectrum of the reaction product of $Zr_{12}O_8(OH)_8(OProp)_{24}$ with a 17-fold excess of acetic acid related to propionate in CD_2Cl_2 at room temperature, b) 1H -NMR spectrum of $Zr_{12}O_8(OH)_8(OAc)_{24}$ (in CD_2Cl_2).

Table 20. $^1\text{H}/^{13}\text{C}$ chemical shifts [ppm] of the reaction product of $\text{Zr}_{12}\text{O}_8(\text{OH})_8(\text{OProp})_{24}$ with an 17-fold excess of acetic acid related to propionate in CD_2Cl_2 at room temperature

	OAc1	OAc2	OAc3	OAc4	OProp1	OProp2	OProp3	OProp4
CH_3	1.82/23.6	1.92/23.8	1.96/23.9	2.03/21.4	1.04/9.3	1.12/9.6	1.14/9.6	1.29/29.9
CH_2	-	-	-	-	2.02/29.8	2.14/29.9	2.22/30.2	2.31/28.7
$\text{C}=\text{O}$	181.0	177.5	n.o.*	176.5	179.0	183.9	n.o.*	n.o.*
$-\text{OH}$	10.66							

* not observed due to mutual exchange

The treatment of the cluster with a 600-fold molar excess of acetic acid led to a complete exchange of the carboxylate ligands. From the signal patterns of the NMR spectra it appears that the cluster core and the overall symmetry of both compounds is the same.

5.7. Reaction of $\text{Zr}_{12}\text{O}_8(\text{OH})_8(\text{OProp})_6(\text{OMc})_{18}$ with propionic acid

Crystals of the cluster $\text{Zr}_{12}\text{O}_8(\text{OH})_8(\text{OProp})_6(\text{OMc})_{18} \cdot 6\text{McOH}^{[102]}$ (Fig. 32) are obtained by reaction of $\text{Zr}(\text{OBU})_4$ with two molar equivalents of propionic acid and five molar equivalents of methacrylic acid. The cluster has the same structure and symmetry as the other zirconium oxo clusters of the type $\text{Zr}_{12}\text{O}_8(\text{OH})_8(\text{OOCR})_{24}$ discussed before. Its structure consists of six propionate (four cluster-bridging and two bridging) and eighteen methacrylate ligands (six chelating and twelve bridging).

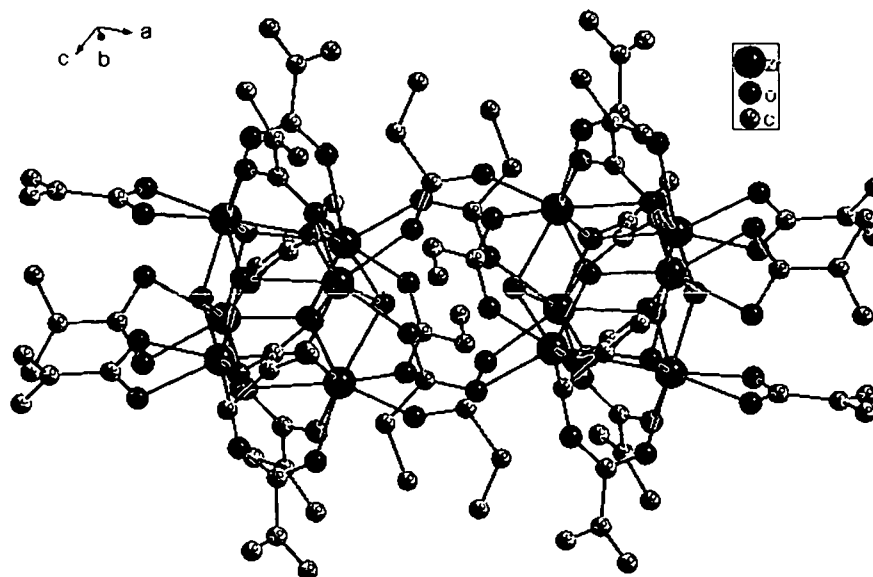


Figure 32. Structure of $Zr_{12}O_8(OH)_8(OProp)_6(OMc)_{18}$

The 1H -NMR spectrum (Fig. 33) of $Zr_{12}O_8(OH)_8(OProp)_6(OMc)_{18}$ in d_8 -toluene at room temperature showed three different methacrylate signals and five different propionate signals. $^1H/^{13}C$ chemical shifts of $Zr_{12}O_8(OH)_8(OProp)_6(OMc)_{18}$ in d_8 -toluene at room temperature are given in Table 21.

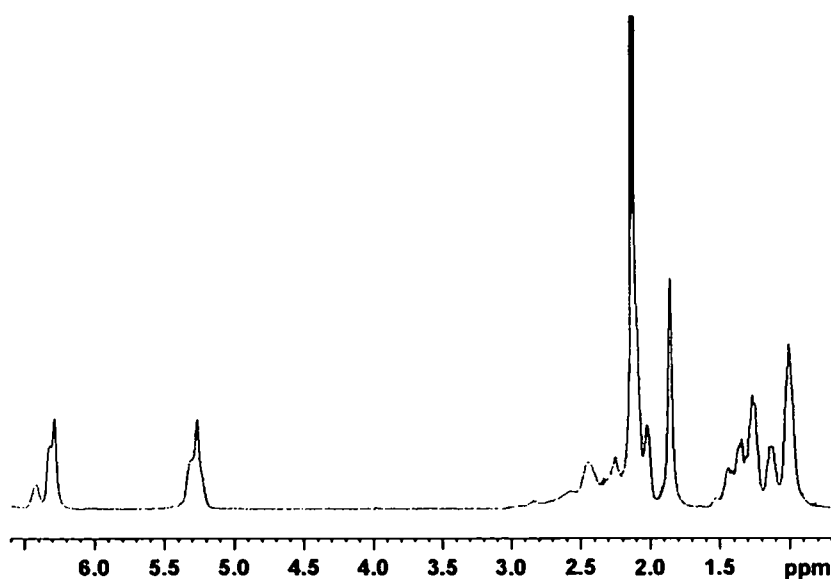
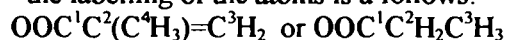


Figure 33. 1H -NMR spectrum of the $Zr_{12}O_8(OH)_8(OProp)_6(OMc)_{18}$ in d_8 -toluene at room temperature.

Table 21. $^1\text{H} / ^{13}\text{C}$ chemical shifts [ppm] of $\text{Zr}_{12}\text{O}_8(\text{OH})_8(\text{OProp})_6(\text{OMc})_{18}$ in C_7D_8 at room temperature

	OMc1	OMc2	OMc3	OProp1	OProp2	OProp3	OProp4	OProp5
C^1	178.3	179.8	184.1	179.8	179.6	178.2	184.2	183.7
C^2	137.5	140.1	139.9	2.11/27.8	2.24/30.2	2.43/30.3	2.57/29.9	2.71/30.2
C^3	6.30, 5.20 /123.1	6.40, 5.29 /123.2	6.26, 5.25 /125.5	0.99/8.3	1.11/9.6	1.24/9.3	1.34/9.7	1.4/9.8
C^4	1.79/18.2	1.86/18.5	1.89/18.4	-	-	-	-	-
-OH	11.70							

^a the labelling of the atoms is as follows:



The intermolecular exchange of carboxylate ligands at the cluster surface against other carboxylates led to the conclusion that the ligand exchange of the mixed carboxylates cluster should be as well possible. This exchange was probed for $\text{Zr}_{12}\text{O}_8(\text{OH})_8(\text{OProp})_6(\text{OMc})_{18}$ with propionic acid. As a reference for this ligand exchange, $\text{Zr}_{12}\text{O}_8(\text{OH})_8(\text{OProp})_{24}$ was prepared by reaction of $\text{Zr}(\text{OBU})_4$ with ten molar equivalent of propionic acid.

The cluster $\text{Zr}_{12}\text{O}_8(\text{OH})_8(\text{OProp})_6(\text{OMc})_{18}$ was reacted with a large excess of propionic acid in CH_2Cl_2 . ^1H -NMR spectra (Fig. 34) showed complete exchange between the cluster-bonded carboxylate ligands and propionic acid in solution. $^1\text{H}/^{13}\text{C}$ -NMR chemical shifts of the propionate compound are given in Table 5.

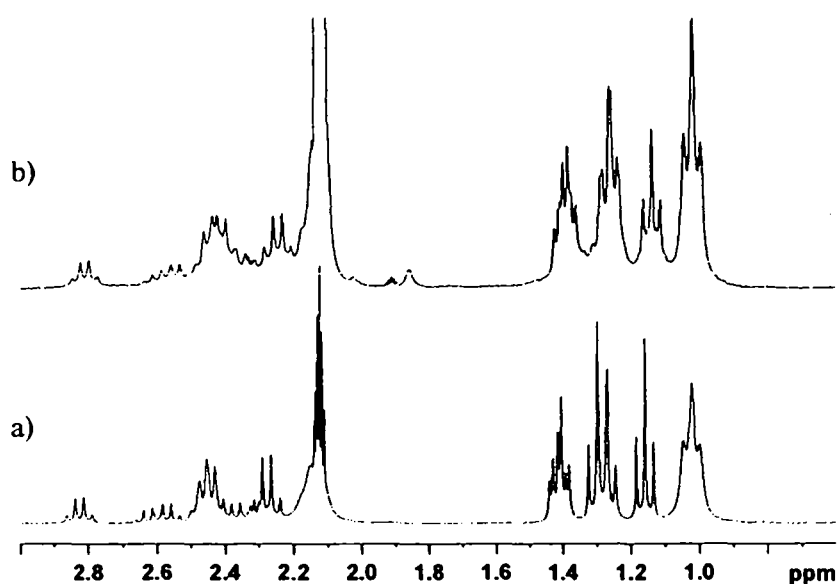


Figure 34. a) $^1\text{H-NMR}$ spectrum of $\text{Zr}_{12}\text{O}_8(\text{OH})_8(\text{OProp})_{24}$ (in C_7D_8), b) $^1\text{H-NMR}$ spectrum of the reaction product of $\text{Zr}_{12}\text{O}_8(\text{OH})_8(\text{OProp})_6(\text{OMc})_{18}$ with an excess of propionic acid in C_7D_8 at room temperature.

The formation of $\text{Zr}_{12}\text{O}_8(\text{OH})_8(\text{OProp})_6(\text{OMc})_{18}$ cluster in solution starting from $\text{Zr}(\text{OBU})_4$, propionic acid and methacrylic acid was followed by NMR spectroscopy. The TOCSY and HMBC spectra (Fig. 35) after 6 h show one signal of the butoxy group at 6.18 ppm, the signals for butyl propionate at 3.93 ppm that correlated to both spectra (TOCSY and HMBC), the signals of the free methacrylic acid at 1.80 ppm and the free propionic acid at 2.19 ppm.

In this experiment one can only observe the formation of butyl propionate, but no butyl methacrylate. This experiment shows that the formation rate of ester from acids plays an important role for the formation of water and thus influences the size and shape of cluster. In conclusion, in the reaction of $\text{Zr}(\text{OR})_4$ with acids, such as propionic or acetic acid, ester formation is fast, and results always in dimeric zirconium clusters of the type $[\text{Zr}_6\text{O}_4(\text{OH})_4(\text{OOCR})_{12}]_2$, while in the reaction of $\text{Zr}(\text{OR})_4$ with acids, such as methacrylic or benzoic acid, the formation of ester is slower and results in the formation of $\text{Zr}_6\text{O}_4(\text{OH})_4(\text{OOCR})_{12}$ but never clusters of the type $\text{Zr}_{12}\text{O}_8(\text{OH})_8(\text{OOCR})_{24}$, except with the mixture with propionic or acetic acid.

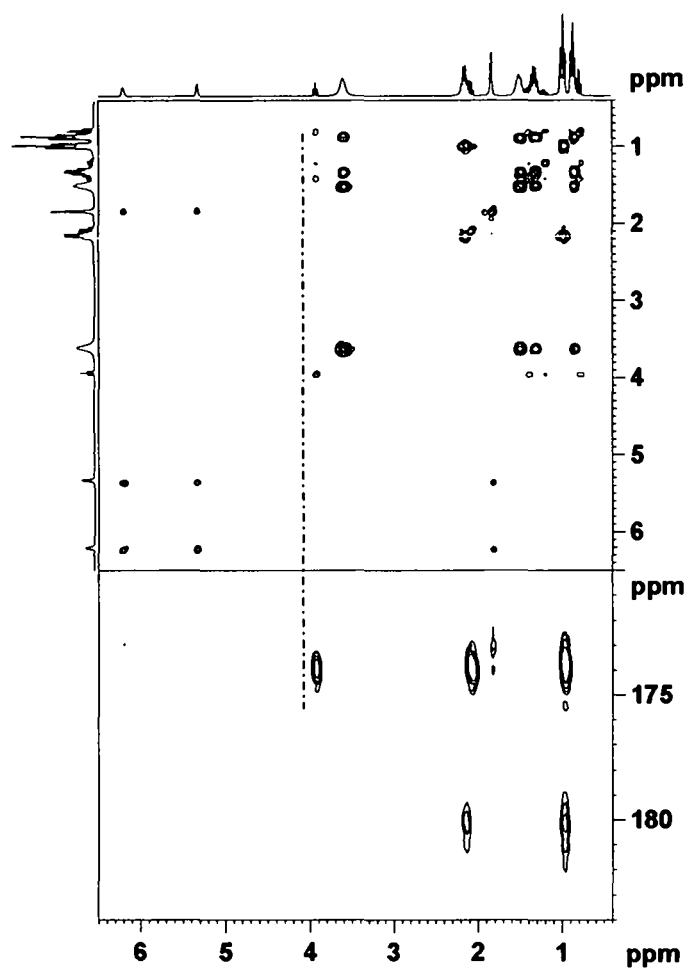


Figure 35. TOCSY spectrum (top) and HMBC spectrum (bottom) of the solvent of $Zr_{12}O_8(OH)_8(OProp)_6(OMc)_{18}$ after 6 h in d_8 -toluene

Zirconium clusters of the type $Zr_6O_4(OH)_4(OOCR)_{12}$ and $Zr_{12}O_8(OH)_8(OOCR)_{24}$ are not through an equilibrium with each other. That is shown by NMR experiments through ligand exchange, as follows:

i) the molecular symmetry of $Zr_6O_4(OH)_4(OMc)_{12}$ is C_{3v} , therefore by NMR at room temperature three signals for three non-equivalent methacrylate ligands were seen [184.7, 169.7 and 171.7 ppm]. After treatment of $Zr_6O_4(OH)_4(OMc)_{12}$ with a large excess of propionic acid $Zr_6O_4(OH)_4(OProp)_{12}$ was obtained. By NMR at room temperature three

signals for three non-equivalent propionate ligands were seen [179.8, 180.3 and 183.9 ppm]. This means that the molecular symmetry of $Zr_6O_4(OH)_4(OProp)_{12}$ is C_{3v} , same as $Zr_6O_4(OH)_4(OMc)_{12}$. Both clusters have the same cluster core $Zr_6O_4(OH)_4$ and the signal peak pattern of ligands after exchange remains unchanged.

ii) zirconium oxo clusters of the type $Zr_{12}O_8(OH)_8(OOCR)_{24}$ have C_{2h} molecular symmetry. From this symmetry, by NMR experiments, seven signals of non-equivalent carboxylate ligands are to expect. But except to $Zr_{12}O_8(OH)_8(OAcMe_2)_{24}$, these signals can be seen only at low temperature, at $-40^\circ C$. After treatment of $Zr_{12}O_8(OH)_8(OProp)_6(OMc)_{18}$ with a large excess of propionic acid $Zr_{12}O_8(OH)_8(OProp)_{24}$ was obtained. By NMR experiments, at $-40^\circ C$ seven signals of seven non-equivalent propionate ligands were seen. That lead to the conclusion that the cluster core $[Zr_{12}O_8(OH)_8]$ and the molecular symmetry after exchange remains unchanged.

6. Inorganic-organic Hybrid Materials

The structurally well-defined metal oxo clusters were used to prepare hybrid materials by the covalent incorporation in organic polymers. Acrylate or methacrylate-substituted tetra- or hexanuclear zirconium, titanium and tantalum oxo clusters [$Zr_4O_2(OMc)_{12}$, $Zr_6O_4(OH)_4(OMc)_{12}$, $Ti_4O_2(OPri)_6(OAc)_6$, $Ti_6O_4(OEt)_8(OMc)_8$, $Ta_4O_4(OEt)_8(OMc)_4$] were polymerized with methyl methacrylate as co-monomers in different molar ratios, where the clusters crosslink the polymer chains very efficiently^[48,103,104]. Hybrid materials were obtained as well by polymerisation of mixed titanium/zirconium oxo clusters [$Ti_2Zr_4O_4(OBu)_2(OMc)_{14}$ or $Ti_4Zr_4O_6(OBu)_4(OMc)_{16}$] with various molar ratios of methacrylic acid or methyl methacrylate as co-monomers^[105].

Poly(methyl methacrylate), PMMA, crosslinked with the titanium / hafnium mixed cluster [$Hf_4Ti_4(OPr)_4(OMc)_{16}$] was prepared in the present work by radical-initiated polymerization, with dibenzoylperoxide as the initiator. Toluene was used as solvent for the reactions. The modified poly(methyl methacrylate) polymers are yellowish glasses. After preparation, they still contained some solvent enclosed in the polymer. The residual amount of solvent was removed by extraction with ethyl acetate, followed by drying at 65°C under reduced pressure. The thermal properties of the synthesized hybrid polymers were investigated by Thermogravimetric Analysis (TGA) and Differential Scanning Calorimetry (DSC). Information about functional groups retained in the polymer matrix were obtained by Infrared Spectroscopy (IR). To verify the cluster proportion on the polymer properties, the swelling behavior of modified PMMA polymers in ethyl acetate was investigated.

6.1. Thermal Behavior

The thermal behavior data of PMMA doped with various amounts of $\text{Hf}_4\text{Ti}_4\text{O}_6(\text{OPr})_4(\text{OMc})_{16}$ (Hf_4Ti_4) as well as that of pure PMMA is shown in Fig. 36 (TGA) and Fig. 37 (DSC).

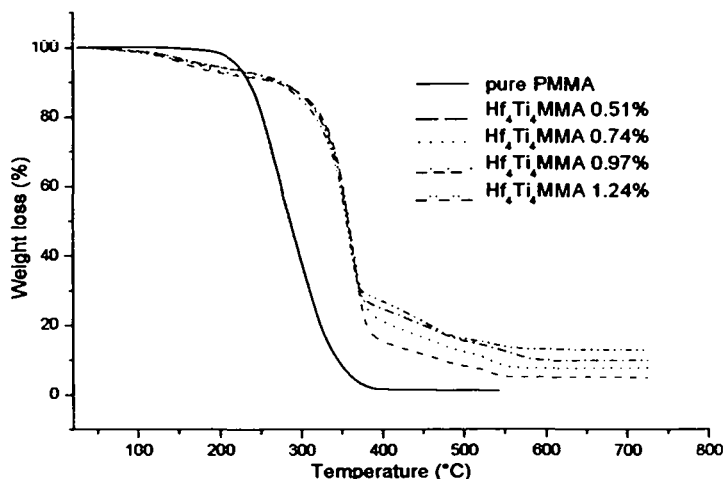


Figure 36. TGA of Hf_4Ti_4 – doped PMMA

Undoped PMMA decomposes above 330°C by depolymerization reactions. All the prepared hybrid materials show an improved thermal stability compared to undoped PMMA prepared under the same conditions. The TGA curves are characterized by two well defined stages. The first weight loss occurs in the temperature range of about 280°C, that corresponds to evaporation of toluene or small oligomers, followed by major thermal degradation in the range 280-550°C. With only 0.51 mol % of added cluster ($\text{Hf}_4\text{Ti}_4\text{MMA}$ 0.51%), the crosslinked polymers no longer depolymerise above 550°C and contain 5.13 wt % $\text{HfO}_2/\text{TiO}_2$. At higher temperatures the polymers are oxidatively degraded. The residual mass corresponds to the theoretical $\text{HfO}_2/\text{TiO}_2$ amount and correlates with the elemental analysis. PMMA doped with 0.74 mol % of cluster ($\text{Hf}_4\text{Ti}_4\text{MMA}$ 0.74%) contains 7.64 wt % $\text{HfO}_2/\text{TiO}_2$, that with 0.97 mol % of cluster ($\text{Hf}_4\text{Ti}_4\text{MMA}$ 0.97%) contains 9.87 wt % $\text{HfO}_2/\text{TiO}_2$ or that with 1.24 mol % of cluster ($\text{Hf}_4\text{Ti}_4\text{MMA}$ 1.24%) contains 12.75 wt % $\text{HfO}_2/\text{TiO}_2$.

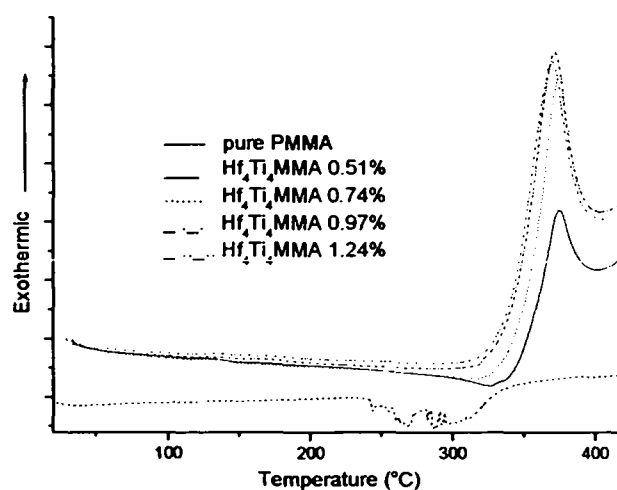


Figure 37. DSC of Hf₄Ti₄ – doped PMMA

DSC of undoped PMMA shows an endothermic event at 330°C. A weaker endothermic event was also observed in the samples with 0.51 mol % of the cluster (Hf₄Ti₄MMA 0.51%), it further decreases when the cluster portion is increased. For crosslinked polymers an exothermic signal above 330°C is observed. This can be attributed to the oxidative degradation of the cluster part of the polymers. The endothermic event is absent with 1.24 mol % of the cluster (Hf₄Ti₄MMA 1.24%).

6.2. Swelling Behavior

A good example for the cluster influence on the polymer properties is their swelling behaviour^[71,104,106]. The swelling behavior of crosslinked polymers and undoped poly(methyl methacrylate), PMMA, are shown in Table 22. The polymers were stored in ethyl acetate for 3 days at room temperature. After this time undoped PMMA was dissolved in the solvent, while crosslinked polymers only swell.

Table 22. Swelling behaviour of the cluster cross-linked PMMA

Swelling Behavior after 3 d	Hf ₄ Ti ₄ O ₈ (OPr) ₄ (OMc) ₁₆ / PMMA 0.51 %	Hf ₄ Ti ₄ O ₈ (OPr) ₄ (OMc) ₁₆ / PMMA 0.74 %	Hf ₄ Ti ₄ O ₈ (OPr) ₄ (OMc) ₁₆ / PMMA 0.97 %	Hf ₄ Ti ₄ O ₈ (OPr) ₄ (OMc) ₁₆ / PMMA 1.24 %
Before swelling [g]	0.1515	0.0788	0.1386	0.0203
After swelling [g]	0.480	0.245	0.440	0.054
g solvent / g polymer	2.16	2.1	2.17	1.66

The amount of uptaken solvent of the cluster-reinforced PMMA in ethyl acetate shows a clear dependence of the degree of crosslinking on the cluster proportion. When a lower amount of cluster is incorporated, a high degree of swelling is observed, and vice versa. The polymer network has a higher mobility and the amount of uptaken solvent increases up to 2.17 g solvent per gram polymer.

7. Experimental Part

7.1. Sample Preparation

7.1.1. General techniques

All operations were carried out in a moisture- and oxygen-free argon atmosphere. All solvents were made water and oxygen-free by standard methods. The following solvents were employed for the NMR experiments: CDCl_3 (99.8%, euriso-top), CD_2Cl_2 (99.6%, euriso-top), d_8 -toluene (99.6%, euriso-top), C_6D_6 (99.6% euriso-top). Metal alkoxides were used as received (Aldrich and ABCR). Iso-butyric acid and dimethylacrylic acid were used as received (Aldrich). Methacrylic acid and methyl methacrylic acid were distilled *in vacuo* prior to use (Aldrich). Propionic acid and acetic acid were distilled and water free used (Aldrich).

7.1.2. Used Chemicals

Chemicals	Provider	CAS-Number	Purification
Methacrylic acid 99%	Aldrich	[79-41-4]	distilled and saturated with argon
Dibenzoylperoxide [DBP]	Aldrich	[94-36-0]	–
Methylmethacrylic acid [MMA]	Aldrich	[80-62-6]	distilled and saturated with argon
Pt-divinyltetramethyldisiloxane	ABCR	[68478-92-9]	saturated with argon
H_2PtCl_6 98 %	ABCR	[16941-12-1]	saturated with argon
Triethylsilane 97 %	ACROS	[617-86-7]	distilled and saturated with argon
Triphenylsilane 97 %	ACROS	[789-25-3]	–
Titanium propoxide 98 %	Aldrich	[3087-37-4]	saturated with argon
Titanium isopropoxide 97 %	ACROS	[546-70-4]	saturated with argon
Zirconium butoxide 80 %	Aldrich	[1071-76-7]	saturated with argon
Hafnium butoxide 95 %	Aldrich	[2172-02-3]	saturated with argon

Yttrium methoxyethoxide 11-18 %	ABCR	[115668-57-0]	saturated with argon
Acetic acid 99 %	Aldrich	[69-19-7]	distilled and saturated with argon
Propionic acid 99,5 %	Aldrich	[79-09-4]	distilled and saturated with argon
Isobutyric acid 99 %	Aldrich	[79-31-2]	distilled and saturated with argon
Dimethylacrylic acid 97%	Aldrich	[541-47-9]	-

7.2. Mixed-Metal oxo clusters

7.2.1. Synthesis of $\text{Ti}_4\text{Y}_2\text{O}_4(\text{OMc})_{14}(\text{MeOCH}_2\text{CH}_2\text{OH})_2$

An amount of 1.02 g (11.8 mmol) of methacrylic acid was added dropwise at room temperature to a stirred mixture of 0.38 g (1.32 mmol) of $\text{Ti}(\text{OPr})_4$ (98% in propanol) and 0.39 mmol of $\text{Y}(\text{OCH}_2\text{CH}_2\text{OMe})_3$ (1.11 g of a 11% methoxyethanol solution). After 7 days at room temperature, 0.31 g of colorless crystals were formed (87% yield relative to Y). The crystals were separated and dried at in vacuo.

Elemental Analysis:

Calc. [%]: C, 41.9; H, 4.9; $\text{TiO}_2/\text{Y}_2\text{O}_3$, 30.6

Found [%]: C, 42.1; H, 4.6; $\text{TiO}_2/\text{Y}_2\text{O}_3$, 32.8 (TGA).

IR-ATR: $\nu = 2927$ (w, CH), 1668 (w, C=C), 1566 (s, sh, COO), 1464 (s), 1424 (s), 1270 (s), 1129 (m), 1031 (m), 978 (m, $\text{CH}_C=\text{CH}_2$), 849 (m), 797 (m) cm^{-1} .

7.2.2. Synthesis of $\text{Ti}_4\text{Y}_2\text{O}_4(\text{OMc})_{14}(\text{MeOH})_2$

An amount of 2.57 g (29.9 mmol) of methacrylic acid was added dropwise at room temperature to a stirred mixture of 1.11 g (3.8 mmol) of $\text{Ti}(\text{OPr})_4$ (98% in propanol) and 0.21 mmol of $\text{Y}(\text{OCH}_2\text{CH}_2\text{OMe})_3$ (0.60 g of a 11% methoxyethanol solution). After 8 days at room temperature, 0.23 g of colorless crystals were formed (quantitative yield relative to Y). The crystals were separated and dried at in vacuo.

Elemental analysis:

Calc. [%]: C, 42.8; H, 4.6; $\text{TiO}_2/\text{Y}_2\text{O}_3$, 30.2

Found [%]: C, 41.6; H, 4.7; $\text{TiO}_2/\text{Y}_2\text{O}_3$, 32.4 (TGA).

IR-ATR: $\nu = 2927$ (w, CH), 1642 (w, C=C), 1546 (s, sh, COO), 1454 (s), 1405 (s, sh), 1241 (s), 1112 (m), 1007 (m), 940 (m, $\text{CH}_C=\text{CH}_2$), 827 (m), 764 (m) cm^{-1} .

7.2.3. Synthesis of $\text{Ti}_4\text{Y}_2\text{O}_4(\text{OMc})_{12}(\text{OCH}_2\text{CH}_2\text{OMe})_2(\text{MeOH})_2$

An amount of 0.74 g (8.6 mmol) of methacrylic acid was added dropwise at room temperature to a stirred mixture of $\text{Ti}(\text{OPr})_4$ (0.23 g, 0.8 mmol, 98% in propanol) and $\text{Y}(\text{OCH}_2\text{CH}_2\text{OMe})_3$ (0.39 mmol, 1.13 g of a ca. 11% methoxyethanol solution). After 3 days at room temperature, 0.31 g of colorless crystals were formed (87% yield relative to Y). The crystals were separated and dried in vacuo.

Elemental Analysis:

Calc. [%]: C, 41.9; H, 4.9; $\text{TiO}_2/\text{Y}_2\text{O}_3$, 30.6

Found [%]: C, 41.9; H, 4.7; $\text{TiO}_2/\text{Y}_2\text{O}_3$, 32.3 (TGA).

IR-ATR: $\nu = 2926$ (w, CH), 1644 (w, C=C), 1571 (s, COO), 1455 (s), 1387 (s, sh), 1369 (s), 1236 (s), 1103 (m), 1065 (m), 1006 (m), 938 (m, $\text{CH}_C=\text{CH}_2$), 826 (m), 736 (m) cm^{-1} .

7.2.4. Synthesis of $\text{Hf}_4\text{Ti}_4\text{O}_6(\text{OPr})_4(\text{OMc})_{16}$

An amount of 1.817 g (21.1 mmol) of methacrylic acid was added dropwise at room temperature to a stirred mixture of 0.77 g (2.65 mmol) of $\text{Ti}(\text{OPr})_4$ (98% in propanol) and 2.54 mmol of $\text{Hf}(\text{O}i\text{Bu})_4$ (1.19 g of a 95% butanol solution). After 7 days at room temperature, 0.23 g of colorless crystals were formed (69% yield). The mother liquid was decanted from crystals, and the crystals were separated and dried at in vacuum.

Elemental analysis:

Calc. [%]: C 35.12; H, 4.19; $\text{TiO}_2/\text{HfO}_2$, 44.59

Found [%]: C 35.04; H 3.93; $\text{TiO}_2/\text{HfO}_2$, 44.29 (TGA).

IR-ATR: $\nu = 2958$ (w); 2925 (w); 1643 (w); 1543 (m); 1455 (s); 1417 (s); 1372 (w); 1245 (m); 1096 (w); 1005 (w); 938 (m); 880 (w); 827 (m); 765 (w) cm^{-1} .

7.3. Zirconium oxo clusters

7.3.1. Synthesis of $\text{Zr}_{12}\text{O}_8(\text{OH})_8(\text{OProp})_{24} \cdot 6\text{PropOH}$

An amount of 1.8 g (24.2 mmol) of propionic acid was added dropwise at room temperature to a stirred mixture of 2.37 mmol of $\text{Zr}(\text{O}i\text{Bu})_4$ (0.91 g of a 80% butanol solution). After 7-8 h at room temperature, 0.53 g of colorless crystals were formed (67% yield relative to alkoxide). The crystals were separated and dried at in vacuo.

Elemental analysis:

Calc. [%]: C 30.39; H 4.65; ZrO_2 41.56

Found [%]: C 29.30; H 4.30; ZrO_2 , 42.86 (TGA).

IR-ATR: $\nu = 3402$ (w); 3259 (w); 2978 (m); 2942 (w); 1717 (m, COOH); 1600 (s, sh, COO⁻); 1533 (s, COO⁻); 1468 (s); 1439 (s, COO⁻); 1374 (m); 1300 (s); 1211 (m); 1078 (m); 1014 (w); 910 (w); 882 (w); 810 (m) cm⁻¹.

NMR-¹H/¹³C: Table 5, page 25.

7.3.2. Synthesis of $\text{Zr}_{12}\text{O}_8(\text{OH})_8(\text{OAc})_{24} \cdot 6\text{AcOH} \cdot 7/2\text{CH}_2\text{Cl}_2$

An amount of 2,62 g (43,66 mmol) acetic acid was added dropwise at room temperature to a solution of 1,7 g (4,44 mmol) of $\text{Zr}(\text{OBu})_4$ (80 % in BuOH) in 5 ml of CH_2Cl_2 under stirring in a Schlenk tube. Within 3 hours at room temperature colourless crystals were obtained. The crystals were separated and dried at in vacuo.

Yield: 1.3 g (68 %)

Elemental analysis:

Calc. [%]: C 21.93; H 2.96; ZrO_2 42.56

Found [%]: C 22.37; H 3.21; ZrO_2 , 47.57 (TGA).

IR-ATR: $\nu = 2960$ (w); 2776 (w); 2607(w); 1757(w); 1709 (m); 1599 (s); 1556 (s); 1449 (s); 1346 (m); 1258(m); 1046 (m); 1026 (m); 910 (w); 883 (w); 791 (w); 735 (w); 669 (m); cm⁻¹.

NMR-¹H/¹³C (C_7D_8 at room temperature): Table 7, page 28.

NMR-¹H/¹³C (C_7D_8 at -40°C): Table 8, page 29.

7.3.3. Synthesis of $\text{Zr}_{12}\text{O}_8(\text{OH})_8(\text{OAcMe}_2)_{24} \cdot 2\text{Me}_2\text{AcOH} \cdot \text{BuOH}$

An amount of 2.516 g (25.13 mmol) of dimethylacrylic acid was added to a solution of 1.31 g (3.41 mmol) of $\text{Zr}(\text{OBu})_4$ (80 % in BuOH) in 10 ml of butanol under stirring. The mixture was allowed to stir for additional 30 min. After 20 days at room temperature colorless crystals were formed. The crystals were separated and dried at in vacuo.

Elemental analysis:Calc. [%]: C 39.95; H 5.0; ZrO₂ 37.00Found [%]: C 40.58; H 4.87; ZrO₂, 35.29 (TGA).

IR-ATR: $\nu = 3648$ (w), 3355 (w, OH), 2911 (w, CH), 1696 (m, C=O), 1651 (s, C=C), 1577 (s), 1520 (s,br, COO_{as}), 1419 (s, COO_s), 1370 (m), 1314 (s), 1234 (m), 1183 (m), 1161 (m), 1077 (m), 862 (m), 819 (m), 722 (m), 638 (m) cm⁻¹.

NMR-¹H/¹³C (CD₂Cl₂ at room temperature): Table 10, page 32.

7.3.4. Synthesis of Zr₁₂O₈(OH)₈(OProp)₆(OMc)₁₈

An amount of 1.37 g (18.49 mmol) of propionic acid and 0.618 g (7.17 mmol) of methacrylic were added dropwise at room temperature to a stirred mixture of 3.72 mmol of Zr(OBu)₄ (1.428 g of a 80% butanol solution). After 1 day at room temperature colorless crystals were formed. The crystals were separated and dried at in vacuo.

NMR-¹H/¹³C (C₇D₈ at room temperature): Table 21, page 57.

7.4. Hafnium oxo cluster**7.4.1. Synthesis of Hf₁₂O₈(OH)₈(OAc)₂₄ · 3AcOH · 3CH₂Cl₂**

An amount of 1,924 g (32,04 mmol) acetic acid was added dropwise at room temperature to a solution of 1,567 g (3,33 mmol) of Hf(OBu)₄ (95 % in BuOH) in 3 ml of CH₂Cl₂ under stirring in a Schlenk tube. After 1 day at room temperature, 2.178 g of colorless crystals were formed (67% yield relative to alkoxide). The crystals were separated and dried at in vacuo. Yield: 2.178 g (67 %).

Elemental analysis:Calc. [%]: C 16.78; H 2.58; HfO₂ 58.87Found [%]: C 17.00; H 2.29; HfO₂, 62.04 (TGA).

IR-ATR: $\nu = 3663$ (w), 3387 (w, OH), 1710 (m, C=O), 1558 (s, COO_{as}), 1453 (s, COO_s), 1261 (m), 1029 (m), 804 (m), 652 (s), 615 (s) cm⁻¹.

NMR-¹H/¹³C (CD₂Cl₂ at room temperature): Table 12, page 36.

7.5. Yttrium Carboxylates

7.5.1. Synthesis of [Y(OMc)₃]_n

An amount of 1,22 g (14,17 mmol) methylacrylic acid was added dropwise at room temperature to a solution of 1,463 g (4,65 mmol) of Y(OCH₂CH₂OMe)₃ (11 % in methoxyethanol solution) in 10 ml of CH₂Cl₂ under stirring in a Schlenk tube. After 7 days at room temperature colorless crystals were formed. The crystals were separated and dried at in vacuo.

IR-ATR: $\nu = 2965$ (w), 1525 (s), 1457 (s), 1420 (s), 1244 (s), 944 (m), 837 (m), 607 (m) cm⁻¹

7.5.2. Synthesis of [Y(OAc)₃]_n

An amount of 0,859 g (14,3 mmol) acetic acid was added dropwise at room temperature to a solution of 1,61 g (5,19 mmol) of Y(OCH₂CH₂OMe)₃ (11 % in methoxyethanol solution) in 10 ml of CH₂Cl₂ under stirring in a Schlenk tube. After 4 days at room temperature colorless crystals were formed. The crystals were separated and dried at in vacuo.

7.6. Cluster Modification Reactions

7.6.1. Attempted hydrosilylation of $Zr_4O_2(OMc)_{12}$

7.6.1.1. Reaction of $Zr_4O_2(OMc)_{12}$ with $HSiPh_3$

- a) A solution of $Zr_4O_2(OMc)_{12}$ (1.01 g, 0.71 mmol) in 8 ml of benzene was treated with 1.74 (6.69 mmol) of $HSiPh_3$. Karstedt catalyst (0.02g) was used. The solution was stirred and heated for 40 hours at 50°C. The product was dried *in vacuo*.

IR-ATR: $\nu = 3069$ (w); 2929 (w), 1722 (m); 1578 (m); 1546 (m); 1462 (s); 1426 (s); 1373 (m); 1306 (w); 1244 (w); 1188 (w); 1108 (s); 998 (w); 728 (s); 697 (s); 678 (s) cm^{-1} .

- b) A solution of $Zr_4O_2(OMc)_{12}$ (1.518 g, 1.07 mmol) in 30 ml of benzene was treated with 3.27g (12.58 mmol) of $HSiPh_3$. H_2PtCl_6 (0.033g) was used as catalyst. The solution was stirred and heated for 20 hours at 60°C. The product was dried *in vacuo*.

IR-ATR: $\nu = 3069$ (w); 2974 (w); 1723 (m); 1550 (m); 1464 (s); 1427 (s); 1375 (m); 1034 (w); 1247 (w); 1188 (w); 1111 (s); 997 (w); 730 (s); 697 (s) cm^{-1} .

7.6.1.2. Reaction of $Zr_4O_2(OMc)_{12}$ with $HSiEt_3$

A solution of $Zr_4O_2(OMc)_{12}$ (0.664 g, 0.468 mmol) in 15 ml of benzene was treated with 4.824g (18.52 mmol) of $HSiEt_3$. H_2PtCl_6 (0.035g) was used as catalyst. The solution was stirred and heated for 20 hours at 60°C. The product was dried *in vacuo*.

IR-ATR: $\nu = 3068$ (w); 3049 (w); 3011 (w); 2122 (m, H-Si); 1588 (w); 1465 (s); 1427 (s); 1304(w); 1187 (s); 1112 (s); 998 (w); 799 (s); 727 (s); 694 (s) cm^{-1} .

7.7. Ligand exchange of metal oxo clusters

7.7.1. Reaction of $Zr_6O_4(OH)_4(OMc)_{12}$ with iso-butyric acid

- a) An amount of 74 mg (0.84 mmol, ~ 6 equivalents) of isobutyric acid was added to a solution of 230 mg (0.135 mmol) of $Zr_6O_4(OH)_4(OMc)_{12}$ in 10 ml of toluene under stirring. The mixture was allowed to stir for additional 30 min. The solvents were then removed, and the resulting residue was dried *in vacuo*. CD_2Cl_2 solutions of the solid were investigated by NMR spectroscopy.

NMR- $^1H/^{13}C$ (CD_2Cl_2 at $-40^\circ C$): Table 17, page 50.

- b) A solution of $Zr_6O_4(OH)_4(OMc)_{12}$ (0.317 g, 0.186 mmol) in 15 ml of toluene was treated with an excess (ca. 20 mmol) of iso-butyric acid, stirred for 10 min and dried *in vacuo*. This process was twice repeated, and then NMR experiments were performed.

7.7.2. Reaction of $Zr_6O_4(OH)_4(OMc)_{12}$ with propionic acid

- a) An amount of 88 mg (1.18 mmol, ~ 6 equivalents) of propionic acid was added to a solution of 332 mg (0.195 mmol) of $Zr_6O_4(OH)_4(OMc)_{12}$ in 15 ml of toluene under stirring. The mixture was allowed to stir for additional 30 min. The solvents were then removed, and the resulting residue was dried *in vacuo*. CD_2Cl_2 solutions of the solid were investigated by NMR spectroscopy.

NMR- $^1H/^{13}C$ (CD_2Cl_2 at $-40^\circ C$): Table 18, page 52.

b) A solution of $Zr_6O_4(OH)_4(OMc)_{12}$ (0.226 g, 0.133 mmol) in 15 ml of toluene was treated with an excess (ca. 20 mmol) of propionic acid, stirred for 10 min and dried *in vacuo*. This process was twice repeated, and then NMR experiments were performed.

NMR- $^1H/^{13}C$ (CD_2Cl_2 at RT): Table 19, page 53.

7.7.3. Reaction of $Zr_{12}O_8(OH)_8(OProp)_{24}$ with acetic acid

An amount of 3.24 g (54.08 mmol) of acetic acid was added to a solution of 0.473 g (0.132 mmol) of $Zr_{12}O_8(OH)_8(OProp)_{24}$ in 5 ml of CH_2Cl_2 under stirring. The mixture was allowed to stir for additional 30 min. The solvents were then removed, and the resulting residue was dried *in vacuo*. CD_2Cl_2 solutions of the solid were investigated by NMR spectroscopy.

NMR- $^1H/^{13}C$ (CD_2Cl_2 at RT): Table 20, page 55.

7.7.4. Reaction of $Zr_{12}O_8(OH)_8(OProp)_6(OMc)_{18}$ with propionic acid

A solution of $Zr_{12}O_8(OH)_8(OProp)_6(OMc)_{18}$ (0.165 g, 0.0428 mmol) in 5 ml of benzene was treated with an excess (1.942 g, 26.21 mmol) of propionic acid, stirred for 10 min and dried *in vacuo*. This process was twice repeated, and then NMR experiments were performed.

NMR- $^1H/^{13}C$ (C_7D_8 at RT): Table 21, page 57.

7.8. Preparation of Inorganic-Organic Hybrid Materials

7.8.1. Synthesis of PMMA doped with $\text{Hf}_4\text{Ti}_4\text{O}_6(\text{OPr})_4(\text{OMc})_{16}$

In a typical synthesis, 0.292 g (0.112 mmol) of $\text{Hf}_4\text{Ti}_4\text{O}_6(\text{OPr})_4(\text{OMc})_{16}$, Hf_4Ti_4 , were dissolved in 4 ml of benzene. 2.216 g (22.13 mmol) of methyl methacrylate were added, and mixture was stirred at room temperature for a few minutes. After addition of 0.232 g (0.096 mmol) the solution was heated at 65°C for 24 hours. The resulting glassy polymer was dried under a vacuum at 65°C for few hours. Residual solvent was removed by extraction with ethyl acetate.

Table 24. Amount of used chemical for the preparation of Hf_4Ti_4 - doped PMMA

Sample name	Cluster g / mmol	Monomer g / mmol	Initiator g / mmol	Solvent ml
$\text{Hf}_4\text{Ti}_4\text{MMA}$ 0.51%	0.292 / 0.112	2.216 / 22.13	0.0232 / 0.096	4
$\text{Hf}_4\text{Ti}_4\text{MMA}$ 0.74%	0.348 / 0.133	1.797 / 17.95	0.0188 / 0.077	5
$\text{Hf}_4\text{Ti}_4\text{MMA}$ 0.97%	0.358 / 0.137	1.409 / 14.07	0.0157 / 0.064	4
$\text{Hf}_4\text{Ti}_4\text{MMA}$ 1.24%	0.502 / 0.193	1.546 / 15.44	0.0174 / 0.071	9

$\text{Hf}_4\text{Ti}_4\text{MMA}$ 0.51%

Elemental analysis [wt %]:

calc. [%]: C 51.58, H 6.75, $\text{HfO}_2 / \text{TiO}_2$ 15.04

found [%]: C 57.35, H 7.25, $\text{HfO}_2 / \text{TiO}_2$ 5.28

IR-ATR: $\nu = 3651$ (s), 3371 (m), 2948 (m), 1726 (s), 1434 (m), 1239 (m), 1144 (s) cm^{-1} .

$\text{Hf}_4\text{Ti}_4\text{MMA}$ 0.74%

Elemental analysis [wt %]:

calc. [%]: C 53.52, H 6.99, $\text{HfO}_2 / \text{TiO}_2$ 11.58

found [%]: C 56.35, H 7.33, $\text{HfO}_2 / \text{TiO}_2$ 4.93

IR-ATR: $\nu = 3649$ (s), 3547 (m), 2948 (m), 1729 (s), 1558 (m), 1241 (m), 1146 (s) cm^{-1} .

Hf₄Ti₄MMA 0.97%**Elemental analysis [wt %]:**calc. [%]: C 54.72, H 7.23, HfO₂ / TiO₂ 9.41found [%]: C 54.61, H 7.08, HfO₂ / TiO₂ 4.21**IR-ATR:** $\nu = 3649$ (s), 3392 (m), 2953 (m), 1728 (s), 1456 (m), 1147 (s) cm⁻¹.**Hf₄Ti₄MMA 1.24 %****Elemental analysis [wt %]:**calc. [%]: C 55.66, H 7.38, HfO₂ / TiO₂ 7.72found [%]: C 53.03, H 6.68, HfO₂ / TiO₂ 6.87**IR-ATR:** $\nu = 3483$ (s,br), 2991 (m), 2949 (m), 1727 (s), 1541 (m), 1434 (m), 1241 (m), 1191 (s, sh), 1146 (s), 989 (m), 829 (m) cm⁻¹.**7.9. Analytical Techniques****7.9.1. Thermal Analysis (TGA, DSC)**

Thermal analysis techniques were used to characterize the thermal behavior of the prepared materials.

Thermogravimetric analysis (TGA) is a thermal analysis method in which the change in sample mass is recorded as a function of temperature. The resulting mass change versus temperature curve provides information concerning the thermal stability and composition of the investigated sample.

TGA measurements on bulk polymers were done in air on a TGA-50 instrument by Shimadzu. A heating rate of 5°C / min was used and the samples were heated from ambient temperature up to 800°C.

Differential scanning calorimetry (DSC) is a thermal analysis technique which is used to measure the temperatures and heat flow associated with transitions in materials as a function of time and temperature. Such measurements provide quantitative and qualitative information about physical and chemical changes that involve endothermic or exothermic processes, or changes in heat capacity.

DSC measurements on bulk polymers were done in air on a Shimadzu DSC-50 instrument. The samples were heated from ambient temperature to 450°C using a heating rate of 5°C / min.

7.9.2. NMR Spectroscopy

7.9.2.1. NMR measurements

NMR spectra were recorded on a Bruker Avance 300 (^1H : 300.13 MHz, ^{13}C : 75.47 MHz) equipped with a 5 mm broadband probe head and a z-gradient unit. 2D spectra were measured by Dr. Michael Puchberger with Bruker standard pulse sequences: COSY (Correlated Spectroscopy), TOCSY (Total Correlation Spectroscopy, mixing time was usually 160ms), ROESY (Rotating Frame Overhauser Effect Spectroscopy, spinlock time was usually 250ms), NOESY (Nuclear Overhauser Effect Spectroscopy, mixing time was usually 250ms), EXSY (Exchange Spectroscopy, mixing time was usually 1s), HSQC (Heteronuclear Single Quantum Correlation), $^1\text{H}/^{13}\text{C}$ -HMBC (Heteronuclear Multiple Bond Correlation).

7.9.3. IR Spectroscopy

IR-ATR spectra of solid samples of oxo clusters and polymers were recorded on a Bruker Tensor 27 with a 2.5 mm diameter sampling area of the ATR crystal. Small amounts of solid can be placed directly on the ATR crystal and pressed using calibrated presses.

7.9.4. Elemental Analysis

Elemental analysis were carried out by Mag. Johannes Theiner at the microanalytical Laboratory at the Institute of Physical Chemistry at the University of Vienna. A 2400 CHN Elemental Analyzer by Perkin Elmer were used.

7.9.5. Single-Crystal X-Ray Diffraction

Selected crystals were mounted on a Siemens SMART diffractometer with a CCD area detector. Graphite-monochromated Mo-K α radiation (71.073 pm) was used for all measurements. The crystal-to-detector distance was 4.40 cm. A hemisphere of data was collected by a combination of three sets of exposures at 173 K. Each set had a different ϕ angle for the crystal, and each exposure took 20 s and covered 0.3° in ω . The data were corrected for polarization and Lorentz effects, and an empirical absorption correction (SADABS) was applied. The cell dimensions were refined with all unique reflections. The structure was solved by direct methods (SHELXS86). Refinement was carried out with the full-matrix least-squares method based on F^2 (SHELXL93) with anisotropic thermal parameters for all non-hydrogen atoms. Hydrogen atoms were inserted in calculated positions and refined riding with the corresponding atom.

7.10. Crystallographic Data

7.10.1. $\text{Ti}_4\text{Y}_2\text{O}_4(\text{OMc})_{14}(\text{MeOCH}_2\text{CH}_2\text{OH})_2$ Table 25. Crystallographic data and structural parameters of $\text{Ti}_4\text{Y}_2\text{O}_4(\text{OMc})_{14}(\text{MeOCH}_2\text{CH}_2\text{OH})_2$

Empirical formula	$\text{C}_{62} \text{H}_{86} \text{O}_{36} \text{Ti}_4 \text{Y}_2$
Formula weight	1776.7
Temperature [K]	173 (2)
Wavelength [pm]	71.073
Crystal system	triclinic
space group	P-1
Unit cell dimensions	$a = 1136.6(1)$ [pm] $b = 1283.3(1)$ [pm] $c = 1493.2(1)$ [pm] $\alpha = 91.410(2)$ [°] $\beta = 103.669(2)$ [°] $\gamma = 110.698(2)$ [°]
$V(\text{pm}^3)$	$1965.6(3) \cdot 10^6$
Z	2
Calculated density [g/cm^3]	1.492
Absorption coefficient μ [mm^{-1}]	1.932
F (000)	902
Crystal size [mm]	0.42 x 0.31 x 0.23
2θ range (°)	2.69 - 28.32
Limiting indices	$-15 \leq h \leq 14$ $-15 \leq k \leq 17$ $-14 \leq l \leq 19$
Reflections coll./ unique	13838 / 9523
Refinement method	Full-matrix least-squares on F^2
Data / parameters	9523 / 485
GOF on F^2	1.024
R1 [$I > 2\sigma(I)$]	R1 = 0.0438, wR2 = 0.1090
R indices (all data)	R1 = 0.0661, wR2 = 0.1212
Largest diff. peak and hole, [$\text{e} \cdot \text{\AA}^{-3}$]	0.716 / -0.315

7.10.2. $\text{Ti}_4\text{Y}_2\text{O}_4(\text{OMc})_{14}(\text{MeOH})_2$ Table 26. Crystallographic data and structural parameters of $\text{Ti}_4\text{Y}_2\text{O}_4(\text{OMc})_{14}(\text{MeOH})_2$

Empirical formula	$\text{C}_{64} \text{H}_{82} \text{O}_{36} \text{Ti}_4 \text{Y}_2$
Formula weight	1796.7
Temperature [K]	173 (2)
Wavelength [pm]	71.073
Crystal system	triclinic
space group	P-1
Unit cell dimensions	a = 1145.83(7) [pm] b = 1249.25(8) [pm] c = 1448.52(9) [pm] $\alpha = 84.884(1) [^\circ]$ $\beta = 82.250(1) [^\circ]$ $\gamma = 76.971(1) [^\circ]$
V(pm ³)	1997.9(2) · 10 ⁶
Z	2
Calculated density [g/cm ³]	1.493
Absorption coefficient μ [mm ⁻¹]	1.902
F (000)	920
Crystal size [mm]	0.30 x 0.24 x 0.18
2 θ range (°)	2.44 - 30.06
Limiting indices	-15 ≤ h ≤ 16 -17 ≤ k ≤ 17 -20 ≤ l ≤ 18
Reflections coll./ unique	15837 / 11271
Refinement method	Full-matrix least-squares on F ²
Data / parameters	11271 / 479
GOF on F ²	1.024
R1 [I > 2 σ (I)]	R1 = 0.0572, wR2 = 0.1469
R indices (all data)	R1 = 0.0890, wR2 = 0.1655
Largest diff. peak and hole, [e·Å ⁻³]	1.024 / -0.630

7.10.3. $\text{Ti}_4\text{Y}_2\text{O}_4(\text{OMc})_{12}(\text{OCH}_2\text{CH}_2\text{OMe})_2(\text{McOH})_2$ Table 27. Crystallographic data and structural parameters of $\text{Ti}_4\text{Y}_2\text{O}_4(\text{OMc})_{12}(\text{OCH}_2\text{CH}_2\text{OMe})_2$
 McO(H)_2

Empirical formula	$\text{C}_{62} \text{H}_{86} \text{O}_{36} \text{Ti}_4 \text{Y}_2$
Formula weight	1776.7
Temperature [K]	173 (2)
Wavelength [pm]	71.073
Crystal system	triclinic
space group	P-1
Unit cell dimensions	$a = 1117.1(1)$ [pm] $b = 1366.1(2)$ [pm] $c = 1409.2(2)$ [pm] $\alpha = 71.659(2)$ [°] $\beta = 75.690(2)$ [°] $\gamma = 76.208(2)$ [°]
$V(\text{pm}^3)$	$1947.6(4) \cdot 10^6$
Z	2
Calculated density [g/cm^3]	1.513
Absorption coefficient μ [mm^{-1}]	1.950
F (000)	910
Crystal size [mm]	0.39 x 0.23 x 0.19
2θ range (°)	2.27 - 28.33
Limiting indices	$-14 \leq h \leq 14$ $-18 \leq k \leq 17$ $-18 \leq l \leq 9$
Reflections coll./ unique	13818 / 9496
Refinement method	Full-matrix least-squares on F^2
Data / parameters	9496 / 469
GOF on F^2	1.007
R1 [$I > 2\sigma(I)$]	R1 = 0.0553, wR2 = 0.1357
R indices (all data)	R1 = 0.0866, wR2 = 0.1523
Largest diff. peak and hole, [$\text{e} \cdot \text{Å}^{-3}$]	1.103 / -0.452

7.10.4. $\text{Hf}_4\text{Ti}_4\text{O}_6(\text{OPr})_4(\text{OMc})_{16}$ Table 28. Crystallographic data and structural parameters of $\text{Hf}_4\text{Ti}_4\text{O}_6(\text{OPr})_4(\text{OMc})_{16}$

Empirical formula	$\text{C}_{76} \text{H}_{108} \text{Hf}_4 \text{O}_{42} \text{Ti}_4$
Formula weight	2599.18
Temperature [K]	193 (2)
Wavelength [pm]	71.073
Crystal system	monoclinic
space group	C2/c
Unit cell dimensions	a = 2762.4(7) [pm] b = 1581.2(4) [pm] c = 2672.4(7) [pm] $\alpha = 90$ [°] $\beta = 117.79(4)$ [°] $\gamma = 90$ [°]
V(pm ³)	$10327(4) \cdot 10^6$
Z	4
Calculated density [g/cm ³]	1.672
Absorption coefficient μ [mm ⁻¹]	4.375
F (000)	5104
Crystal size [mm]	0.80 x 0.36 x 0.16
2 θ range (°)	1.67 - 26.37
Limiting indices	$-34 \leq h \leq 34$ $-9 \leq k \leq 19$ $-33 \leq l \leq 32$
Reflections coll./ unique	28626 / 10451 [R(int) = 0.0531]
Refinement method	Full-matrix least-squares on F ²
Data / restraints / parameters	10451 / 6 / 569
GOF on F ²	1.108
R1 [I > 2 σ (I)]	R1 = 0.0664, wR2 = 0.1468
R indices (all data)	R1 = 0.1095, wR2 = 0.1752
Largest diff. peak and hole, [e·Å ⁻³]	4.386 / -1.922

7.10.5. $Zr_{12}O_8(OH)_8(OProp)_{24} \cdot 6PropOH$ Table 29. Crystallographic data and structural parameters of $Zr_{12}O_8(OH)_8(OProp)_{24} \cdot 6PropOH$

Empirical formula	$C_{90} H_{155} O_{76} Zr_{12}$
Formula weight	3547.78
Temperature [K]	173 (2)
Wavelength [pm]	71.073
Crystal system	monoclinic
space group	P-1
Unit cell dimensions	$a = 1709.2(6)$ [pm] $b = 1935.6(6)$ [pm] $c = 2156.1(7)$ [pm] $\alpha = 86.951(7)$ [°] $\beta = 88.241(8)$ [°] $\gamma = 78.973(7)$ [°]
$V(\text{pm}^3)$	$6990(4) \cdot 10^6$
Z	2
Calculated density [g/cm ³]	1.686
Absorption coefficient μ [mm ⁻¹]	0.951
F (000)	3566
Crystal size [mm]	0.36 x 0.28 x 0.24
2 θ range (°)	1.46 to 23.26
Limiting indices	$-18 \leq h \leq 15$ $-21 \leq k \leq 19$ $-23 \leq l \leq 21$
Reflections collected	30393 / 19224 [R(int) = 0.0585]
Refinement method	Full-matrix least-squares on F^2
Data / restraints / parameters	19224 / 0 / 1605
GOF on F^2	1.028
R1 [$I > 2\sigma(I)$]	R1 = 0.0697, wR2 = 0.1836
R indices (all data)	R1 = 0.1172, wR2 = 0.2150
Largest diff. peak and hole, [e·Å ⁻³]	3.211 and -1.466

7.10.6. $Zr_{12}O_8(OH)_8(OAc)_{24} \cdot 6AcOH \cdot 7/2CH_2Cl_2$ Table 30. Crystallographic data and structural parameters of $Zr_{12}O_8(OH)_8(OAc)_{24} \cdot 6AcOH \cdot 7/2CH_2Cl_2$

Empirical formula	$C_{63.5} H_{103} Cl_{3.5} O_{76} Zr_{12}$
Formula weight	3473.79
Temperature [K]	173 (2)
Wavelength [pm]	71.073
Crystal system	monoclinic
space group	P2(1)/c
Unit cell dimensions	a = 1253.7(6) [pm] b = 2414.9(11) [pm] c = 2050.8(10) [pm] $\alpha = 90$ [°] $\beta = 104.9(10)$ [°] $\gamma = 90$ [°]
V(pm ³)	6000.5(5) · 10 ⁶
Z	4
Calculated density [g/cm ³]	1.896
Absorption coefficient μ [mm ⁻¹]	1.255
F (000)	3382
Crystal size[mm]	0.34 x 0.10 x 0.09
2 θ range (°)	1.92 to 28.36
Limiting indices	-16 ≤ h ≤ 15 -32 ≤ k ≤ 32 -27 ≤ l ≤ 27
Reflections collected	69801 / 14888 [R(int) = 0.0763]
Refinement method	Full-matrix least-squares on F ²
Data / restraints / parameters	14888 / 0 / 766
GOF on F ²	1.039
R1 [I > 2 σ (I)]	R1 = 0.0574, wR2 = 0.1415
R indices (all data)	R1 = 0.0980, wR2 = 0.1620
Largest diff. peak and hole, [e · Å ⁻³]	2.293 and -1.077

7.10.7. $Zr_{12}O_8(OH)_8(OAcMe_2)_{24} \cdot 2Me_2AcOH \cdot BuOH$ Table 31. Crystallographic data and structural parameters of $Zr_{12}O_8(OH)_8(OAcMe_2)_{24} \cdot 2Me_2AcOH \cdot BuOH$

Empirical formula	$C_{148} H_{214} O_{74} Zr_{12}$
Formula weight	4271.83
Temperature [K]	173 (2)
Wavelength [pm]	71.073
Crystal system	triclinic
Space group	P-1
Unit cell dimensions	$a = 1675.8(10)$ [pm] $b = 1745.6(11)$ [pm] $c = 1969.8(12)$ [pm] $\alpha = 86.452(10)$ [°] $\beta = 72.838(10)$ [°] $\gamma = 63.784 (10)$ [°]
V(pm)	$4923.9(5) \cdot 10^6$
Z	1
Calculated density [g/cm ³]	1.441
Absorption coefficient μ [mm ⁻¹]	0.688
F (000)	2174
Crystal size	0.40 x 0.35 x 0.23 mm
2 θ range (°)	2.03 to 25.00
Limiting indices	$-18 \leq h \leq 19$ $-20 \leq k \leq 20$, $-23 \leq l \leq 23$
Reflections collected	31945 / 17261 [R(int) = 0.0600]
Refinement method	Full-matrix least-squares on F ²
Data / restraints / parameters	17261 / 1920 / 1054
GOF on F ²	1.098
R1 [I > 2 σ (I)]	R1 = 0.1025, wR2 = 0.2554
R indices (all data)	R1 = 0.1519, wR2 = 0.2768
Largest diff. peak and hole, [e·Å ⁻³]	1.892 and -1.159

7.10.8. $\text{Hf}_{12}\text{O}_8(\text{OH})_8(\text{OAc})_{24} \cdot 3\text{AcOH} \cdot 3\text{CH}_2\text{Cl}_2$ Table 32. Crystallographic data and structural parameters of $\text{Hf}_{12}\text{O}_8(\text{OH})_8(\text{OAc})_{24} \cdot 3\text{AcOH} \cdot 3\text{CH}_2\text{Cl}_2$

Empirical formula	$\text{C}_{66} \text{H}_{102} \text{Cl}_{12} \text{O}_{76} \text{Hf}_{12}$
Formula weight	4678.76
Temperature [K]	173 (2)
Wavelength [pm]	71.073
Crystal system	monoclinic
Space group	P2 (1) / c
Unit cell dimensions	a = 1255.9(9) [pm] b = 2419.5(2) [pm] c = 2049.7(15) [pm] $\alpha = 90$ [°] $\beta = 104.993(10)$ [°] $\gamma = 90$ [°]
V(pm)	$6016.3(8) \cdot 10^6$
Z	2
Calculated density [g/cm ³]	2.583
Absorption coefficient μ [mm ⁻¹]	10.672
F (000)	4348
Crystal size [mm]	0.21 x 0.18 x 0.12
2 θ range (°)	2.22 - 25.00
Limiting indices	$-14 \leq h \leq 14$ $-28 \leq k \leq 28$ $-23 \leq l \leq 24$
Reflections collected	38319 / 10582 [R(int) = 0.0497]
Refinement method	Full-matrix least-squares on F ²
Data / restraints / parameters	10582 / 1358 / 743
GOF on F ²	1.296
R1 [I > 2 σ (I)]	R1 = 0.0748, wR2 = 0.1469
R indices (all data)	R1 = 0.0811, wR2 = 0.1491
Largest diff. peak and hole, [e·Å ⁻³]	4.411 and -2.234

7.10.9. $[\text{Y}(\text{OMc})_3]_n$ Table 33. Crystallographic data and structural parameters of $[\text{Y}(\text{OMc})_3]_n$

Empirical formula	$\text{C}_{12} \text{H}_{15} \text{O}_6 \text{Y}$
Formula weight	344.15
Temperature [K]	173(2)
Wavelength [pm]	71.073
Crystal system,	orthorhombic
space group	$\text{Cmc}2(1)$
Unit cell dimensions	$a = 1453.61(2)$ [pm] $b = 1280.33(1)$ [pm] $c = 768.02(9)$ [pm] $\alpha = 90$ [°] $\beta = 90$ [°] $\gamma = 90$ [°]
Volume (pm ³)	$1429.4(3) \cdot 10^6$
Z	1
Calculated density[g/cm ³]	1.599
Absorption coefficient μ [mm ⁻¹]	4.098
F(000)	696
Crystal size [mm]	0.20 x 0.20 x 0.20
2 θ range (°)	2.12 - 25.00
Limiting indices	$-17 \leq h \leq 17,$ $-15 \leq k \leq 10,$ $-8 \leq l \leq 9$
Reflections coll. / unique	3748 / 1161
Refinement method	Full-matrix least-squares on F^2
Data / restraints / parameters	1161 / 1 / 97
GOF on F^2	1.055
R1 [$I > 2\sigma(I)$]	$R1 = 0.0289, wR2 = 0.0725$
R indices (all data)	$R1 = 0.0308, wR2 = 0.0732$
Largest diff. peak and hole, [e-Å ⁻³]	0.718 / -0.416

7.10.10. $[\text{Y}(\text{OAc})_3]_n$ Table 34. Crystallographic data and structural parameters of $[\text{Y}(\text{OAc})_3]_n$

Empirical formula	$\text{C}_6 \text{H}_9 \text{O}_6 \text{Y}$
Formula weight	266.1
Temperature [K]	293(2)
Wavelength [pm]	71.073
Crystal system,	monoclinic
space group	Cc
Unit cell dimensions	$a = 1584.37(11)$ [pm] $b = 1646.41(11)$ [pm] $c = 8.3242(6)$ [pm] $\alpha = 90$ [°] $\beta = 115.8310(10)$ [°] $\gamma = 90$ [°]
Volume (pm ³)	$1954.4(2) \cdot 10^6$
Z	4
Calculated density[g/cm ³]	1.788
Absorption coefficient μ [mm ⁻¹]	5.963
F(000)	1032
Crystal size [mm]	0.20 x 0.18 x 0.15
2 θ range (°)	2.47 - 25.00
Limiting indices	$-18 \leq h \leq 18,$ $-19 \leq k \leq 19,$ $-9 \leq l \leq 9$
Reflections coll. / unique	8727 / 3336
Refinement method	Full-matrix least-squares on F^2
Data / restraints / parameters	3336 / 2 / 235
GOF on F^2	1.054
R1 [$I > 2\sigma(I)$]	R1 = 0.0673, wR2 = 0.1924
R indices (all data)	R1 = 0.0702, wR2 = 0.1953
Largest diff. peak and hole, [e-Å ⁻³]	6.621 / -1.077

8. Summary

The chemical modification of metal alkoxides by nucleophilic ligands leads to the formation of new molecular precursors which exhibit different chemical reactivity and functionality.

In the present work, carboxylate-substituted clusters were synthesized by reaction of the alkoxides with carboxylic acids.

Titanium-yttrium mixed-metal oxo clusters capped by polymerizable methacrylate ligands were prepared by reaction of mixtures of $\text{Ti}(\text{O}^n\text{Pr})_4$ and $\text{Y}(\text{OCH}_2\text{CH}_2\text{OMe})_3$ with methacrylic acid. Only the ratio between the two alkoxides was varied while the metal alkoxide/methacrylic acid ratio was kept constant. The reaction of metal alkoxides $[\text{Ti}(\text{O}^n\text{Pr})_4 + \text{Y}(\text{OCH}_2\text{CH}_2\text{OMe})_3]$ with a seven-fold of methacrylic acid resulted in a various mixed-metal clusters which were isolated in high yields and structurally characterized by single crystal diffraction. All clusters had the general composition $\text{Ti}_4\text{Y}_2\text{O}_4\text{X}_{14}(\text{HZ})_2$ ($\text{X}, \text{Z} = \text{OMc}$ and/or $\text{OCH}_2\text{CH}_2\text{OMe}$) despite the different Ti/Y ratio in the precursor mixture. The cluster differed by the distribution of X and Z, and by the arrangement of the titanium and yttrium polyhedra. The reaction of titanium propoxide and yttrium methoxyethoxide with methacrylic acid in a molar ratio of 2 : 1 : 7 resulted in the formation of $\text{Ti}_4\text{Y}_2\text{O}_4(\text{OMc})_{14}(\text{MeOCH}_2\text{CH}_2\text{OH})_2$. Increasing the proportion of the titanium propoxide relative to the yttrium methoxyethoxide to a molar ratio 3.5 : 1 lead to the formation of $\text{Ti}_4\text{Y}_2\text{O}_4(\text{OMc})_{14}(\text{McOH})_2$, and the cluster $\text{Ti}_4\text{Y}_2\text{O}_4(\text{OMc})_{12}(\text{OCH}_2\text{CH}_2\text{OMe})_2(\text{McOH})_2$ was obtained from a molar ratio 18 : 1. The basic structural motif of $\text{Ti}_4\text{Y}_2\text{O}_4(\text{OMc})_{14}(\text{MeOCH}_2\text{CH}_2\text{OH})_2$ and $\text{Ti}_4\text{Y}_2\text{O}_4(\text{OMc})_{14}(\text{McOH})_2$ is a zigzag chain of two central $[\text{YO}_8]$ dodecahedra and two terminal $[\text{TiO}_6]$ octahedra to which two additional $[\text{TiO}_6]$ octahedra are condensed. The structures are very similar to that of the previously obtained titanium-zirconium mixed-metal cluster $\text{Ti}_4\text{Zr}_2\text{O}_4(\text{OBu})_6(\text{OMc})_{10}$. In the $\text{Ti}_4\text{Y}_2\text{O}_4(\text{OMc})_{12}(\text{OCH}_2\text{CH}_2\text{OMe})_2(\text{McOH})_2$, only two of the oxo ligands are μ_3 , while the other two oxo ligands are μ_2 , each $\text{OCH}_2\text{CH}_2\text{OMe}$ ligand must occupy three coordination sites. The structural motif of $\text{Ti}_4\text{Y}_2\text{O}_4(\text{OMc})_{12}(\text{OCH}_2\text{CH}_2\text{OMe})_2(\text{McOH})_2$ consists of a ring of four corner-sharing $[\text{TiO}_6]$ octahedra to which two $[\text{YO}_8]$ dodecahedra are condensed.

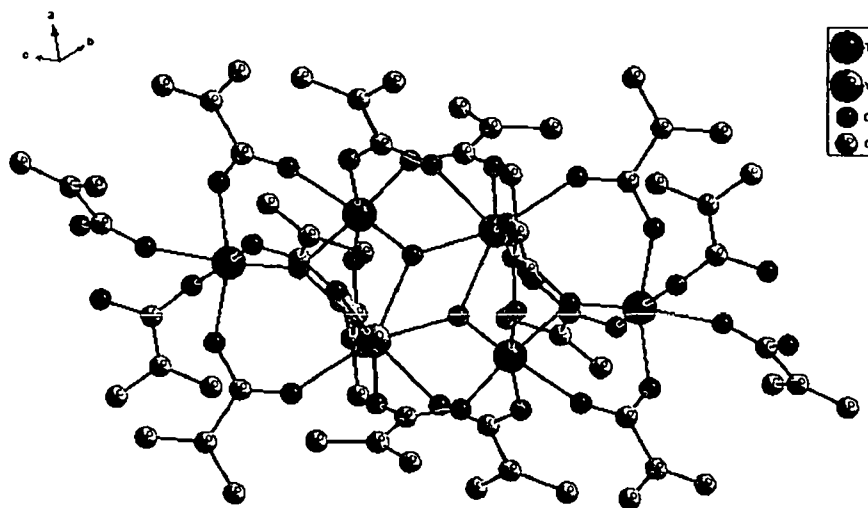


Figure 38. Molecular structure of $\text{Ti}_4\text{Y}_2\text{O}_4(\text{OMc})_{14}(\text{McOH})_2$.

Another noteworthy feature of the clusters $\text{Ti}_4\text{Y}_2\text{O}_4(\text{OMc})_{14}(\text{MeOCH}_2\text{CH}_2\text{OH})_2$, $\text{Ti}_4\text{Y}_2\text{O}_4(\text{OMc})_{14}(\text{McOH})_2$ and $\text{Ti}_4\text{Y}_2\text{O}_4(\text{OMc})_{12}(\text{OCH}_2\text{CH}_2\text{OMe})_2(\text{McOH})_2$ is the presence of monodentate carboxylate ligands and coordinated alcohol or acid molecules. Both types of ligands are always in a *cis* position at the same metal. This allows the formation of a hydrogen bridge between the alcoholic or carboxylic OH group and the C=O group of the monodentate methacrylate ligand, which probably stabilizes this unusual ligand combination. The conversion of a bidentate carboxylate ligand to a monodentate ligand, with concomitant coordination of a neutral ligand to the opened coordination site, may be connected to the reactivity of the clusters.

This result shows that the relative molar ratio of the involved alkoxides plays an important role in the formation of the mixed-metal oxo clusters.

The reaction of a mixture of titanium propoxide and hafnium butoxide with methacrylic acid in a molar ratio of 1 : 1 : 4 resulted in the formation of $\text{Hf}_4\text{Ti}_4\text{O}_6(\text{OPr})_4(\text{OMc})_{16}$. A similar cluster with butoxy groups, $\text{Hf}_4\text{Ti}_4\text{O}_6(\text{OBu})_4(\text{OMc})_{16}$, was obtained when titanium propoxide was replaced by titanium butoxide. This result shows that the kind of titanium alkoxide has no big influence on the structure of the formed clusters.

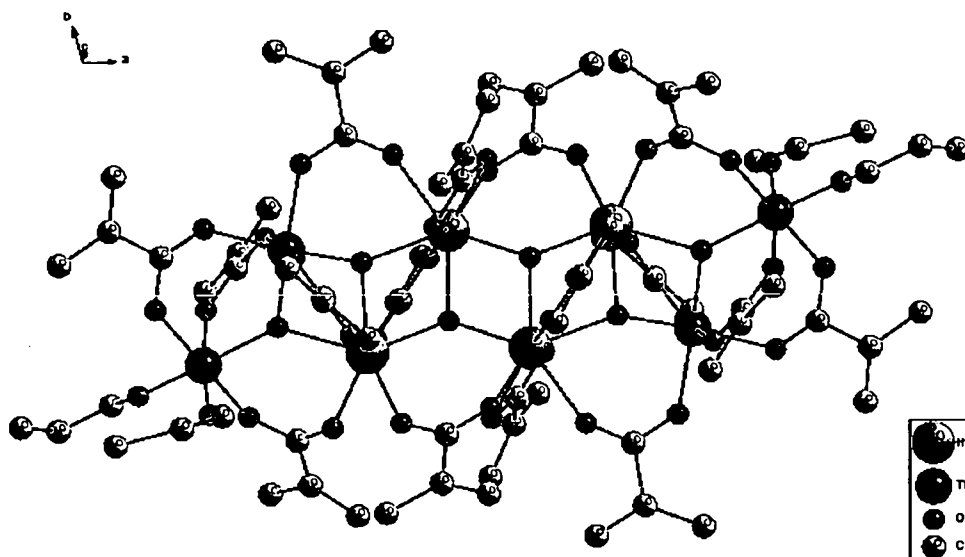


Figure 39. Molecular structure of $\text{Hf}_4\text{Ti}_4\text{O}_4(\text{OPr})_4(\text{OMc})_{16}$.

Reaction of zirconium butoxide with a 10-fold molar excess of propionic or acetic acid, respectively, led to the formation of zirconium oxo clusters of the type $\text{Zr}_{12}\text{O}_8(\text{OH})_8(\text{OOCR})_{24}$. The same cluster was obtained with various other molar ratios of the corresponding acids to metal alkoxide. The same cluster type was formed when zirconium butoxide was reacted with 7 molecular equivalents of dimethylacrylic acid.

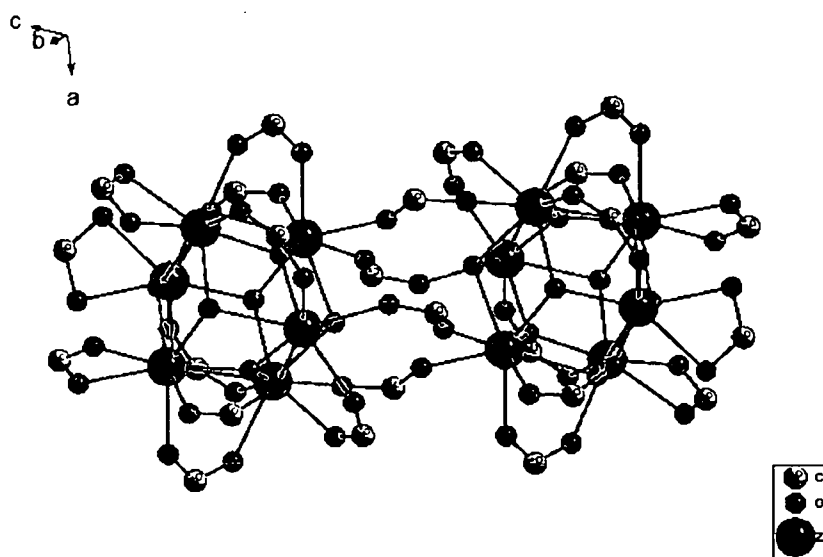


Figure 40. Cluster core of connected zirconium, oxygen and carbon atoms in the type $\text{Zr}_{12}\text{O}_8(\text{OH})_8(\text{OOCR})_{24}$ clusters. For clarity the organic groups were omitted.

Reaction of hafnium butoxide with a 10-fold molar excess of acetic acid led to the formation of a hafnium oxo cluster of the type $\text{Hf}_{12}\text{O}_8(\text{OH})_8(\text{OAc})_{24}$. The cluster had the same symmetry and geometry as zirconium clusters of the type $\text{Zr}_{12}\text{O}_8(\text{OH})_8(\text{OOCR})_{24}$.

Organically modified metal oxo clusters bearing polymerizable ligands on the surface can be used as co-monomer for the preparation of hybrid materials. In attempts to reduce the number of polymerizable ligands for a given cluster type either hydrosilylation reactions or exchange of surface bonded ligands against others was tested. The hydrosilylation reaction was investigated for $\text{Zr}_4\text{O}_2(\text{OMc})_{12}$ in the presence of catalytic amounts of either Karstedt catalyst or H_2PtCl_6 . Several reactions with an stoichiometric or over-stoichiometric cluster : HSiPh_3 or HSiEt_3 ratio were carried out. The possibility that the hydrosilylation reactions took place was not confirmed by spectroscopic methods in any of the investigated reactions mixtures.

Complete carboxylate exchange with an excess of carboxylic acid can be achieved for clusters of the type $\text{Zr}_6\text{O}_4(\text{OH})_4(\text{OOCR})_{12}$, $[\text{Zr}_6\text{O}_4(\text{OH})_4(\text{OOCR})_{12}]_2$ or $[\text{Zr}_6\text{O}_4(\text{OH})_4(\text{OOCR})_x(\text{OOCR}')_y]_2$. However, partial exchange is also feasible.

The cluster $\text{Zr}_6\text{O}_4(\text{OH})_4(\text{OMc})_{12}$ was reacted with six molar equivalents of iso-butyric acid in toluene. The NMR spectra of the resulting solid clearly showed that the cluster contains both methacrylate and iso-butyrate ligands. Their ratio was in this case approximately 1:1, that means the mixed carboxylate cluster $\text{Zr}_6\text{O}_4(\text{OH})_4(\text{OIsob})_6(\text{OMc})_6$ was obtained. Treatment of $\text{Zr}_6\text{O}_4(\text{OH})_4(\text{OMc})_{12}$ with a large excess of iso-butyric acid led to nearly complete exchange of the methacrylate ligands.

The addition of six equivalents of propionic acid to $\text{Zr}_6\text{O}_4(\text{OH})_4(\text{OMc})_{12}$ led to a compound with the propionate : methacrylate ratio of approximately 5 : 7, i.e. the approximate composition was $\text{Zr}_6(\text{OH})_4\text{O}_4(\text{OProp})_5(\text{OMc})_7$ (determined by integration of the ^1H NMR signals). Treatment of $\text{Zr}_6\text{O}_4(\text{OH})_4(\text{OMc})_{12}$ with a large excess of propionic acid led to nearly complete exchange of the methacrylate ligands. The cluster core remained unchanged.

The addition of a 17-fold excess of acetic acid related to propionate of $\text{Zr}_{12}\text{O}_8(\text{OH})_8(\text{OProp})_{24}$ lead to a compound with the propionate : acetate ratio of approximately 1 : 2, i.e. the approximate composition was $\text{Zr}_{12}\text{O}_8(\text{OH})_8(\text{OProp})_8(\text{OAc})_{16}$ (determined by integration of the ^1H NMR signals). Treatment of $\text{Zr}_{12}\text{O}_8(\text{OH})_8(\text{OProp})_6(\text{OMc})_{18}$ with a large excess of propionic acid lead to nearly complete exchange of the methacrylate ligands. $\text{Zr}_{12}\text{O}_8(\text{OH})_8(\text{OProp})_{24}$ was prepared as a reference for the exchange experiments. The NMR analysis showed that the spectrum of the reaction product of $\text{Zr}_{12}\text{O}_8(\text{OH})_8(\text{OProp})_6(\text{OMc})_{18}$

with propionic acid corresponds to the spectrum of $Zr_{12}O_8(OH)_8(OProp)_{24}$, this means that the cluster core, $Zr_{12}O_8(OH)_8$, and the molecular symmetry, C_{2h} , after exchange is the same as before exchange.

These results show that through ligand exchange is possible to control the ratio of different ligands on the cluster-surface and that the zirconium clusters of the type $Zr_6O_4(OH)_4(OOCR)_{12}$ and $Zr_{12}O_8(OH)_8(OOCR)_{24}$ are not connected through an equilibrium to each other, while the cluster core and the symmetry of clusters after ligand exchange remains unchanged.

The mechanism of the carboxylate exchange may be as follows: a carboxylic acid molecule after conversion of a bridging carboxylate ligand to a monodentate coordination mode, could be coordinated. After proton transfer from the incoming to the outgoing carboxylic acid via a hydrogen bridge, the old carboxylate could be eliminated and the new carboxylate regains a bridging coordination. This hypothesis is supported by the structure of $Ti_4Y_2O_4(OMc)_{14}(McOH)_2$ (Fig. 38), where a vacated coordination site is occupied by a carboxylic acid, $RCOOH$. In the Y/Ti cluster, an (anionic) OMc and a (neutral) HOMc ligand are bonded to the same metal atom.

Radical-initiated polymerization of 0.5-1.24 mol % of $Hf_4Ti_4O_6(OPr)_4(OMc)_{16}$ with methyl methacrylate in toluene at $65^\circ C$, with dibenzoylperoxide as the initiator, resulted in yellowish glassy polymers. The thermal behavior of the modified polymers was studied by Thermogravimetric Analysis (TGA) and Differential Scanning Calorimetry (DSC) and compared to pure poly(methyl methacrylate) PMMA. Undoped PMMA depolymerizes at $330^\circ C$. This decomposition reaction is suppressed when the polymers were crosslinked by the oxo cluster. The degree of depolymerization decreases as the cluster proportion increases. While undoped PMMA dissolves in ethyl acetate, the cluster crosslinked polymers only swell. The solvent uptake can be correlated with the proportion of the incorporated cluster.

9. Literature

1. C. J. Brinker, G. W. Scherer, *Sol-Gel Science; The Physics and Chemistry of Sol-Gel Processing*, Academic Press, New York, (1990).
2. J. Livage, M. Henry, C. Sanchez, *Prog. Solid State Chem.* **18**, 259 (1988).
3. L. G. Hubert-Pfalzgraf, *New J. Chem.*, **11**, 663, (1987).
4. G. W. Scherer, *J. Non-Cryst. Solids* **100**, 77, (1988).
5. C. Sanchez, F. Ribot, *New J. Chem.*, **18**, 1007, (1994).
6. D. C. Bradley, R. C. Mehrotra, D. P. Gaur, *Metal Alkoxides*, Academic, London, (1978).
7. B. Vaartstra, J. C. Daran, P. S. Gradef, L. G. Hubert-Pfalzgraf, J. C. Huffman, S. Parraud, K. Yunlu, K. G. Caulton, *Inorg. Chem.*, **29**, 3126, (1990).
8. P. Tolendo, F. Ribot, C. Sanchez, *Acta Cryst.*, **C46**, 1419, (1990).
9. F. Babonneau, S. Doeuff, A. Léaustic, C. Sanchez, C. Cartier. M. Verdaguer, *Inorg. Chem.*, **27**, 3166, (1988).
10. E. A. Barringer, H. K. Bowen, *Langmuir* **1**, 420, (1985).
11. D. Kundu, D. Ganguli, *J. Mater. Sci. Lett.* **5**, 293, (1986).
12. C. Sanchez, J. Livage, *New J. Chem.* **14**, 513, (1990).
13. J. C. Pouxviel, J. P. Boilot, J. C. Boloeil, J. Y. Lallemand, *J. Non-Cryst. Solids* **89**, 345, (1987).
14. K. G. Caulton, L. G. Hubert-Pfalzgraf, *Chem. Rev.* **90**, 969, (1990).
15. S. Doeuff, M. Henry, C. Sanchez, J. Livage, *J. Non-Cryst. Solids* **89**, 206, (1987).
16. A. Larbot, I. Laaziz, C. Giuzard, L. Cot, *Precurseurs Moleculaires de Materiaux Inorganiques* **2**, 269, (1989).
17. B. E. Yoldas, *J. Mater. Sci.* **21**, 1087, (1986).
18. R. E. Reeves, L. W. Mazzeno Jr., *J. Am. Chem. Soc.* **76**, 2533, (1953).
19. J. Chaibi, M. Henry, H. Zarrouk, N. Gharbi, J. Livage, *J. Non-Cryst. Solids* **170**, 1, (1994).
20. C. Sanchez, M. In, *J. Non-Cryst. Solids*, **147/148**, 1, (1992).
21. C. Sanchez, J. Livage, M. Henry, F. Babonneau, *J. Non-Cryst. Solids*, **100**, 65, (1988).
22. R. Nass, H. Schmidt, *J. Non-Cryst. Solids*, **121**, 329, (1990).
23. R. C. Mehrotra, R. Bohra, D. P. Gaur, *Metal β -diketonates and Allied Derivatives*, Academic, London, (1978).
24. H. Unuma, T. Tokoda, T. Y. Susuki, T. Furusaki, K. Kodaira, T. Hatsushida, *J. Mater. Sci. Lett.*, **5**, 1248, (1986).

25. J. C. Debsikar, *J. Non-Cryst. Solids*, **87**, 343, (1986).
26. J. C. Debsikar, *J. Mater. Sci.*, **20**, 44, (1985).
27. J. Livage, C. Sanchez, *J. Non-Cryst. Solids*, **145**, 11, (1992).
28. P. Papet, N. LeBars, J. F. Baumard, A. Lecomte, A. Dauger, *J. Mater. Sci.*, **24**, 3850, (1989).
29. A. Léaustic, F. Babonneau, J. Livage, *J. Chem. Mater.*, **1**, 240, (1989).
30. F. Ribot, P. Tolendano, C. Sanchez, *Chem. Mater.*, **3**, 759, (1991).
31. G. D. Smith, C. N. Gaughlan, J. A. Campbell, *Inorg. Chem.*, **11**, 2989, (1972).
32. P. Toledano, M. In, C. Sanchez, *C. R. Acad. Sci., Paris Ser. II*, **313**, 1247, (1991).
33. P. D. Moran, C. E. F. Rickard, G. A. Bowmaker, R. P. Cooney, J. R. Bartlett and J. L. Woolfrey, *Inorg. Chem.*, **37**, 1417, (1998).
34. B. K. Keppler, C. Friesen, H. G. Moritz, H. Vongerichten, E. Vogel, *Structure and Bonding*, **78**, 97, (1991).
35. P. Toledano, M. In, C. Sanchez, *C. R. Acad. Sci., Paris Ser. II*, **311**, 1161, (1990).
36. C. Sanchez, M. In, P. Toledano, P. Griesmar, *Mater. Res. Soc. Symp. Proc.* **271**, 669, (1992).
37. J. V. Silverton, J. L. Hoard, *Inorg. Chem.* **2**, 243, (1963).
38. N. W. Alcock, V. M. Tracy, T. C. Waddington, *J. Chem. Soc., Dalton Trans.*, 2243, (1976).
39. I. Laaziz, A. Larbot, C. Guizard, J. Durand, L. Cot, *Acta Cryst.* **C46**, 2332, (1990).
40. S. Doeuff, Y. Dromzee, C. Sanchez, *C. R. Acad. Sci., Paris Ser. II*, **308**, 1409, (1989).
41. S. Doeuff, Y. Dromzee, F. Taulelle, C. Sanchez, *Inorg. Chem.* **28**, 4439, (1989).
42. I. Gautier-Luneau, A. Mosset, J. Galy, *Z. Kristallogr.*, **180**, 83, (1987).
43. T. J. Boyle, T. M. Alam, C. J. Tafoya, *Inorg. Chem.* **37**, 5588, (1998).
44. T. J. Boyle, R. P. Tyner, T. M. Alam, B. L. Scott, J. W. Ziller, B. G. Potter Jr., *J. Am. Chem. Soc.* **121**, 12104, (1999).
45. X. Lei, M. Shang, T. P. Fehlner, *Organometallics* **15**, 3779, (1996).
46. X. Lei, M. Shang, T. P. Fehlner, *Organometallics* **16**, 2589, (1997).
47. H. Shimomura, X. Lei, M. Shang, T. P. Fehlner, *Organometallics* **16**, 5302, (1997).
48. B. Moraru, N. Hüsing, G. Kickelbick, P. Fratzl, H. Peterlik, U. Schubert, *Chem. Mater.*, **14**, 2732, (2002).
49. G. Kickelbick, U. Schubert, *Eur. J. Inorg. Chem.* **159**, (1989).
50. U. Schubert, E. Arpac, W. Glaubitt, A. Helmerich, C. Chau, *Chem. Mater.* **4**, 291, (1992).

51. R. Papiernik, L. G. Hubert-Pfalzgraf, J. Vaissermann, M.C. Henriques Baptista Goncalves, *J. Chem. Soc., Dalton Trans.*, 2285, (1998).
52. I. Laaziz, A. Larbot, C. Guizad, A. Julbe, L. Cot, *Mat. Res. Soc. Symp. Proc.* 271, 71, (1992).
53. G. Kickelbick, U. Schubert, *Chem. Ber.* 130, 473, (1997).
54. G. Kickelbick, P. Wiede, U. Schubert, *Inorg. Chem. Acta* 284, 1, (1999).
55. B. Moraru, S. Gross, G. Kickelbick, G. Trimmel, U. Schubert, *Monatsh. Chem.*, 132, 993, (2001).
56. G. Kickelbick, U. Schubert, *J. Chem. Soc., Dalton Trans.*, 1301, (1999).
57. S. Gross, G. Kickelbick, M. Puchberger, U. Schubert, *Monatsh. Chem.*, 134, 1053, (2003).
58. B. Moraru, G. Kickelbick, U. Schubert, *Eur. J. Inorg. Chem.*, 1295, (2001).
59. W. Noll, *Chemistry and Technology of Silicones*, Academic, New York, (1968).
60. V. W. Day, T. A. Eberspacher, W. G. Klemperer, C. W. Park, F. S. Rosenberg, *J. Am. Chem. Soc.* 113, 8190, (1991).
61. N. Steunou, F. Robert, K. Boubekour, F. Ribot, C. Sanchez, *Inorg. Chim. Acta* 279, 144, (1998).
62. R. Schmid, A. Mosset, J. Galy, *J. Chem. Soc., Dalton Trans.*, 1999, (1991).
63. C. F. Campana, Y. Chen, V. W. Day, W. G. Klemperer, R. A. Sparks, *J. Chem. Soc., Dalton Trans.*, 691, (1996).
64. V. W. Day, T. A. Eberspacher, Y. Chen, J. Hao, W. G. Klemperer, *Inorg. Chem. Acta* 229, 391, (1995).
65. B. Morosin, *Acta Cryst.* B33, 303, (1977).
66. N. Steunou, F. Ribot, K. Boubekour, J. Maquet, C. Sanchez, *New J. Chem.*, 23, 1079, (1999).
67. V. W. Day, T. A. Eberspacher, W. G. Klemperer, C. W. Park, *J. Am. Chem. Soc.* 115, 8469, (1993).
68. N. Steunou, F. Robert, K. Boubekour, F. Ribot, C. Sanchez, *Inorg. Chem. Acta*, 279, 144, (1998).
69. N. Steunou, G. Kickelbick, K. Boubekour, C. Sanchez, *J. Chem. Soc., Dalton Trans.*, 3653, (1999).
70. U. Schubert, *Chem. Mater.*, 13, 3847, (2001).
71. D. A. Loy, K. J. Shea, *Chem. Rev.*, 95, 1431, (1995).
72. P. Judenstein, C. Sanchez, *J. Mater. Chem.*, 6, 511, (1996).

73. G. Kickelbick, U. Schubert, *Monatsh. Chem.*, **132**, 13, (2001).
74. F. Ribot, C. Sanchez, *Comments Inorg. Chem.*, **20**, 327, (1999).
75. C. Sanchez, G. J. de A. A. Soler-Illia, F. Ribot, T. Lalot, C. R. Mayer, V. Cabuil, *Chem. Mater.*, **13**, 3061, (2001).
76. U. Schubert, N. Hüsing, A. Lorenz, *Chem. Mater.*, **7**, 2010, (1995).
77. J. Kramer, R. K. Prud'homme, *J. Colloid Interface Sci.*, **118**, 294, (1987).
78. J. Kramer, R. K. Prud'homme, P. Wiltzius, P. Mirau, S. Knoll, *Colloid Polym. Sci.*, **266**, 145, (1988).
79. G. Monchatre, *L'Actualite Chimique*, 11, January 1984.
80. G. Trimmel, S. Gross, G. Kickelbick, U. Schubert, *Appl. Organomet. Chem.* **15**, 401, (2001).
81. G. Trimmel, P. Fratzl, U. Schubert, *Chem. Mater.*, **12**, 602, (2000).
82. U. Schubert, G. Trimmel, B. Moraru, W. Tesch, P. Fratzl, S. Gross, G. Kickelbick, N. Hüsing, *Mat. Res. Soc. Symp. Proc.*, **628**, CC2.3.1, (2000).
83. O. Poncelet, L. G. Hubert-Pfalzgraf, J. C. Daran, R. Astier, *J. Chem. Soc. Chem. Comm.*, 1846, (1989).
84. R. P. Turcotte, J. M. Haschke, M. S. Jenkins, L. R. Eyring, *J. Solid State Chem.*, **2**, 593, (1970).
85. F. L. Corter, F. von Batchelder, J. F. Murray, P. H. Klein, *Proc. 9th Rare Earth Res. Conf.*, **2**, 752, (1971).
86. E. G. Pogodilova, A. I. Grigorev, A. V. Novoselova, *Russ. J. Inorg. Chem.*, **14**, 913, (1969).
87. A. I. Grigorev, E. G. Pogodilova, *J. Struct. Chem.*, **10**, 43, (1969).
88. A. S. Antsyshkina, L. M. Dikareva, L. Kh. Minacheva, M. A. Poraikoshits, *Proc. Semin. Crystallochem. Coord. Metalloorg. Comp.*, 2nd, p. 9, (1973).
89. R. C. Merhrotra, R. Bohra, *Metal Carboxylates*, Academic Press, London, (1983).
90. F. Ribot, P. Toledano, C. Sanchez, *Inorg. Chim. Acta* **239**, 185, (1991).
91. P. A. Agaskar, *J. Am. Chem. Soc.* **111**, 6858, (1989).
92. Karstedt B.D., U.S. Patent 3, 775, 452, (1973).
93. B. Ameduri, B. Boutevin, J. J. E. Moreau, H. Moutaabbid, M. W. Chi Man, *J. Fluor. Chem.*, **104**, 185, (2000).
94. C. Aguilera, J. Bartulin, B. Hisgen, H. Ringsdorf, *Makromol. Chem.* **184**, 253, (1983).
95. P. J. Miller, K. Matyjaszewski, *Macromolecules*, **33**(26), 8760, (1999).
96. D. Hoebbel, T. Reinert, K. Endres, H. Schmidt, A. Kayan, E. Arpac, *Proc. 1st Europ.*

- Workshop on Hybrid Organic-Inorganic Materials*, Eds. C. Sanchez, F. Ribot, 319, (1993).
97. H. E. Katz, M. L. Schilling, S. M. Stein, F. M. Houlihan, R. S. Hutton, G. N. Taylor, *Chem. Mater.*, **7**, 1534, (1995).
 98. I. Mijatovic, G. Kickelbick, M. Puchberger, U. Schubert, *New J. Chem.*, **27**, 3, (2003).
 99. I. Mijatovic, G. Kickelbick, U. Schubert, *Eur. J. Inorg. Chem.*, 1933, (2001).
 100. T. Lis, *Acta Crystallogr., Sect. B*, **32**, 2042, (1980).
 101. F. R. Kogler, M. Jupa, M. Puchberger, U. Schubert, *J. Mater. Chem.*, **14**, 3133, (2004).
 102. S. Gross, G. Kickelbick, U. Schubert, *unpublished*.
 103. S. Gross, V. Di Noto, G. Kickelbick, U. Schubert, *Mat. Res. Soc. Symp. Proc.*, **726**, Q4.1.1, (2002).
 104. G. Trimmel, B. Moraru, S. Gross, V. Di Noto, U. Schubert, *Macromol. Symp.*, **175**, 357, (2001).
 105. B. Moraru, Dissertation, TU Wien, (2001).
 106. U. Schubert, *J. Sol-Gel Sci. Technol.*, **31**, 19, (2004).

Lebenslauf

Name *Jupa Myhedin*

Geboren *09.04.1972 in Molliq, Gjakove, Kosovo*

Familienstand *Verheiratet mit Lumturije Jupa, 1999*

Kinder *Sohn Blendi, geb. 1999
Sohn Bleon, geb. 2001*

Ausbildung *1978 - 1986 Volksschule in Molliq*
1986 – 1990 Gymnasium in Gjakove
*1990 – 1996 Universität von Prishtina, Fakultät der Natur-
Wissenschaft, Sektion Chemie. Sponson am 04.06.1996*
1996 – 1998 Chemielehrer ans Gymnasium in Gjakove
*1999 – 2000 Vorstudienlehrgang der Wieneruniversitäten –
Wien, Deutsch Sprachkurs für Fortgeschrittene*
*Seit 01.06.2002 beschäftigt als Wissenschaftlicher
Mitarbeiter in Ausbildung an der Technische Universität
Wien, Institut für Materialchemie*
*Dissertation zum Thema: Herstellung und Modifizierung von
Carboxylat-substituierten Metall Oxo Clustern.*

Muttersprache *Albanisch*

Fremdsprachen *Deutsch, Englisch, Serbisch.*

Wien, am 23.05.2005

Mag .rer. nat. Myhedin Jupa
